MICROGLIAL DYSFUNCTION AS AN EARLY SUSCEPTIBILITY TO ALZHEIMER'S DISEASE: THE EXACERBATING ROLE OF DEVELOPMENTAL TOXICITY

by

Annalise N. vonderEmbse

June 2017

Director of Dissertation: Jamie C. DeWitt, Ph.D.

Major Department: Pharmacology and Toxicology

The association between perturbations to neuroimmune development and susceptibility to adult neurodegenerative diseases, like Alzheimer's disease (AD), may undersore a putative pathogenic role for gradual microglial dysfunction. In the present thesis, gene and environment (GxE) interactions were evaluated in the propagation of microglial dysfunction within the context of AD. We hypothesized that postnatal toxicant exposure in a mouse model of AD (Tg) would disrupt neuroimmune development preferentially in females, in parallel with human AD sex bias, incurring altered regulation of microglial response phenotypes early in life that then functionally persists as the reduced capacity to adapt later in life, thereby promoting synaptic dysfunction and increasing susceptibility to AD. Following postnatal exposure to lead acetate (Pb) from postnatal day (PND) 5-15, earlier and more severe amyloid accumulation was observed in the hippocampus concomitant to reduced microglial activation (densitometric Iba1+, $CD45^{lo}/CD11b^{+}$ characterization) in females compared to males by PND 50, inferring that non-neuroprotective microglia exacerbated AD susceptibility with female bias. In order to determine the extent of microglial dysfunction at the level of the synapse, deficits in neuroprotective capabilities, such as microglial ferritin expression and polarization profiles (CD86:CD209), in the amyloid-stressed environment of older animals were investigated following a similar exposure period to Pb from

PND 5-10. Congruent with our previous findings, Pb-exposed Tg females preferentially exhibited gross abnormalities in healthy microglia:neuron signaling, such as atypical TrkB expression in the CA3 region, that transitioned to maladaptive over time. The addition of a wildtype (WT) mouse comparison substantiated the selective GxE synergism in microglial maladaptation, prompting investigation for early epigenetic regulation for a dysfunctional phenotype of susceptibility that could persist into adulthood. As hypothesized, deleterious expression patterns for miR-124, miR-132, and miR-34a, critical to homeostatic neuroimmune maturation, were observed in Pb-exposed Tg females by PND 10 and 21, suggesting persistent, epigenetic re-patterning of the microglial response phenotype and limited adaptability. The results presented in this thesis converge to describe a newly established critical window of postnatal developmental sensitivity for female-specific microglial maladaptation. Collectively, this set of experiments provides insight into the potentiative effects of GxE during development and neuroimmune-related susceptibility to AD.

MICROGLIAL DYSFUNCTION AS AN EARLY SUSCEPTIBILITY TO ALZHEIMER'S DISEASE: THE EXACERBATING ROLE OF DEVELOPMENTAL TOXICITY

A Dissertation

Presented to the Faculty of the Department of Pharmacology and Toxicology

East Carolina University Brody School of Medicine

In Partial Fulfillment of the Requirements for the Degree of

Doctor of Philosophy in Pharmacology and Toxicology

by

Annalise Noelle vonderEmbse

June 2017

MICROGLIAL DYSFUNCTION AS AN EARLY SUSCEPTIBILITY TO ALZHEIMER'S DISEASE: THE EXACERBATING ROLE OF DEVELOPMENTAL TOXICITY

by

Annalise Noelle vonderEmbse

APPROVED BY:

DIRECTOR OF
DISSERTATION: _____
(Jamie C. DeWitt, PhD)

COMMITTEE MEMBER: _____
(Ken Soderstrom, PhD)

COMMITTEE MEMBER: _____
(Lisa Domico, PhD)

COMMITTEE MEMBER: _____
(Kymberly Gowdy, PhD)

COMMITTEE MEMBER: _____
(Tuan Tran, PhD)

CHAIR OF THE DEPARTMENT OF
PHARMACOLOGY AND TOXICOLOGY: _____
(David Taylor, PhD)

DEAN OF THE
GRADUATE SCHOOL: _____
(Paul J. Gemperline, PhD)

ACKNOWLEDGEMENTS

I would like to express my sincere gratitude to Dr. Jamie DeWitt, my PI and mentor for the last five years, for her guidance, patience, and humor. I would also like to thank Adam, my parents, siblings, and friends, as well as my lab family – Qing, Jacqui, and Jason, for their unending support and kindness. Additionally, I want to thank the faculty, staff, and students of the Department of Pharmacology and Toxicology for trusting in my potential and selflessly assisting me, including Jackie Hooker, Jackie Masterson, Dr. Van Dross, and Dr. Taylor. Exta-departmentally, I would like to acknowledge the support of Joani Zary, Kristen Hall, Dale and the entire Department of Comparative Medicine, the IT guys, and Dr. Muller-Borer. Finally, I want to thank my committee members, Dr. Kym Gowdy, Dr. Lisa Domico, Dr. Tuan Tran, and Dr. Ken Soderstrom, for their valuable input into this thesis.

TABLE OF CONTENTS

LIST OF TABLES

LIST OF FIGURES

LIST OF SYMBOLS OR ABBREVIATIONS

Aβ	Amyloid-β
ACH	Amyloid Cascade Hypothesis
AD	Alzheimer's disease
ANOVA	Analysis of variance
APC	Allophycocyanin
APP	Amyloid precursor protein
ATP	Adenosine triphosphate
BBB	Blood-brain barrier
BDNF	Brain-derived neurotrophic factor
CCL	Chemokine ligand
CNS	Central nervous system
CSF	Cerebrospinal fluid
CSF-1	Colony stimulating factor-1
C_t	Threshold cycle
Ctl	Control
Cy5	Cyanine 5
DAB	Diaminobenzidine

DAP12	DNAX activation protein 12kDa
DAPI	4',6-diamidino-2-phenylindole
DG	Dentate gyrus
DIT	Developmental immunotoxicity
DMH	Dysfunctional/Dystrophic Microglia Hypothesis
DOAD	Developmental Origins of Adult Disease
EDTA	Ethylenediaminetetraacetic acid
EOAD	Early-onset Alzheimer’s disease
FACS	Fluorescence-activated cell sorting
FCS	Fetal calf serum
FFPE	Formalin-fixed, paraffin-embedded
FITC	Fluorescein isothiocyanate
FMO	Fluorescence minus one
GC	Granule cell
GxE	Gene x Environment
HSP	Hebbian synaptic plasticity
IACUC	Institutional Animal Care and Use Committee
Iba1	Ionized calcium binding adaptor molecule 1

IF	Immunofluorescence
IgG	Immunoglobulin G
IHC	Immunohistochemistry
IL	Interleukin
Indo	Indomethacin
LOAD	Late-onset Alzheimer’s disease
LTP/LTD	Long-term potentiation/depression
MFP	Mossy fiber pathway
miRNA	microRNA
NFT	Neurofibrillary tangles
NO	Nitric oxide
NSAID	Non-steroidal anti-inflammatory drug
Pb	Lead (II) acetate
PBS	Phosphate buffered saline
PD	Parkinson’s disease
PGE_2	Prostaglandin E_2
PND	Postnatal day
ppm	Parts per million

PtdSer	Phosphatidylserine
qRT-PCR	Quantitative real-time polymerase chain reaction
ROI	Region of interest
RT	Reverse transcriptase
SEM	Standard error of the mean
SGZ	Subgranular zone
SVZ	Subventricular zone
Tg	3xTgAD triple transgenic mouse model
TNFα	Tumor necrosis factor α
TPBS	Phosphate buffered saline with tween
TREM2	Triggering receptor expressed on myeloid cells 2
TrkB	Tyrosine kinase B
WT	Wildtype

Chapter 1:

General Introduction

1.1 Developmental Origins of Adult Disease (DOAD)

The Developmental Origins of Adult Disease (DOAD) hypothesis refers to the burgeoning research field that interrelates adult diseases, such as neurodegeneration, that develop gradually over time with factors that influence the developmental environment (Gluckman et al., 2010). DOAD has a relatively strong biological basis in developmental plasticity. However, due to the complexity of development, incompletely described thresholds of maladaptation, and subtle, slow-developing pathologies, the link between early and late life is inherently more difficult to experimentally corroborate.

During development, organisms undergo overlapping critical windows of development for all cells, organs, organ systems, and interactions therein. It is during these sensitive and often singular events that cells grow and mature, not only via genetic instruction, but through cues from both the immediate and external environment. In fact, interactions between genes and environment, and the subsequent plethora of phenotypic variability, are ubiquitous phenomena found throughout biology. Nowhere is this more prevalent than during development, where exogenous influences help shape an organism to adapt and thrive in a particular environment by capitalizing on phenotypic plasticity (West-Eberhard, 1989). The DOAD hypothesis selectively investigates particular critical windows during these variable environmental conditions to determine limits of plasticity and persistence of consequences as an etiologic function for slow-developing diseases.

The research avenues within the DOAD paradigm are expansive, first described in the 1980s as the Barker hypothesis, in which poor developmental conditions were correlated with increased risk of coronary heart disease (Gluckman et al., 2010). Additionally, there are considerable data supporting developmental origins of hypertension, osteoporosis, Type I diabetes mellitus, and allergies, among numerous other diseases (Fox et al., 2012; Dietert, 2011). Many of these studies focus on heightened genetic and environmental risk factors and highlight a critical role for both toxicological analysis and evidence, or biomarkers, of these gene-environment interactions, with functional implications on the scope and limitations of adaptation. In this regard, epigenetics has been leading the forefront.

1.1.1 *Gene x Environment: Epigenetics and Developmental Immunotoxicity (DIT)*

Epigenetics, considered “the bridge between genotype and phenotype” (Goldberg et al., 2007), refers to DNA modifications, often initiated by or in response to environmental signals that then determine functional phenotype. Classic examples, such as alterations to chromatin accessibility, include covalent, post-transcriptional acetylation and methylation, as well as non-covalent chromatin remodeling, histone repositioning, and dynamic looping and topographic modifications. Non-coding RNAs are also included in this list of epigenetic modifiers. MicroRNAs (miRNAs), for example, act as post-transcriptional inhibitors of mRNA expression, and it has been estimated that 60% of all protein-encoding genes may be regulated by miRNAs (Friedman et al., 2009). Of particular note are NeurimmiRs, or miRNAs that affect both neuronal and immune cellular phenotype, as they are involved in CNS development and disease (Soreq and Wolf, 2011). Epigenetic modifications are particularly useful as quantifiable footprints from a

developmental event or environmental exposure, written and rewritten into the epigenome through a variety of mechanisms even after the initiating stimulus is gone (Chin-Chan et al., 2015). For example, Coppieters and colleagues (2014) recently described their Latent Early-life Associated Regulation model in a study of global methylation/hydroxymethylation patterns within the aging and Alzheimer's disease (AD) brain, implicating environmental factors as well as the epigenome in the regulatory elements involved in heightened aging-related vulnerability.

Beyond epigenetics, altered developmental conditions can interfere with critical stages of maturation and facilitate the formation of atypical, and transiently beneficial adaptations, such as a "primed" phenotype to increase the likelihood of a particular stereotyped response and susceptibility to dysfunction. Arguably the greatest depth and breadth of these atypical adaptations is seen in the field of developmental immunotoxicity (DIT). The development of the immune system is distinct from other organ systems through a prolonged critical period of maturation, pervasiveness throughout the entire body, and reliance on the body's environmental cues for learning and development of normal function (Burns-Naas, et al., 2008). The mounting evidence linking DIT to cancer, pediatric-related immune dysfunction, and even deficits in cognition emphasizes the potential for developmental immune-related phenotypic plasticity to play a considerable role in a multitude of later-life adult diseases.

1.2 Alzheimer's disease

There are data to suggest the DOAD hypothesis may be applicable in neurodegenerative diseases, such as Alzheimer's disease (AD), that have highly complex etiologies and aging as a common denominator (Miller and O'Callaghan, 2008). AD is defined

as a progressive, late-onset neurodegenerative disease that presents as gradual cognitive decline, memory loss, and personality changes, somewhat akin to accelerated dementia. In fact, AD is the most common form of dementia, accounting for 60-80% of dementia cases in elderly, preferentially affecting women more than men (Schmidt et al., 2008). The hierarchy of AD subtypes can be defined by genetic predilection, including sporadic AD, with high variability in onset and severity and no discernable genetic component, and the less common gene-related familial AD (Pericak-Vance and Haines, 1995). AD subtypes are also defined by timing of disease onset. A very rare form, known as early-onset AD (EOAD), develops before the age of 50 and is more likely to have a genetic predisposition due to mutations in amyloid precursor protein (APP) and presenilins 1 and 2. Conversely, late-onset AD (LOAD), which typically develops after 65, accounts for nearly 95% of all AD cases and may or may not have any genetic predisposition. Genetic association studies, though beneficial in elucidating partial molecular mechanisms, ultimately fall short in characterizing the etiology for sporadic LOAD, thus implicating a potential role for exogenous influences and, perhaps, atypical development.

1.2.1 *AD Pathophysiology*

Beyond irreversible neurodegeneration with specificity for cholingergic neurons, two hallmark molecular pathologies associated with AD are extracellular senile plaques and intracellular neurofibrillary tangles (NFTs), defined by the accumulation of misfolded proteins, such as amyloid-β and tau, respectively. Additionally, chronic inflammation, decreased neurogenesis, and altered metabolism are observed in the typical AD brain. Neurodegeneration often occurs with remarkable selectivity for specific regions of the brain, such as the neocortical-

hippocampal pathway, leading to deficits in learning, memory, and executive function (Armstrong, 2009).

The pathogenesis of AD is still incompletely understood despite decades of research due to the complexity and variability of presentation, and lack of a discernible etiologic catalyst. This is exemplified by inconsistent biomarkers for pre-clinical stages, and weak efficacy of therapeutics. For years pathogenesis has been thought to follow the Amyloid Cascade Hypothesis (ACH), which posits initiation of AD molecular pathologies, such as senile plaque and neurofibrillary tangle formation, occur subsequent to increased amyloid load in the brain. This hypothesis has been substantiated by numerous studies demonstrating the neurotoxicity of amyloid beta oligomers, both in vitro and in vivo, and correlation to cognitive decline (Forny-Germano et al., 2014; Baglioni et al., 2006; Näslund et al., 2000; Lambert et al., 1998). The presence of these oligomeric "seeds" is thought to be due, in part, by disruption of the unfolded protein response within the endoplasmic reticulum, a process known to be upregulated in AD (Hoozemans et al., 2005). However, the structure, function, and neurotoxicity of oligomeric amyloid beta is highly dependent on their immediate environment (Li et al., 2009), implicating their persistence and gradual accumulation as insoluble fibrils in ACH-related neurotoxicity. Ultimately, this weakens the ACH by underscoring the lack of phagocytosis and passive diffusion into the cerebrospinal fluid (CSF) rather than the production of amyloid beta. Furthermore, recent evidence suggests these misfolded proteins may, in fact, be a reactive pathological event to oxidative stress (Naidoo, 2009). New studies have shown a surprising protective role for the reactive appearance of amyloid beta, acting as a potent antioxidant similar in efficacy to superoxide dismutase (Lee et al., 2004). Additionally, the relatively late appearance of these proteins in disease pathogenesis, as well as the inconsistent causal

relationship between amyloid aggregation and initiation of NFT formation argue against this long-held AD dogma.

Even though this neuroprotective hypothesis has yet to gain substantial footing in amyloid research, there is a transitional tone towards anti-ACH research avenues, much of which is now centered on enhanced susceptibility to disease due to aging, genetic, and environmental factors. In other words, the complex etiology has yet again been deemed too complex for a single catalyst like amyloid to initiate the cascade. Although disheartening for many therapeutic approaches, this new perspective allows for greater acceptance of novel hypotheses to describe the muddled and seemingly compensatory nature of disease pathogenesis – even as obscure and unintuitive as a developmentally-derived proclivity to adult neurodegeneration.

1.3 Microglia

We hypothesized that the cognate cell type involved in the DOAD-related relationship for atypical development and AD vulnerabilities is microglia, the resident innate immune cell within the central nervous system (CNS). Not only do these cells shoulder nearly the entire burden of immune protection within the blood brain barrier (BBB), but also possess such phenotypic and functional variability as to direct circuitry development, provide phagocytic and trophic support, and homeostatically monitor neuronal microenvironments. Although microglia, much like amyloid, have been assigned a neurotoxic misnomer in AD pathogenesis, they may, in fact, have a more subtle, and critical, role in the developmental susceptibility to disease.

1.3.1 *Microglia Background*

Microglia are tissue-resident macrophages in the CNS, and act as first responders against infectious, inflammatory, and pathophysiological stimuli. They are unique in their biophysical independence within the CNS to respond via morphological remodeling of phenotype, highly dependent on the type and duration of stimuli (Walker et al., 2014). The functional diversity of these cells is exemplified in the heterogeneous protein expression of both ramified, mature states, as well as with the continuum of activated, often amoeboid, states (Hanisch, 2013). Microglia also vary within different areas of the brain, depending on the cytoarchitectural differences within each microenvironment to develop phenotypes to more acutely respond to region-specific demands (Olah et al., 2011). For example, the differences in microglial phenotype between white and grey matter, being longitudinally or radially branched, respectively, as well as differences in size and density (Walker et al., 2014), are reflective of the specific needs of myelin-dense regions and the complexity of factors involved in phenotypic heterogeneity. Additionally, several subtypes have been described, attributable to the fluctuations in transcription factors upon challenge (Nayak et al., 2014), demonstrating a critical intersection in the maturation and temporal regulation involved in microglial “decision-making.”

By maintaining such dynamic, highly specific, and strictly regulated phenotypic potential, microglia are capable defenders of the CNS in homeostasis and disease. But what happens when microglia themselves are subject to atypical development? In what way, if at all, does the brain adapt? To address these inquiries, the developing environment for these multifaceted cells must first be considered.

1.3.2 *Microglia within the Developing Brain*

Microglia are of peripheral mesodermal origin, as opposed to the neuroectodermal origin of neurons, astrocytes, and oligodendrocytes (Chan et al., 2007). There are three general milestones of microglial development: proliferation, migration, and differentiation into mature cells fully integrating into the healthy CNS. Microglial precursors migrate into the CNS during late embryonic and early postnatal development, and proliferate in a highly organized manner distinct from peripheral macrophages (Kierdorf et al., 2013). After birth microgliogenesis expands the pool of pre-microglia in response to interleukin 34 (IL-34), released by neurons, and colony stimulating factor 1 (CSF-1), directed by the hematopoietic transcription factor PU.1 (Salter and Beggs, 2014). The tissue-specific development and maturation of these effector parenchymal cells takes part in a stepwise fashion mimicking the developmental milestones, again segregated into three distinct transitional phases based on expression of certain genes: highly proliferative early microglia, pre-microglia involved in synaptogenesis and synaptic pruning, and fully mature adult microglia that actively participate in immune surveillance and CNS homeostasis (Matcovitch-Natan, et al., 2016). Around postnatal day (PND) 10 approximately 1/3 of microglia visibly transition from the immature, activated amoeboid state into mature, ramified phenotypes, while the other 2/3 of amoeboid microglia undergo apoptosis that parallels developmental apoptotic synaptic pruning (Parakalan et al., 2012). Microglial maturation also occurs with distinct sexual dimorphism in the timing of this transition, with the greatest number of amoeboid microglia present in males around PND 4 and in females around PND 30 (Schwarz et al., 2012).

During the postnatal period microglia are most vital to proper CNS development, but are generally considered expendable during other periods of maturation. This is likely due to the

vital role of microglia in both synaptogenesis and synaptic pruning that occurs during postnatal development, though various physiologic factors such as secretion of brain-derived neurotrophic factor (BDNF), as well as apoptotic and phagocytic factors, like signaling through the chemokine receptor CX3CR1, complement activation of CR3, and modulation of glutamatergic receptors, NMDA and AMPA (Salter and Beggs, 2014). Additionally, early microgliogenesis coincides with the first wave of synaptogenesis, around embryonic day 14-15 in rodents and before the appearance of astrocytes (Ziebell et al., 2015), suggesting early proliferation between neurons and microglia is critically interrelated. The high rate of synaptic turnover and maturation during this time creates a very specific instructive environment for microglia, and synaptic pruning via activation of microglial CD11b and DNAX activation protein 12 kDa (DAP12) immunoreceptors is required for proper neuronal maturation, circuitry formation, and healthy adult brain function (Wakselman et al., 2008; Paolicelli et al., 2011). The intracellular adaptor protein DAP12 associates with triggering receptor on myeloid cells 2 (TREM2) on microglia that mediates developmental synaptic pruning by inducing phagocytosis while concurrently down-regulating pro-inflammatory cytokine production to produce what is known as a “silent” activated microglial phenotype (Kiialainen et al., 2005). Interestingly, mutations in either TREM2 or DAP12 have been linked to a progressive form of dementia, known as Nasu-Hakola Disease (Thrash et al., 2009). The importance of the postnatal window on adult CNS plasticity has been shown in studies of environmental enrichment or alcohol exposure during this period, producing persistent effects on neurogenesis, cognitive ability, and synaptic changes (Koo et al., 2003; Klintsova et al., 2007).

Concurrent and synchronized neuronal:microglial maturation during this instructive period for both cell types guides the development of balanced signaling relationships between the two that is necessary for adult homeostasis and plasticity. This functional crosstalk regulates

critical processes, such as long-term potentiation (LTP) in the hippocampus, through a series of inhibitory connections, activity-dependent interactions, and variable release of positive- and negative-feedback molecules in a timely manner (Fig 1.1).

The continuum of microglial activation has been of particular research interest, as microglia bear the sole weight of the “CNS immune privilege” moniker (Carson et al., 2006). The activation states are very often classified by the macrophage activation terminology, M1 (pro-inflammatory) and M2 (anti-inflammatory), loosely, with considerable variation in gene expression, cytokine secretion, physiology, and surface markers between different phenotypic states. Further segmentation into states, such as M2c, M2b, and a potential M3 subcategory, highlight the extraordinary depth of responsiveness microglia possess to protect and maintain a healthy CNS environment. Additionally, ramified microglia are equally important in this endeavor, if not more so, by actively surveying the immediate microenvironment and making active contacts with neurons, which help maintain the tight regulation of inhibitory signals for microglial activation. A recent study demonstrated the neuroprotective capabilities of mature ramified microglia in a model of NMDA-induced toxicity, whereby the presence of activated microglia coincided with regional neuronal vulnerability and the presence of ramified microglia resulted in neuroprotection (Vinet et al., 2012).

1.3.3 *Microglia:Neuron Interactions in Health and Disease*

In the healthy CNS, the finely tuned functional capacity of microglia is extremely sensitive to the type, duration, and strength of stimulus due to appropriate and often redundant inhibitory signals from the immediate microenvironment, many of which derive from the neurons

themselves. Homeostatic balance is achieved via dynamic microglia:neuron crosstalk. For example, certain combinations of neuronal “off” signals to microglia cannot be present if microglia are to become activated towards a particular polarization bias, thereby protecting this post-mitotic organ with limited regenerative capabilities from a potentially neurotoxic phenotype. Likewise, damaged neurons, no longer capable of maintaining “off” signaling, can function to activate microglia. In this way the CNS limits the spread of inflammatory signaling molecules, maintains regional specificity, and develops precise support when necessary.

Microglia:neuron interactions throughout life are multifaceted, specifically at synaptic junctions, and can encompass signaling through neurotransmitters, peptides, and direct contact (Fig 1.1). As innate immune cells, microglia respond to pro-inflammatory cytokines or signaling through toll-like receptors (TLRs) to mount a localized response, as well as paracrine signaling from injured neurons and activated astrocytes through adenosine triphosphate (ATP), phosphatidylserine (PtdSer), tumor necrosis factor alpha (TNFα), nitric oxide (NO), glutamate, and remote vesicular transport of chemokine ligand 21 (CCL21), among many others (Kim et al., 2013). Moreover, microglia possess metabotropic and inotropic glutamate receptors, $GABA_B$ receptors, and adenosine receptors to monitor the activity of neurons, reflecting their integral role in the “quad-partite synapse” (Bessis et al., 2007). Direct contact with synapses also allows for frequent sampling of neuronal health, and ramified microglia will make transient connections with synapses at a rate of five minutes every hour in the healthy adult CNS (Wake et al., 2009). These ramified microglia with regional synaptic specializations are capable of modulating neurotransmitter release, neuronal activity, and even influence long-term potentiation (LTP) and long-term depression (LTD). In much the same way, neurons can influence microglial morphology and frequency of interactions through modulation of neuronal activity, such as with chronic stress (Walker et al., 2014). Thus, healthy function of one cell type promotes the

balanced, healthy interaction with the other, resulting in a multifaceted reciprocity with substantial versatility to address the unique requirements of the brain.

Synapse dynamics are of particular interest to our global research inquiry, not only due to the robust interdependence of microglia and neurons in nearly every region of the brain, but also the emerging theory that synaptic dysfunction may underlie some of the earliest molecular pathologies in AD (Du et al., 2010). Activity-dependent synaptic plasticity and refinement of neuronal circuitry contributing to overall cognitive ability is a combination of two forms of plasticity that are critically dependent on healthy microglial presence and function. The first, known as Hebbian synaptic plasticity (HSP), encompasses classic LTP/LTD activity-dependent modulation of synapse strength through early receptor activation and late protein synthesis that is the anatomical substrate parallel to memory, specifically within the hippocampus. The other form of plasticity, synaptic scaling, is a process by which homeostatic balance is maintained in dynamic, saltatory conductive cells exposed to high amounts of metabolic stress and toxic mediators. It has been suggested in recent literature that synaptic scaling abrogates positive feed-back mechanisms from inducing hyper- or hypo-excitable neuronal circuitry and gradual destabilization through dynamic AMPAR trafficking (Garay and McAllister, 2010). Notably, nearly all effects on synaptic plasticity mediated by microglia have been linked to microglial secretion of BDNF, the deprivation of which resulted in deficits in plasticity and learning (Parkhurst et al., 2013).

Adult neurogenesis in the subventricular zone (SVZ) and subgranular zone (SGZ) of the dentate gyrus is also critically instructed by appropriate microglia:neuron interactions. Microglia adopt distinct functions based on brain region, and the neurogenic niche is no exception. Following the “birth” of a granule cell (GC) neuron there exists a four week critical window of

maturation in which only a small percentage of newborn GCs become fully incorporated into the granule cell layer. Notably, microglia-dependent apoptosis and phagocytosis of non-essential immature GCs occurs within the first 1-4 days (Sierra et al., 2010), thereby promoting neurogenic homeostasis and controlling necrotic mediators from affecting neighboring cells. In addition, microglia can act as multipotent stem cells for neurons and glia, as well as provide trophic support to developing hippocampal pathways (Yokoyama et al., 2004). The Mossy Fiber Pathway (MFP), along which GC axons project to the CA3 region via non-associate LTP, is of particular interest due to the sole utilization of glutamate for non-associate LTP and the presence of balancing GABAergic interneurons, all of which are supported by region-specific microglia. Chronic reductions in neurogenesis, observed early in the pathogenesis of AD (Demars et al., 2010), has been shown to produce atypical maturation of mossy fiber axons, altered connectivity with GABAergic interneurons, and cytoarchitectural changes to the CA3 region (Schloesser et al., 2013).

In addition to GC pruning, microglial-mediated synapse homeostasis throughout the brain also includes more traditional innate immune cell-like responses, such as in the case of aging, disease, and injury. For example, circuit reorganization following acute neuronal injury is first preceded by an influx of predominantly M1-activated microglia to the area, phagocytizing debris and inducing apoptosis of unhealthy neurons to reduce the risk of excitotoxicity (Yamada et al., 2011). With tight regulation for sequence-specific functionality, microglia then adopt an M2-activated phenotype over time to promote circuitry repair by secretion of trophic factors, such as BDNF (Perry et al., 2010). Recent studies have shown the time and sequence-dependency of progression for microglial phenotypes in acute versus chronic neuronal injury, and have subsequently developed numerous models of morphological transition states (Walker

et al., 2014). How these transitions slowly develop and adapt over a lifetime after developmental injury, and to what degree one phenotype dominates over another, remain unclear.

1.4 Experimental DOAD Model of AD

In order to address these questions of atypical microglia:neuron interactions, connections between developmental immunotoxicity and AD, and phenotypes of susceptibility, we proposed a set of unified, cohesive experiments utilizing a "double-hit" model of gene x environment (GxE) interactions via postnatal toxicant exposure in a 3xTgAD mouse model of AD. The 3xTgAD transgenic mouse (B6;129-Psen1^{tm1Mpm}Tg(APPSwe,tauP301L)1Lfa/Mmjax) used in our studies progressively develops amyloid and tau molecular pathologies, specifically within the hippocampus and cerebral cortex, as well as behavioral and cognitive changes that sequentially parallel pathological progression observed in AD human brains (Sterniczuk et al., 2010). Amyloid deposition is observable by 3-4 months of age, followed by deficits in cognition and LTP by 6 months of age, and female-preferential symptomology characteristic in humans (JAX® mouse strain datasheet; Oddo et al., 2003). A recent publication by Overk and colleagues (2013) reported atypical sex steroid hormone levels in 3xTgAD mice, noting an age-related increase in male mice testosterone levels that was in direct opposition of epidemiological human data. While we did observe considerable sex differences throughout our experiments, none of our hypotheses were directly or critically related to sex steroid hormones, and instead focused on differences in sexually dimorphic brain development and parenchymal maturation prior to any putative age-related hormone discrepancies. Although we recognize this drawback in our rodent model and recommend that future studies include an alternative genetic model for comparison, we believe that the targeted approach of our experimental paradigm minimized this

minor translational conundrum. In that regard, the 3xTgAD model has been well-described and utilized in numerous studies, demonstrating decreased neurogenesis, atypical hippocampal excitability preceding overt neuronal death, and altered GABAergic interneuron populations relevant to AD neuronal dysfunction (Davis et al., 2014; Rodríguez et al., 2008).

The environment side of our GxE experimental design was addressed as postnatal toxicant exposure via oral gavage of lead acetate (Pb, 100ppm) dissolved in sterile water. This well-characterized, model toxicant was employed due to the plethora of information available on the mechanism of developmental neurotoxicity (Toscano and Guilarte, 2005), acting, in a sense, like a functional assay in itself. Additionally, Pb exposure has been correlated with amyloidogenesis and AD (Wu et al., 2008; Basha et al., 2005), as well as glial activation (Liu et al., 2015; Sobin et al., 2013; Liu et al., 2012), but there still exist significant gaps in the literature connecting Pb, Alzheimer's disease, and microglia in a Developmental Origin of Adult Disease model of Developmental Immunotoxicity to mechanistically focus on subtle, progressive dysfunction and relevant phenotypes. Likewise, although the field of AD research has slowly begun to shift away from investigating mechanisms of microglial neurotoxicity, the burgeoning research avenue of microglial senescence in the Dysfunctional Microglia Hypothesis (DMH) in aging and Alzheimer's disease, championed by Streit and colleagues (2014, 2010, 2009, 2006), has its own translational and therapeutic drawbacks. Specifically, an opinion article published by Smith and Dragunow (2014), detailing differences in microglia derived from rodents versus humans, highlighted the ineffectiveness of neurotoxic microglia-targeted therapeutics for AD that were developed based on rodent research. The authors commented that human data revealed the presence of dystrophic microglia morphologies and cytorrhexis consequent to senescence and aging, a process that does not necessarily translate well from rodents. We addressed this limitation in using an etiological approach within our DOAD rodent model,

hypothesizing accelerated aging in senescent microglia was not, itself, a pathologic catalyst, but rather a symptom of gradual dysfunction propagated by developmental immunotoxicity. Accordingly, the following set of experiments was designed to validate our model with internal corroboration, and concurrently minimize inherent translational drawbacks. As with all Socratic research models, judicious allocation of experimental parameters with biological relevance ultimately determines the degree of translational capacity.

1.5 Study Objectives and Research Hypothesis

Exponentially more toxicological studies are now contributing to a multidisciplinary knowledge base, out of which the DOAD hypothesis was derived. Despite this growth in evidentiary support, there are still considerable gaps in knowledge, both figuratively and literally, that connect early-life events to later-life health and disease. Specifically in the contended role of microglia in Alzheimer's disease, there are relatively few theories and even less data demonstrating a definitive mechanistic link between GxE interactions in atypical microglial development and the latent exacerbation of AD. **Our global hypothesis was that postnatal toxicant exposure in a mouse model of AD would disrupt neuroimmune development preferentially in females, incurring altered regulation of microglial response phenotype early in life that then functionally persists as the reduced capacity to adapt later in life, thereby promoting synaptic dysfunction and increasing susceptibility to AD.** Our overall study objectives therein were as follows:

1. Evaluate the validity and efficacy of our DOAD model of AD, and explore sex bias in a critical window of microglial development
    - Does timely Pb exposure affect microglial function months later?
    - In what way, if at all, is microglial function associated with susceptibility for classical AD molecular pathologies?
2. Investigate the putative contribution of microglia dysfunction in AD etiopathologies
    - Do microglia default on neuroprotective capabilities at the level of the synapse at later stages of pathological progression?
    - Is GxE a limiting variable in the determination of a microglial maladaptive threshold?
3. Analyze conjectural GxE contributions to DIT latency in the neuroimmune-related exacerbation of AD
    - Is there evidence for sex bias in the promotion of poor developmental conditions for neuroimmune maturation?
    - Is early epigenetic regulation of phenotypic plasticity sustained beyond cessation of exposure?
    - How are sex-biased phenotypes of susceptibility differentially influenced by type of toxicant and stage of microglial maturation?

Our first study objective is addressed in Chapter 2, to establish our Developmental Origins of Adult Disease model and verify the cognate parenchymal target utilized throughout our global research directive. In this study we hypothesized that postnatal Pb exposure would increase AD susceptibility via earlier and more severe amyloid accumulation in females

compared to males by disrupting healthy microglia function months after cessation of exposure, thereby implicating dysfunction of this innate immune cell in the pathological progression of AD within a DOAD experimental paradigm. Although the field of research of the role of microglia in AD is transitioning away from accusations that the sole resident immune cell of the central nervous system acts as an unrestrained neurotoxic mediator in aging, the majority of microglial developmental toxicity studies are still focused on priming for chronic pro-inflammatory phenotypes (Williamson et al., 2011; Bilbo and Schwarz, 2009). Consequently, our first study provides novel insight into the early correlation of non-neuroprotective microglia and GxE susceptibility in AD.

The second study objective is addressed in Chapter 3, in which we investigated the extent to which GxE interactions exacerbate the reduced capacity for microglial neuroprotection by evaluating the severity of, and maladaptation to, disrupted synapse dynamics, considered one of the earliest molecular pathologies in AD (Du et al., 2010). We hypothesized that synaptic dysfunction would occur earlier and more severely in females consequent to GxE interactions, and that maladaptive measures for microglial dysfunction and reduced neuroprotection would occur preferentially in these mice. Through the inclusion of a wildtype (WT) comparison and later pathological time points, we were able to investigate disruptions to both glial- and immune-related functions of microglia as alterations to healthy microglia:neuron crosstalk, with greater clarity and specificity at the synapse, as well as GxE interactions on capacity for compensation. In demonstrating female-specific reductions in adaptability for microglia:neuron crosstalk, this study underscored an important link between a GxE female specificity with early microglial maladaptation, a potential catalyst for the senescence phenotype observed in AD human microglia. Furthermore, it prompted a final inquiry into how and why this unbalanced microglial phenotype was promoted during development, and what was the mechanistic driver of latency.

Accordingly, our final study objective, addressed in Chapter 4, was to investigate early derivations of sex bias and epigenetic catalysts of maladaptive microglia:neuron crosstalk. We hypothesized transgenic female mice exposed postnatally to Pb would preferentially develop a detrimental microRNA profile for interrelated neuroimmune maturation, thereby re-patterning response phenotypes for subtle imbalances between the two cell types later in life and limiting adaptability. Thus, we explored epigenetic reprogramming of developmental phenotypic plasticity, and delineated a previously unreported sensitive period of female susceptibility for neuroimmune maladaptation. In addressing the global research directive, the current set of distinct, cohesive experimental studies aimed to address significant knowledge gaps in the relationship between GxE interactions and DOAD models of AD, as well as the role of microglia in AD, through utilization of a targeted, macroscopic-to-microscopic approach, and careful experimental design.

Fig. 1.1. Microglia:neuron crosstalk is mediated via contact, neurotransmitters, and various signaling molecules. Graphical schematic summary depicting some of the molecular actors of information flow between microglia and neurons. (adapted from Kim et al., 2013 and Bessis et al., 2007)

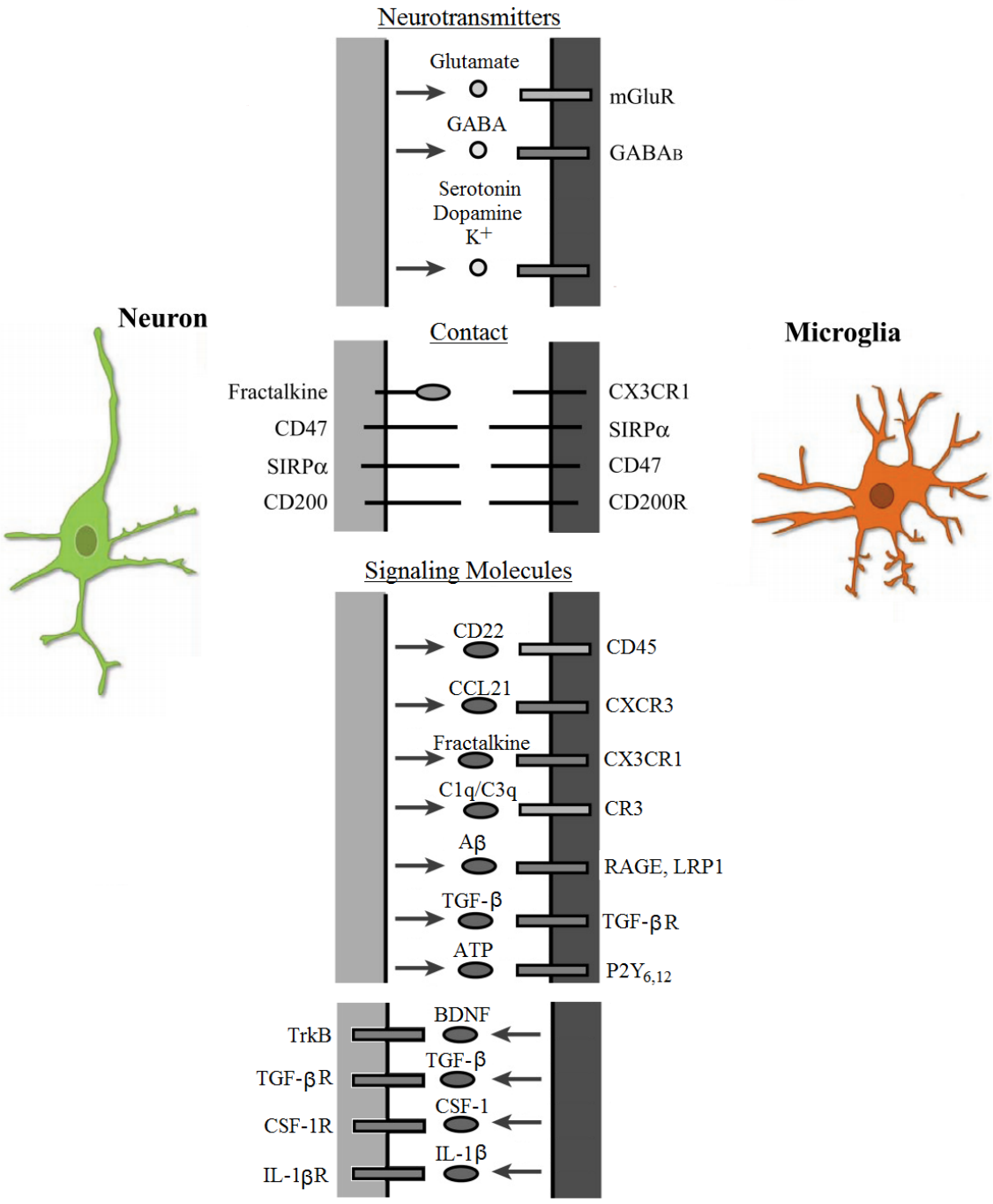
Neurotransmitters
Glutamate
mGluR
GABA
GABAB
Serotonin
Dopamine
K+
Neuron
Contact
Microglia
Fractalkine
CX3CR1
CD47
SIRPα
SIRPα
CD47
CD200
CD200R
Signaling Molecules
CD22
CD45
CCL21
CXCR3
Fractalkine
CX3CR1
C1q/C3q
CR3
Aβ
RAGE, LRP1
TGF-β
TGF-βR
ATP
P2Y6,12
BDNF
TrkB
TGF-β
TGF-βR
CSF-1
CSF-1R
IL-1β
IL-1βR

Chapter 2:

Developmental toxicant exposure in a mouse model of Alzheimer's disease induces differential sex-associated microglial activation and increased susceptibility to amyloid accumulation

2.1 Introduction

Recent studies of the developmental origins of adult disease (DOAD) hypothesis have demonstrated that early life events may contribute to the pathogenesis of many adult diseases, including Alzheimer's disease (AD) and other neurodegenerative diseases (Bilbo, 2010; Miller and O'Callaghan, 2008; Basha et al., 2005; Barker, 2004). One system at risk from these early life events is the immune system. The developing immune system is highly sensitive to exogenous insults and can be associated with systematic changes that persist into adulthood (DeWitt et al., 2012). These persistent effects have been associated with pediatric diseases, and are predictive of later-life disease onset (Dietert and Zelikoff, 2009). However, little headway has been made to uncover the myriad mechanisms and systemic interactions that underlie the risk of adult disease following an early life insult.

Microglia, the innate immune cells of the central nervous system (CNS), are thought to be potential targets of developmental disruption, subsequently contributing to a variety of adult diseases within the CNS (Streit et al., 2014; Harry and Kraft, 2012). These neuroimmune cells have a multitude of homeostatic functions in the developing brain, including promoting synaptogenesis and synaptic pruning (Santambrogio et al., 2001). Likewise, they are the first responders to brain injury, pathogens, and toxicants through a sensitive, stimuli-dependent

response typically involving a phenotypic change to an activated state (Olah et al., 2011; Gehrmann et al., 1995). The role of microglia in neurodegenerative diseases, however, is unclear in the later stages of pathology, and even less is known about their potential contribution to the developmental origins of these diseases. Furthermore, as the exact mechanism of developmental microglial dysfunction in AD is unknown, the methods of analysis are similarly lacking (Walker and Lue, 2015).

The brain undergoes sexually dimorphic development that, in part, is thought to be due to the direct involvement of microglial activation; thus, specifically-timed disruption of this tightly regulated signaling may result in sex-dependent susceptibility to AD and other neurodegenerative disorders (Lenz et al., 2013). As females are at greater risk of developing AD correlation to periods of distinct developmental sexual dimorphism is of particular interest. In this study, we investigated the role of microglia in the etiopathology of AD as a consequence of early toxicant exposure during a critical window of development for microglia, defined by microglia-driven postnatal brain development during this time. The prototypical toxicant utilized during this critical window was lead acetate, a well-defined developmental immuno- and neurotoxicant, at a physiologically relevant dose to mimic an acute, low-level exposure to environmental lead. This time-sensitive dosing paradigm was applied in a genetically predisposed mouse model for AD (3xTgAD) to assess the pathological consequences of early toxicant exposure. An advantage to this “double-hit” model is that we could more clearly differentiate increased vulnerability to AD, as evidenced by earlier or more severe pathological markers, consequent to precise postnatal disruption of neuroimmune-relevent development. In addition, the 3xTgAD mouse model was reported to exhibit female bias in amyloid accumulation similar to that in humans, increasing the translational power of the model and interpretation of sex-specific results (Carroll et al., 2010). We hypothesized that microglia would become

activated in a sex-dependent manner following early postnatal lead exposure and that this change in activation would be inversely correlated with earlier or more severe AD pathologies, suggesting an early role for microglia in the pathological progression of AD.

Here we demonstrate the utility of this double-hit DOAD model, specifically in the context of the developing neuroimmune parenchyma and microglia, in detecting early changes involved in the pathophysiology of AD. We report that postnatal toxicant exposure increased AD pathologies in females to a greater extent than in males, and that this may be correlated with early disruption of female microglia functionality.

2.2 Materials and Methods

2.2.1 *Animal handling*

All experimental animal handling and dosing was carried out in accordance with procedures approved by the East Carolina University Institutional Animal Care and Use Committee (IACUC). Pregnant transgenic dams (3xTgAD; B6;129-Psen1^{tm1Mpm}Tg(APPSwe,tauP301L)1Lfa/Mmjax) were obtained from the seed colony in the ECU Department of Comparative Medicine and kept on a 12:12 hour light/dark cycle, with access to food and water ad libitum. Litters were culled to six after birth (postnatal day, PND 1), weaned at PND 21, and housed by sex in groups of no more than three.

2.2.2 *Dosing and tissue preparation*

Dosing solution concentration of lead acetate was prepared weekly (100 ppm in sterile water, at 10 µL • g-1 body weight • day-1; Sigma-Aldrich, St. Louis, MO, USA), and dosing was performed based on daily body weight. This concentration was determined based on rodent model toxicity and risk assessment recommendations (Moser et al., 2005; Zoetis and Walls, 2005), as well as previous reports of long term potentiation impairment due to microglial activation following exposure to Pb at this concentration (Liu et al., 2012). From PND 5-15, neonates were dosed with lead acetate (Pb) or vehicle (ctl) once per day using a modified gavage technique (Butchbach et al., 2007). No overt signs of lead-induced toxicity, such as changes in body weight, or behavioral abnormalities such as decreased feeding or huddling, were observed in any of the animals. One mouse per sex, litter, and treatment group was euthanized at either PND 50, 90, or 180. These terminal endpoints were chosen based on reports of the 3xTgAD mouse strain displaying amyloid beta immunoreactivity as early as three months of age (Oddo et al., 2003). Sample sizes included 3-6 mice/sex/age/exposure. Immediately following euthanasia, the brain was carefully removed and hippocampi dissected in ice cold PBS. For histochemical analysis, hippocampi were fixed for 24 hours in 10% neutral buffered formalin followed by 70% ethyl alcohol before paraffin embedding. For flow cytometric analysis, the remaining brain tissue sans cerebellum was placed in FACS buffer (3% FCS, 0.1% sodium azide, and 10mM EDTA in PBS) for subsequent homogenization the same day as extraction.

2.2.3 *Flow cytometry*

Brain tissue was homogenized in a 15 mL Tenbroek glass homogenizer and filtered through a 70 µm nylon mesh filter. Myelin removal was accomplished via centrifugation in 30%

isotonic Percoll (GE Healthcare, Uppsala, Sweden), and the fatty layer was removed from the top of the cell suspension. Cells were then resuspended in blocking buffer (5% normal mouse serum, 5% normal rat serum, 1% Fcr block [polyclonal anti-mouse IgG CD16/32; eBioscience Inc., San Diego, CA, USA] in FACS buffer) and incubated for 10 minutes. Cells were passed through a 40 µm nylon mesh filter, centrifuged, resuspended in incubation buffer (10% FBS, PBS), and incubated with the following primary antibodies for one hour: APC-conjugated CD11b (1:100, rat monoclonal IgG2b kappa [M1/70]; Abcam, Cambridge, MA, USA) and FITC-conjugated CD45R (1:100, rat monoclonal IgG2a kappa [C363.16A]; eBioscience). Following incubation, cells were centrifuged, resuspended in FACS buffer, and read using a BD Accuri C6 flow cytometer (BD Biosciences, Franklin Lakes, NJ, USA). A total of 10,000 events were recorded. Color compensation was performed using isotype controls, and quadrants were determined based on fluorescence minus one (FMO) positive controls. Figure 2.1a depicts the gating schematic used to differentiate resident microglia ($CD45^{lo}$) from peripheral macrophages ($CD45^{hi}$). The data were analyzed using the BD Accuri C6 software (BD Biosciences), and are represented as the mean CD11b mean fluorescence intensity (MFI) ± SEM.

2.2.4 *Immunohistochemistry*

Formalin-fixed, paraffin-embedded (FFPE) hippocampi were sliced on a rotary microtome at 5 µm and mounted on Superfrost Plus slides (Azer Scientific, Morgantown, PA, USA). Briefly, slides were dewaxed in Histo-Clear II (Electron Microscopy Sciences, Halfield, PA, USA), followed by washes in 100% and 95% ethyl alcohol and PBS. Antigen unmasking was accomplished using a heat-mediated citrate buffer, followed by incubation in 0.3% hydrogen peroxide for 30 minutes. All subsequent staining was performed using Sequenza-Coverplate racks (Thermo Scientific, Waltham, MA, USA). Sections were permeabilized with

TPBS and blocked with diluted normal serum (ABC Vectastain; Vector Laboratories, Burlingame, CA, USA). Slides were then incubated with primary antibody, ionized calcium binding adaptor molecule 1 (Iba1, 1:500; Wako Chemicals USA, Inc., Richmond, VA, USA), for 60 minutes at room temperature or overnight at 40˚C. Sections were visualized using ABC Vectastain and DAB kits (Vector Laboratories) and counterstained with Harris' Alum Hematoxylin. After sequential washing in ethyl alcohol and Histo-Clear, slides were coverslipped with Permount (Fisher Scientific, Fair Lawn, NJ, USA) and cured overnight prior to visualization.

Slides were visualized using a Leica DM1000 light microscope at 20x magnification with a SPOT^{TM} Idea camera attachment and SPOT Advanced Imaging software. Two regions of interest (ROI) per hippocampal section were selected at random, with the viewing frame containing as much tissue as possible, and the % immunopositive microglia/ROI was analyzed using ImageJ (Schneider et al., 2012). All data are represented as the mean percent microglia density per ROI ± SEM.

2.2.5. *Immunofluorescence*

FMO control optimizations, the use of fluorphores with relatively distinct emission spectra, and a sequential double staining immunofluorescence procedure were utilized to reduce cross-reactivity and spectral bleed-through. Slide dewaxing, rehydration, and antigen retrieval were performed in a similar manner to immunohistochemistry. Slides were blocked with 10% donkey serum in TPBS for 30 minutes at room temperature, followed by a one-hour incubation with primary antibody for amyloid-β (1:1000, rabbit pAb; Abcam). Subsequent incubation with Cy5-conjugated secondary antibody (1:1000, goat anti-rabbit IgG-Cy5; Abcam)

was performed and cell nuclei were stained with DAPI (300 nM; Life Technologies, Eugene, OR, USA). Slides were coverslipped with ProLong Gold antifade reagent (Life Technologies), cured for 24 hours, and stored upright protected from light.

Hippocampal sections were visualized with a Zeiss LSM 700 laser scanning confocal microscope with the EC Plan-Neofluar 10x/0.30 M27 objective. Two counting frames per animal (640.17 µm x 640.17 µm) were used for ROIs. Amyloid load density was defined as % amyloid beta + immunoreactivity/ROI area, and the two ROIs were averaged per animal. Fluorescence intensity was considered positive over the background fluorescence threshold. Data are represented as mean ± SEM.

2.2.6 *Statistical analysis*

All analyses were performed using Statistical Analysis System (SAS Institute, Cary, NC, USA). Two-way analysis of variance (ANOVA) for sex and exposure effects was performed for immunohistochemistry and flow cytometry at each age. Individual pairwise comparisons between sex within treatment and between treatments within sex were made with a t-test or a Tukey's studentized range distribution method. All data in bar charts are represented as mean ±SEM. $p < 0.05$ was used to define statistical significance.

2.3 Results

2.3.1 *Developmental Pb exposure increased microglial activation only in males at PND 50*

To determine how toxicant exposure during a critical window of development altered microglia and markers of AD, we employed two techniques to assess microglial activation: upregulation of activation surface markers with flow cytometry and microglial density with immunohistochemistry.

Flow cytometry was carried out using markers of microglial/macrophage activation, CD45 and CD11b (Nikodemova and Watters, 2012; Stevens et al., 2001; Ford et al., 1995; Sedgwick et al., 1991). $CD45^{lo}$ microglia were discriminated from peripheral macrophages (Fig. 2.1a), and CD11b expression was used to determine activation and general functionality, as CD11b (CR3A) is part of the innate complement system and involved in phagocytosis, migration, and chemotaxis (Kobayashi et al., 2013; Roy et al., 2006). Microglial activation was higher in Pb-exposed males than in females at PND 50, with Pb-exposed female microglial responsiveness comparable to ctl mice (Fig. 2.1b). By PND 90, the sex difference in Pb-exposed mice was still detectable, but there was no change in CD11b expression between ctl and Pb mice of either sex at PND 90 and 180.

The hippocampus is vulnerable to damage with AD, and associated with amyloid beta deposition and accumulation in the 3xTgAD mouse model (Oddo et al., 2003). Therefore, microglial activation within this region of the brain was assessed at three time points (Fig. 2.2a). To determine microglial abundance and activation, hippocampi were stained for Iba1, a general marker for microglia. As more infiltrating microglia would increase overall density, and activated microglia take up more space due to enlarged somas and thickened processes, microglial density was used as a general maker for neuroprotective microglial presence (Schwarz et al., 2012). Immunohistochemical evaluation indicated that Pb-exposed male mice had greater

microglial density than the ctl males at PND 50, and Pb-exposed females had significantly lower microglial density than Pb-exposed males (Fig. 2.2b). Female mice had consistently lower microglial density at all time points, with Pb-exposed females differing significantly from Pb-exposed males at the earliest (PND 50) and latest (PND 180) time points.

2.3.2 *Developmental Pb exposure increased amyloid-β load density*

Amyloid-β load density, encompassing both immature aggregates of amyloid deposits as well as later plaque formation, was used to determine changes in AD pathological severity. Immunofluorescent evaluation of FFPE hippocampi revealed increased amyloid density in Pb-exposed females at PND 50 but not in Pb-exposed males, indicative of increased pathological severity due to an earlier appearance of amyloid deposits compared to 3xTgAD controls (Fig. 2.3b). At PND 90 Pb exposure increased amyloid density in both males and females, with the first appearance of diffuse plaque-like amyloid aggregates only seen in the Pb exposed groups (Fig. 2.3a, insets). By PND 180 the 3xTgAD controls had detectable plaques and increased amyloid density. Likewise, Pb-exposed animals also exhibited mature, hollow plaques, but to a greater degree than controls at the latest time point. There were no differences between control males and females at any time point. PND 180 could be considered relatively early in the 3xTgAD pathological progression; there have been previous reports of virtually no detectable plaques in 4-6 month 3xTgAD hippocampi and no discernable sex difference in plaque number until 13-14 months (Overk et al., 2013). However, this is contrasted by the Pb-exposed females that had significantly increased amyloid burden at PND 50, and a general trend towards greater pathology than males at all time points (Fig. 2.3b). Altogether, Pb exposure during a critical window of postnatal development increased amyloid burden and AD pathology in both males

and females at later time points. Furthermore, Pb-exposed females were affected earlier (PND 50) than Pb-exposed males (PND 90), potentially contributing to the sex-related bias seen in AD.

Fig. 2.1. Developmental Pb exposure increased CD11b expression in males at PND 50. There was no observable change in CD11b associated with Pb exposure at PND 90 and 180. (a) Representative flow cytometric plots and gating schematic for discrimination of doublets, live/dead and peripheral macrophages ($CD45^{hi}$, $CD11b^{+}$). (b) Bar graphs depicting CD11b expression as a result of early Pb exposure at PND 50, 90 and 180 in males and females. n = 3–6 mice/sex/age/exposure. Data are presented as mean ± S.E.M. $p<0.05$ was considered statistically significant compared with age-matched control values. * = significant between exposure, # = significant between sex. PND, postnatal day; FSC, forward scatter; SSC, side scatter; MFI, mean fluorescence intensity; ctl, control; Pb, lead.

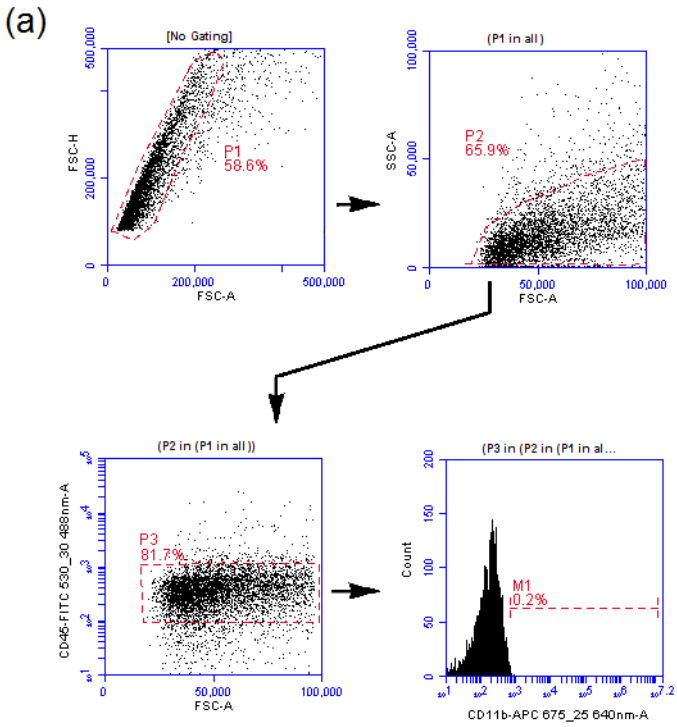
(a)
[No Gating]
FSC-H
FSC-A
P1
58.6%
(P1 in all)
SSC-A
FSC-A
P2
65.9%
(P2 in (P1 in all))
CD45-FITC 530_30 488nm-A
FSC-A
P3
81.7%
(P3 in (P2 in (P1 in al...
Count
M1
0.2%
CD11b-APC 675_25 640nm-A

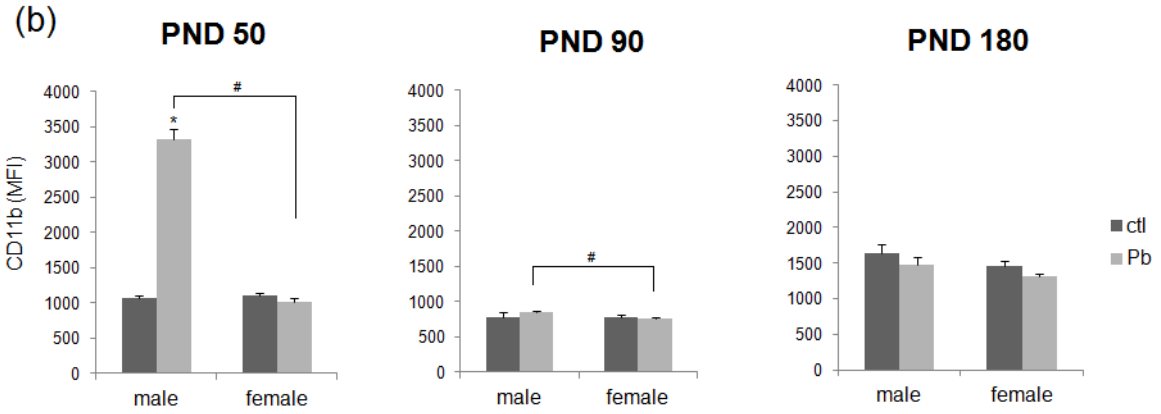
(b)
PND 50
PND 90
PND 180
CD11b (MFI)
male
female
ctl
Pb

Fig. 2.2. Developmental Pb exposure increased microglial density in males at PND 50, as assessed by ionized calcium-binding adapter molecule 1 (Iba1) + immunohistochemistry (IHC) and semiquantitative morphometric analysis of activation state. Ctl males at PND 50 and 90 had greater microglial density than females, whereas at PND 180, Pb-exposed males had higher density than females. (a) Representative images of microglial density at PND 50, 90 and 180 in the hippocampus of control- and Pb-treated male mice. Scale bar = 50 μm. (b) Bar graphs representing IHC morphometric analysis of microglial density at PND 50, 90 and 180 in males and females. n = 3 mice/sex/age/exposure. Data are presented as mean ± S.E.M. $p< 0.05$ was considered statistically significant compared with age-matched control values. * = significant between exposure, # = significant between sex. ROI, region of interest; ctl, control; Pb, lead acetate.

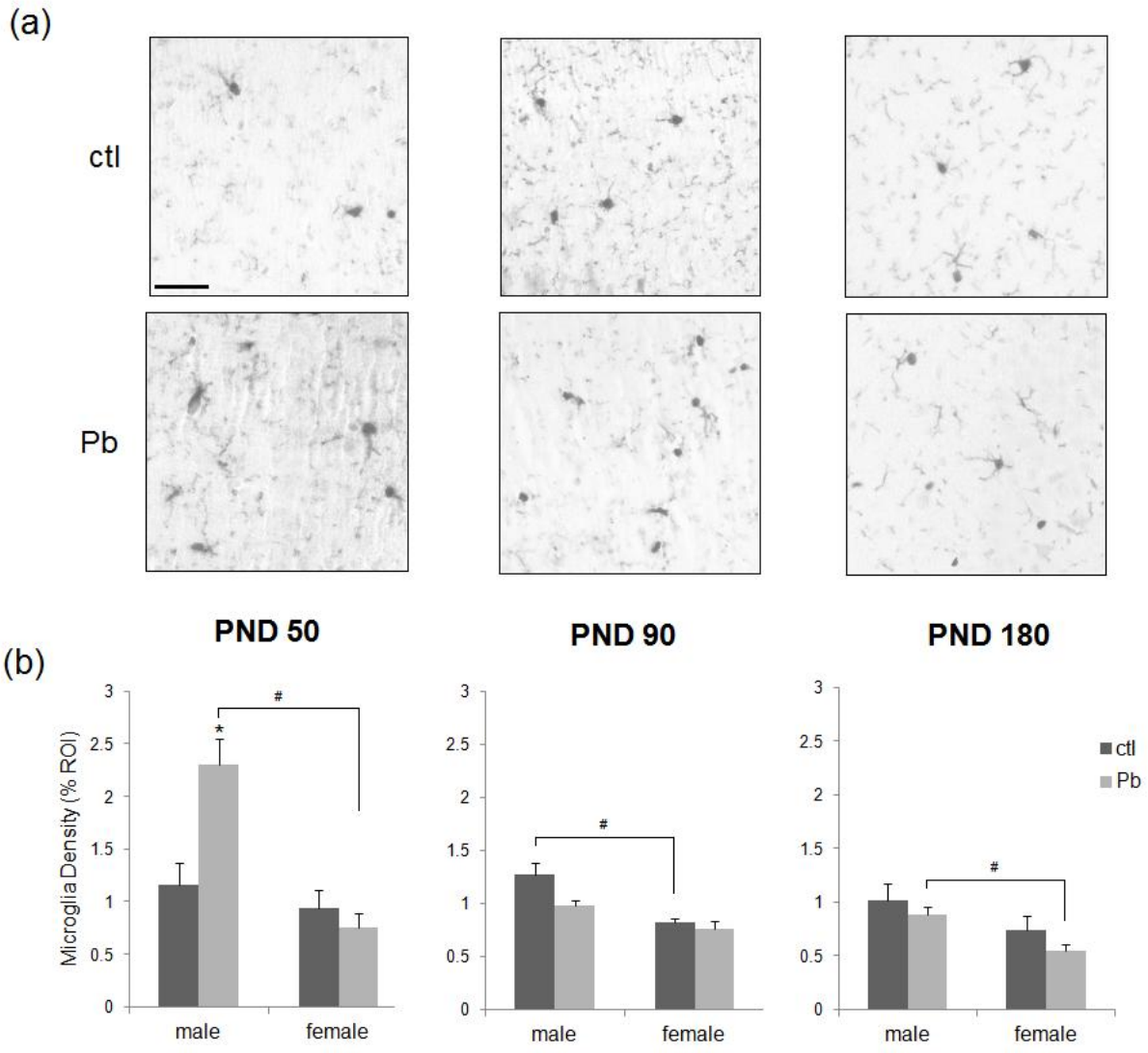
(a)
ctl
Pb
(b)
PND 50
PND 90
PND 180
Microglia Density (% ROI)
male
female
ctl
Pb
*
#

Fig. 2.3. Developmental Pb exposure increased amyloid density in the hippocampus of male and female triple transgenic murine model for AD (3xTgAD) mice at PND 90 and PND 180, and only in females at PND 50. (a) Representative immunofluorescence images of amyloid-β immunoreactivity at PND 50, 90 and 180. Insets, representative plaques that progressed from dense clusters (PND 90) to more mature, hollow configurations (PND 180). Scale bar = 50 μm. (b) Summary graphs of amyloid density at each time point. Data are represented as mean density ± S.E.M. n = 3 mice/sex/age/exposure. $p<0.05$ was considered statistically significant compared with age-matched control values. * = significant between exposure, # = significant between sex. ROI, region of interest; ctl, control; Pb, lead acetate; PND, postnatal day.

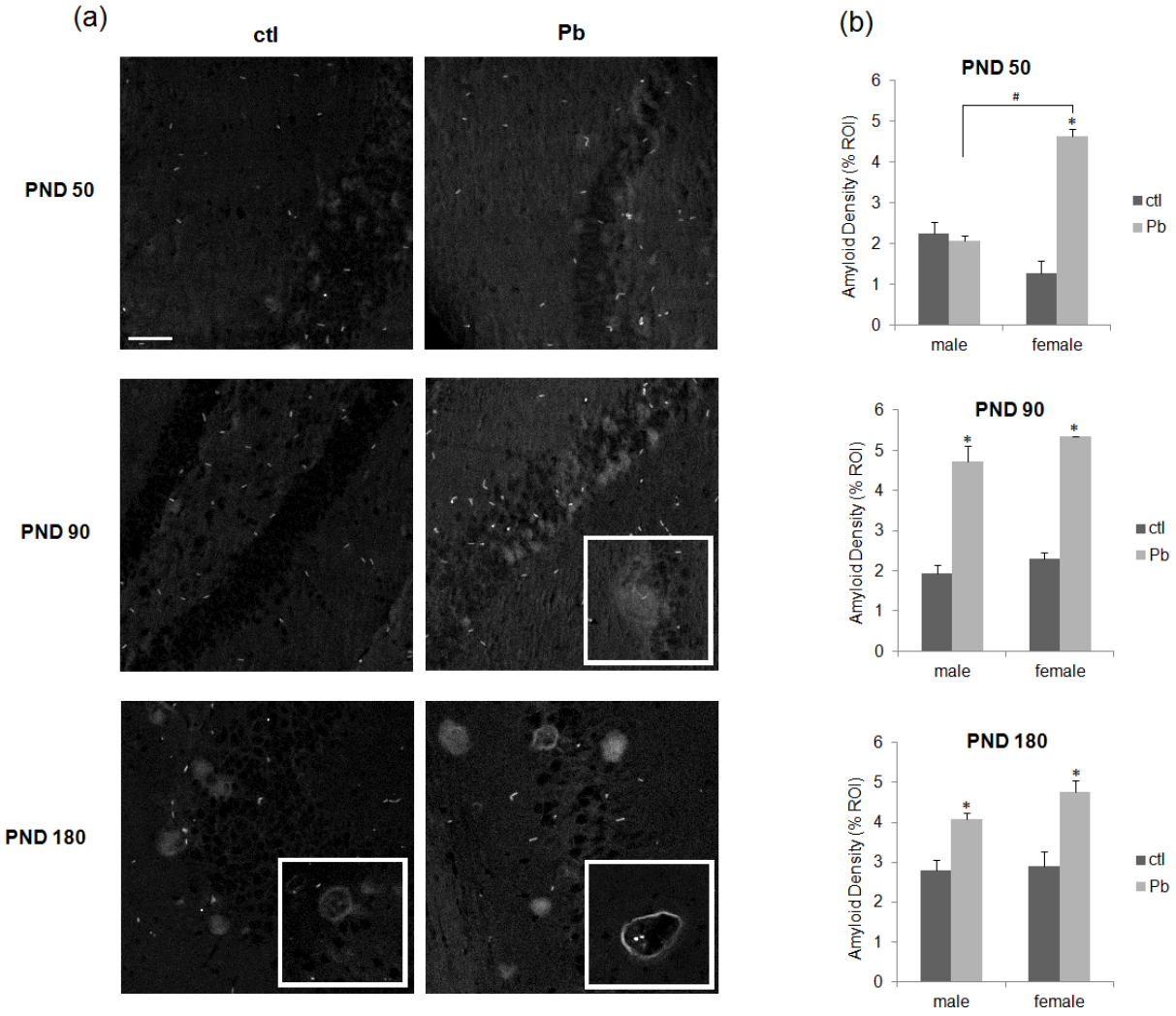
(a)
ctl
Pb
PND 50
PND 90
PND 180
(b)
PND 50
PND 90
PND 180
Amyloid Density (% ROI)
male
female
ctl
Pb
#
*

2.4 Discussion

Previous studies have established a correlation between microglia and AD, many of which interpret the pathological role of microglia as an inflammatory propagator due to increased overall activation (Solito and Sastre, 2012; Hooper et al., 2009; El Khoury et al, 1998; Banati et al., 1993). The gaining momentum of DOAD hypotheses has propelled investigations into microglial priming and altered inflammatory sensitivity following a developmental immune insult as potential contributors to adult disease (Perry and Teeling, 2013; Krstic et al., 2012; Leifer and Dietert, 2001; Wu et al., 2008). However, there is a disjointed understanding of this early role for microglia, particularly in neurodegenerative diseases, due to a lack of standardized markers for the various states of activation, compounded by numerous disease models and conflicting data collection time points (Walker and Lue, 2015; Olah et al., 2011). In this study, we investigated the role of early toxicant exposure during a critical window of development for microglia in the exacerbation of AD pathologies. Our results support the utility and validity of this DOAD exposure paradigm, namely through demonstrating a persistent change in pathological severity months after exposure. Furthermore, our results demonstrate a sex-related vulnerability seen only in females at early stages of AD that are paralleled by the sex differential in early microglial responsiveness following Pb exposure. As microglial proliferation and activation were once thought to contribute to pathology, this correlation highlights the necessity of utilizing DOAD models to better define the putative role of microglia in AD.

During normal brain development activated microglia migrate, proliferate, and mature to a ramified morphology by PND 28 (Nayak et al., 2014). Developmental microglial activation is functionally distinct from activation in the adult CNS due to its critical role in neuronal

synaptogenesis and pruning, the absence of which can result in the development of atypical brain circuitry (Paolicelli et al., 2011). This perinatal critical window of microglial development may be further temporally segmented, varying in susceptibility by sex. Both rodent and human brains develop in a sexually dimorphic manner, and microglia are critical to this process through various feedforward mechanisms, such as those involving estrogens and prostaglandins (Lenz et al., 2013; Schwarz and Bilbo, 2012). Likewise, microglial-mediated processes, such as phagocytosis and proliferation, also proceed in surges that temporally vary in concert with steroid hormone signaling (Lenz and McCarthy, 2015). At PND 4, male mice experience a testosterone surge that coincides with a peak in microglia numbers in various brain regions like the hippocampus, whereas female mice experience this microglial migration and proliferation later in development, around PND 21 (Crain et al., 2013; Schwarz et al., 2012). Although there are data to suggest females are less vulnerable to long term changes compared to males following early postnatal infection (Bilbo, 2010), sex-related microglial vulnerability may be more dependent on the concentration and type of toxicant rather than timing only. Our results demonstrate an increase in amyloid-β burden in Pb-exposed mice, with female mice exhibiting greater and earlier pathological severity associated with developmental toxicant exposure (Fig. 2.3). The Pb-related exacerbation of pathology was not seen in male mice at PND 50. An inverse sex bias was also present at PND 50 for markers of microglial activation, with greater microglial responsiveness in Pb-exposed males than females (Fig. 2.1 and 2.2), implying the early heightened microglia responsiveness in males likely was neuroprotective against signs of AD neuropathology. Conversely, the detectable sex differences at PND 50 supports the identification of a window of vulnerability for female microglia during a period of development previously mainly attributed to male vulnerability. The mechanisms by which females were more vulnerable than males may be consequent to the low concentration of Pb (100 ppm) and later exposure window (PND 5-15) used in our study.

A recent study by Sobin et al. reported atypical and differential microglial disruption depending on a high (330 ppm) or low (30 ppm) postnatal exposure to Pb, with no evidence of neuroinflammatory propagation at PND 28. Furthermore, dose-dependent reduction in microglia numbers correlated with decreased dentate gyrus volume, suggesting reduced later-life resiliency and cognitive function. This contrasts sharply with many investigations into the role of microglia in developmental Pb exposure paradigms that implicate microglia as propagators of bystander neuronal death and neuroinflammation (Kumawat et al., 2014; Liu e tal., 2012; Zurich et al., 2002; Bunn et al., 2001). Our results provide a similar early glimpse into microglial disruption following acute, low levels of Pb. By PND 90 Pb-exposed males still had higher CD11b expression compared to females, but by PND 180 there was no sex- or Pb-related effect detectable (Fig. 2.1). This could be due, in part, to latent and persistent neurotoxicity, resulting in male microglia eventually developing a similar dysfunctional phenotype to females over time; CD11b-associated phagocytosis decreased and amyloid deposition increased. As an alternative, there could be fewer total numbers of microglia present to differentiate from controls. However, although Pb-exposed females had lower microglial density at PND 180 than males, there was no significant difference between control and Pb-exposed mice at that time in either sex (Fig. 2.2). Further studies are warranted to determine sex differences in microglial functionality, if any, at later stages of AD.

Increases in amyloid density following developmental Pb exposure persisted over time, although there was no direct age-related correlation with markers of microglial activation. This suggests that if there were a causative role for microglia in pathological exacerbation, as our results imply, it would occur very early in pathological progression. Many AD studies that evaluate microglia function typically do so at later time points, after pathology has been well

established, producing conflicting data in terms of how the presence of microglia changes amyloid pathology. For example one study showed prevention of neuronal loss and no change in amyloid-β plaques following selective microglial elimination, while another demonstrated that formation and maintenance of amyloid-β plaques were not influenced by the presence or absence of microglia (Spangenberg et al., 2016; Grathwohl et al., 2009). Conversely, the colocalization of activated microglia with senile plaques has been extensively cited, with the pro-inflammatory phenotype frequently implicated as the major instigator of chronic inflammation and neurotoxicity in AD (Marlatt et al., 2014; Bolmont et al., 2008; Hickman et al., 2008; Combs et al., 2001; Stalder et al., 1999; Banati et al., 1993; Cras et al., 1990). Our data support the inverse association between microglial activation and early pathological exacerbation, inferring changes in classical markers of inflammation, such as IL-1β, TNF-α, and iNOS, evaluated at a single point in time may not necessarily indicate a causative role for microglial inflammation in AD. Had we evaluated time points only at PND 90 or later, when the 3xTgAD model was anticipated to exhibit cognitive decline (Oddo et al., 2003), any sex differences or correlations with microglial activation would not have been as significant or detectable, as developmental damage to microglia would have already occurred. This could potentially contribute to the mass of conflicting reports for the role of microglia in AD, or even account for the inefficiencies of NSAIDs as AD therapeutics.

Along with demonstrating a link between very early microglia dysfunction and exacerbated amyloid burden, our results revealed a female bias in early susceptibility to AD following postnatal Pb exposure. For both amyloid density and microglial activation, the sex-related bias was most significant at PND 50, suggesting an early role for microglia. Our exposure window, at the overlap of previously established male/female microglial windows of vulnerability, as well as the relatively low concentration of Pb, likely contributed to the increased

susceptibility in females via steroid hormones, imbalances in neuronal apoptosis and neurogenesis, or even changes in transcriptional regulation of microglial activation. Additional studies to determine how steroid hormones skew microglia to varying responses throughout life and how early-life toxicants disrupt this process are warranted.

The role of microglia in the developmental etiopathology of AD is unclear and, as shown here, complicated by a variety of intrinsic factors, like sex biases and mechanistic roles, as well as extrinsic factors, such as appropriate models, exposure scenarios, and timing of data collection. Here, we attempted to characterize a standardized double-hit model for exploring the role of microglia in the developmental origins of AD following early postnatal Pb exposure. The results indicated that microglia are activated by postnatal toxicant exposure in a sexually dimorphic manner, with activation in males at the earliest time point coinciding with greater neuroprotection against amyloid accumulation. Likewise, the critical window of Pb exposure used in this study defined a period of female microglial vulnerability and correlated with earlier pathological severity, suggesting that microglia likely are early contributors to AD via dysfunctional responsiveness to pathological stimuli and impaired neuroprotectiveness. Further investigations are warranted to determine the causative versus correlational role for microglia in AD, and the mechanisms of early sex bias to disease progression.

Chapter 3:

Evidence of sex bias in microglial and synaptic susceptibility to Alzheimer's disease following postnatal toxicant exposure

3.1 Introduction

The etiology of certain adult neurodegenerative diseases, such as Alzheimer's disease (AD), may stem from atypical brain development, as a variation of the developmental origin of adult disease (DOAD) hypothesis (Mathew and Ayyar, 2012). Sex-biased CNS diseases, such as autism spectrum disorders, schizophrenia, and AD, can be traced back to sex-specific genes and distinct stages of sexually dimorphic brain development (Shi et al., 2016). Additionally, studies of early-life immune activation demonstrate persistent effects of atypical development on later-life cognitive endpoints and sex biases (Bilbo, 2010; Schwarz and Bilbo, 2012). As the resident innate immune cells of the central nervous system (CNS), microglia have been implicated in several nervous system disorders, but the correlation between postnatal microglial dysfunction and their role in the development of sex-biased neurodegeneration is not well understood.

In highly complicated disease pathologies with etiologies that potentially arise from immune dysfunction over a lifetime, the likelihood of waves of compensation is greatly increased. Moreover, the transition from adaptive to maladaptive responses characteristic of a lifetime-long etiology is of particular importance with microglia, which are critical to neuronal homeostasis and adult neurogenesis. We have previously reported that postnatal exposure to a model neurotoxicant, lead acetate (Pb), not only preferentially increased disease susceptibility

in females, but also correlated with decreased microglial activation (vonderEmbse et al., 2017). This suggests a gene x environment-mediated vulnerability related to microglial neglect or dysfunction may be consequent to interference with the closure of a critical window of development for integrated microglia and neuronal maturation, persisting into adulthood. Furthermore, as this relatively acute, low dose exposure is severe enough to exacerbate AD pathologies and alter microglia months after exposure cessation, the exposure paradigm is more analogous to the formation of unfavorable developmental conditions promoting adaptation for survival.

In the current study, we investigated patterns of timing and fluctuations for hallmarks of microglial dysfunction, as well as synapse dishomeostasis, considered one of the earliest molecular pathologies in AD (Du et al., 2010; Masliah et al., 2001). To assess beneficial vs detrimental adaptation, we analyzed neuroprotective, functional endpoints for microglia, as well as cognate neuronal markers. Microglia function was measured using surface expression markers for activation polarization skew for M1:M2 to determine relative shifts in polarization, and neuroprotective capabilities were analyzed via expression of the iron sequestration molecule, ferritin. Likewise, neuronal consequences were measured through the trophic receptor, tyrosine kinase B (TrkB), as well as synaptic proteins, SNAP25 and synaptophysin. We hypothesized that the combination of both genetic proclivity and postnatal toxicant exposure, as a DOAD model of gene x environment interactions, would preferentially increase female susceptibility to synaptic aberrations due to dysfunctional microglia. Furthermore, this dysfunctional phenotype would be evident through later-life alterations in functional endpoints for microglia, homeostatic signaling molecules between microglia and neurons, and synaptic proteins critical to processes known to be perturbed early in AD.

The postnatal exposure window utilized in this study corresponds to a critical window of development for neuronal and microglial maturation, as well as maturation of synaptic receptors in the hippocampus critical to long term potentiation (LTP), synaptic plasticity, and adult neurogenesis (Bessis et al., 2007; Garay and McAllister, 2010). By perturbing this dual learning and maturation period via low levels of Pb, the neuroimmune parenchyma is critically and persistently altered; beyond interference with closure of this critical window of development, the resulting phenotype could manifest as abnormal neuronal wiring patterns, atypical epigenetic regulation, and re-patterned functional phenotypes.

Our purpose in the current study was to delineate markers of dysfunction in microglia:neuron crosstalk originating during atypical development, and integrating the timeline of maladaptation to known pathological markers in a genetic model of AD. By utilizing this model of postnatal gene x environment interactions, we propose a novel analysis of early, sexually dimorphic microglial dysfunction in AD, and interrelated functional endpoints with synaptic aberrations.

3.2 Materials and Methods

3. 2.1 *Animal handling*

All experimental animal handling and dosing was carried out in accordance with procedures approved by the East Carolina University Institutional Animal Care and Use Committee (IACUC). Pregnant wildtype (SFN) and transgenic dams (3xTgAD; B6;129-Psen1^{tm1Mpm}Tg(APPSwe,tauP301L)1Lfa/Mmjax) were obtained from the seed colony in the ECU

Department of Comparative Medicine and kept on a 12:12 hour light/dark cycle, with access to food and water ad libitum. Litters were culled to eight after birth (postnatal day, PND 1), weaned at PND 21, and separated by sex into cages of no more than four animals/cage.

3.2.2 *Dosing and tissue preparation*

Dosing solutions of lead acetate (100 ppm) dissolved in sterile water were prepared weekly. From PND 5-10 neonates were dosed with lead acetate or vehicle once per day using a modified gavage technique (Butchbach et al., 2007). One mouse per sex, litter, and treatment group was randomly assigned and euthanized at PND 120, 180, or 240. As per ethical use protocol, animals were euthanized with isoflurane and decapitation, and the brain was carefully removed and hippocampi dissected in ice cold phosphate buffered saline (PBS). For histochemical analysis the left hippocampi was fixed for 24 hours in 10% neutral buffered formalin followed by 70% ethyl alcohol before paraffin fixation. For flow cytometric analysis the remaining left hemisphere sans hippocampus was placed in FACS buffer (3% fetal calf serum (FCS), 0.1% sodium azide, and 10mM ethylenediaminetetraacetic acid (EDTA) in PBS) for subsequent homogenization. The right hemisphere and cerebellum were minced and slowly frozen in cryopreserve (0.32 M sucrose, 10% dimethyl sulfoxide (DMSO), PBS) for Western blot analysis.

3.2.3 *Flow cytometry*

Papain (~200 U/mL) was activated 30 min prior to use at 37˚C with activation buffer (1.1 mM EDTA, 0.067 mM β-mercaptoethanol, 5.5 mM L-cysteine). The left hemisphere sans

hippocampus was gently minced and enzymatically digested with activated papain (20 U/mL) for 20 min at 37˚C. Enzyme halt buffer (20% FBS, PBS) was added, and the homogenate was filtered through a 70 µm nylon mesh filter before centrifugation at 1000 g for 5 min. Myelin removal was accomplished via resuspension in 30% isotonic Percoll (GE Healthcare, Uppsala, Sweden) and centrifugation at 500 g for 20 min. Brain homogenates sans myelin were then resuspended in RBC Lysis Bufer (eBioscience, San Diego, CA, USA) for 10 min and passed through a 40 µm nylon mesh filter. Briefly, cells were washed with FACS buffer (3% FCS, 0.1% sodium azide, 120 mM EDTA) twice with a series of resuspensions and centrifugations at 1000 g for 5 min. Following analysis for yield and viability, samples were aliquoted to $1x10^5$ cells/tube in incubation buffer (10% FBS, PBS) for 30 min on ice. The following primary antibodies (1:100) were added for 30 min at 4˚C, protected from light: CD86-PE and CD209-APC (abcam). Following incubation, cells were washed with PBS and centrifuged at 350 g for 5 min, resuspended in PBS, and read using a BD Accuri C6 flow cytometer (BD Biosciences, Franklin Lakes, NJ, USA). A total of 10,000 events were recorded per sample. Doublet exclusion and live/dead gating was performed, and quadrant crosshairs were determined via fluorescence minus one (FMO) positive controls. The data are represented as the log-transformed fold change of ratio of the % $CD86^+$ to $CD209^+$ cells.

3.2.4 *Immunohistochemistry*

Formalin-fixed, paraffin-embedded (FFPE) hippocampi were sliced on a rotary microtome at 16 µm and mounted on Superfrost Plus slides (Azer Scientific, Germany). Briefly, slides were dewaxed in Histo-Clear II (Electron Microscopy Sciences, Halfield, PA), followed by washes in 100% and 95% ethyl alcohol and PBS. Antigen unmasking was accomplished using

a heat-mediated citrate buffer, followed by incubation in 0.3% hydrogen peroxide for 30 minutes. All subsequent staining was performed using Sequenza-Coverplate racks (Thermo Scientific, Waldorf, Germany). Sections were permeabilized with PBS with Tween 20 (TPBS) and blocked with diluted normal serum (ABC Vectastain; Vector Laboratories, Burlingame, CA, USA). Slides were then incubated with anti-ferritin primary antibody (1:1000; Abcam, Cambridge, MA, USA), for 60 minutes at room temperature or overnight at 4˚C. Sections were visualized using ABC Vectastain and diaminobenzidine (DAB) kits (Vector Laboratories) and counterstained with Harris' Alum Hematoxylin. After sequential washing in ethyl alcohol and Histo-Clear slides were coverslipped with Permount (Fisher Scientific, Fair Lawn, NJ, USA) and cured overnight prior to visualization.

Slides were visualized using a Leica DM1000 light microscope at 20x magnification with a SPOT^{TM} Idea camera attachment and Advanced Imaging software. Two regions of interest (ROI) per animal were chosen at random along the dentate gyrus, with the viewing frame containing as much tissue as possible. Immunopositive ferritin reactivity was determined via FIJI (Schindelin et al., 2012) analysis over a predetermined background threshold and color deconvolution. The % area ferritin^{+}/ROI was determined and averaged per animal, and results are represented as the mean ± SEM.

3.2.5 *Immunofluorescence*

Slide dewaxing, rehydration, and antigen retrieval were performed in a similar manner to immunohistochemistry. Following insertion into the Sequenza racks and two-5 min washes with TPBS, slides were incubated with blocking buffer (10% donkey serum, 0.1% Triton X-100, PBS)

for 60 minutes at room temperature. Overnight incubation at 4˚C was carried out with the primary antibody cocktail, diluted in blocking buffer: TrkB (4 µg/mL, rabbit anti-mouse IgG; Abcam) and Iba1 (1:200, goat anti-mouse pAb; Abcam). Sections were washed twice with TPBS, and the secondary antibody cocktail, diluted in TPBS, was applied for 60 min protected from light: AlexaFluor555-conjugated donkey anti-rabbit (1:500, Abcam) and FITC-conjugated donkey anti-goat (1:500, Abcam). Nuclei were stained with 4',6-diamidino-2-phenylindole (DAPI, 1.5 µM; Life Technologies, Eugene, OR, USA) and, after two washes with PBS, treated with TrueBlack Lipofuscin Autofluorescence Quencher (Biotium, Fremont, CA, USA) for 30 seconds. Briefly, slides were washed and coverslipped with ProLong Gold antifade reagent (Life Technologies), left to cure for 24 hours, and stored upright protected from light.

Hippocampal sections were visualized with a Zeiss LSM 700 laser scanning confocal microscope with the EC Plan-Neofluar 10x/0.30 M27 objective. The dentate gyrus (DG) and CA3 region were identified based on standardized hippocampal landmarks, and two counting frames per region (150 µm x 97 µm) were used as the ROI. Fluorescence intensity was considered positive over a predetermined threshold above background fluorescence. Data are represented as mean relative fluorescence intensity ± SEM.

3.2.6 *Western blot*

3.2.6.1 Synaptosome preparation

Crude synaptosomal fractions (P-2) were prepared from minced, cryopreserved right hemispheres and cerebellums. Frozen tissue was quickly thawed in a warm water bath and centrifuged at 1000g for 5 minutes at 4˚C. The supernatant was discarded and the pellet was

resuspended in Homogenization Buffer, consisting of protease inhibitor cocktail (Halt™ Single-Use, Thermo Scientific, Rockford, IL, USA), three parts PBS, and one part 4x Gradient Buffer (1.28M sucrose, 4mM EDTA, 20mM Tris, pH 7.4). Briefly, tissue was homogenized in a chilled 15 mL Tenbroeck glass homogenizer and centrifuged at 1000g for 10 minutes. The supernatant was then collected and further centrifuged at 10,000g for 20 minutes, and the remaining pellet was considered the P-2 synaptosome fraction. Aliquots of the P-2 fraction were either immediately analyzed or routinely cryopreserved at -80˚C until further analysis.

3.2.6.2 Protein concentration and Western blotting analysis

The P-2 fraction was resuspended in PBS and total protein concentration was determined with BCA Protein Assay (Thermo Scientific). Synaptosomes were diluted to 10 µg/mL in NuPAGE LDS reducing agent, LDS sample buffer (Invitrogen, Carlsbad, CA, USA), and denatured on a 70˚C heating block for 10 minutes. Samples were then electrophoresed on 10% Bis-Tris Mini Gels (Invitrogen) and transferred onto a 0.45 µm nitrocellulose membrane. Following overnight incubation with constant agitation in Blocking Buffer (Rockland, Gilbertsville, PA, USA), membranes were probed for one hour with the appropriate primary antibodies (Abcam) in Blocking Buffer with 0.1% Tween-20: either SNAP25 (0.02 µg/mL, goat pAb) or synaptophysin (1:500, mouse mAb), with beta actin (1:10,000, rabbit pAb). Membranes were washed four times with TPBS for 5 minutes each and incubated for one hour with the cognate secondary antibody cocktail (1:25,000; Li-Cor, Lincoln, NE, USA) diluted in Blocking buffer and 0.1% Tween-20: either donkey anti-rabbit IRDye 680RD and donkey anti-goat IRDye 800CW, or goat anti-rabbit IRDye 680RD and goat anti-mouse IRDye 800CW. Membranes were washed four times with TPBS and once with PBS for 5 minutes each, left to dry for at least 24 hours,

and read on a Li-Cor Odyssey CLx. Densitometric quantification was performed using Li-Cor Image Studio™. Results are expressed as fold change over sex- and age-matched vehicle-treated controls corrected for equal loading to beta actin.

3.2.7 *Statistics*

All analyses were performed using Statistical Analysis System (SAS Institute, Cary, NC, USA). Two-way analysis of variance (ANOVA) for sex and age effects was performed for each strain for microglial polarization, treatment and sex effects for each age and strain for ferritin and TrkB analysis, and treatment and age effects for each sex for synaptic protein expression. Individual pairwise comparisons were made with a t-test or a Tukey's studentized range distribution method. All data in bar charts are represented as mean ±SEM. $p < 0.05$ was used to denote statistical significance.

3.3 Results

3.3.1 *Postnatal Pb exposure persistently altered microglial polarization profiles*

Microglia were characterized from brain homogenates via flow cytometry to evaluate functional alterations in their activation profiles using CD86 and CD209 as M1- and M2-associated surface markers, respectively (Fig 3.1a). The M1:M2 ratio was used to describe a microglial activation skew towards a more pro-inflammatory, M1-like profile, or anti-inflammatory and M2-like. Postnatal Pb exposure elicited an M2 skewed microglial phenotype in Tg females

compared to controls at PND 120, while both WT males and females, as well as Tg male mice, exhibited activation profiles with greater M1 skew (Fig 3.1b,c). Although microglia gradually adopt a pro-inflammatory phenotype over time due to aging-related factors (Lee et al., 2013), these effects were not yet seen in these younger mice, and there was a general trend towards M2 polarization bias compared to strain-, age-, and sex-matched controls over time. This trend occurred earlier in WT mice compared to Tg mice at PND 180. By the latest time point, Tg females had adopted a strongly M2-like activation profile compared to controls (Fig 3.1b).

3.3.2 *Pb-exposed 3xTgAD females exhibited reduced iron sequestration over time*

To further assess microglial function and health, we evaluated the hippocampus, a region of the brain particularly vulnerable to AD pathologies, for expression of the iron sequestration protein, ferritin. Isolated ferritin expression, although indicative of neurotoxic iron in the immediate microenvironment, is also an indicator of microglial neuroprotective capabilities to sequester potentially neurotoxic agents (Kaneko et al., 1989). Ferritin expression was highly localized along the mossy fiber pathway, specifically around the dentate gyrus hilus and CA3 subregions (Fig 3.2a,b).

At PND 120, weeks following the cessation of Pb exposure, ferritin expression was increased in Tg mice, with greater ferritin immunoreactivity in the hippocampi of Tg males compared to females (Fig 3.3a,d). Moreover, total ferritin expression decreased over time in Pb-exposed WT mice and Tg females, but increased in Tg males at PND 240 (Fig 3.3). Although Tg females developmentally exposed to Pb had decreased overall ferritin expression at PND 240, there were detectable ferritin crystallite aggregates, plaque-associated and otherwise (Fig

3.2c-e, Fig 3.3d), suggesting the reduction in total expression seen in all three groups might not be functionally equivalent.

3.3.3 *Pb-exposed 3xTgAD females exhibited earlier, more extensive synaptic protein aberrations compared to males*

To determine the implications of Pb-induced microglial dysfunction on synaptic endpoints, synaptosomes were evaluated for altered levels of the presynaptic proteins synaptophysin and SNAP25, involved in synaptogenesis and vesicular fusion, respectively. Both synaptophysin and SNAP25 were significantly reduced at PND 120 in Pb-exposed Tg females (Fig 3.4a,c), whereas males exhibited reductions in only synaptophysin at this earliest time point (Fig 3.4d). By PND 240, however, there were reduced levels of both proteins in Pb-exposed Tg males, whereas females recovered synaptophysin levels and significantly increased SNAP25 compared to PND 120 levels. Interestingly, at PND 240 the western blots revealed the presence of SNAP25 cleavage products in both control and Pb-exposed mice (Fig 3.4).

3.3.4 *TrkB expression in the CA3 hippocampal subregion is reduced over time in a sex-dependent manner*

To investigate trophic synaptic signaling between microglia and neurons, immunofluorescence was used to evaluate expression of TrkB in the CA3 subregion of the hippocampus (Fig 3.5a). Ionized calcium binding adaptor molecule 1 (Iba1) was also used to identify microglia within the hippocampus (Fig 3.5b). In 3xTgAD mice, developmental Pb

exposure increased TrkB expression at PND 120 (Fig 3.6a). TrkB expression in WT mice was also significantly altered at PND 120, with increased TrkB expression in males but decreased TrkB in females (Fig 3.6b). For all four groups this trend was reversed at PND 180. Notably, by the latest time point CA3 TrkB expression was significantly depleted in Tg males (Fig 3.6c). However, Tg females at PND 240 had comparable levels of TrkB to the control, whereas in WT females TrkB was decreased.

Fig. 3.1. Developmental Pb exposure persistently altered microglial polarization profiles, differentially based on sex. (a) Representative gating schematic and flow cytometry output plots. (b,c) Quantification of CD86:CD209 expression ratio as mean ±SEM log-transformed fold change over to age-, sex-, and strain-matched controls. n = 3-9 mice/sex/age/treatment/strain. $p < 0.05$ was considered statistically significant. * = significant among ages. # = significant between sex. PND: postnatal day, WT: wildtype, FSC: forward scatter, SSC: side scatter.

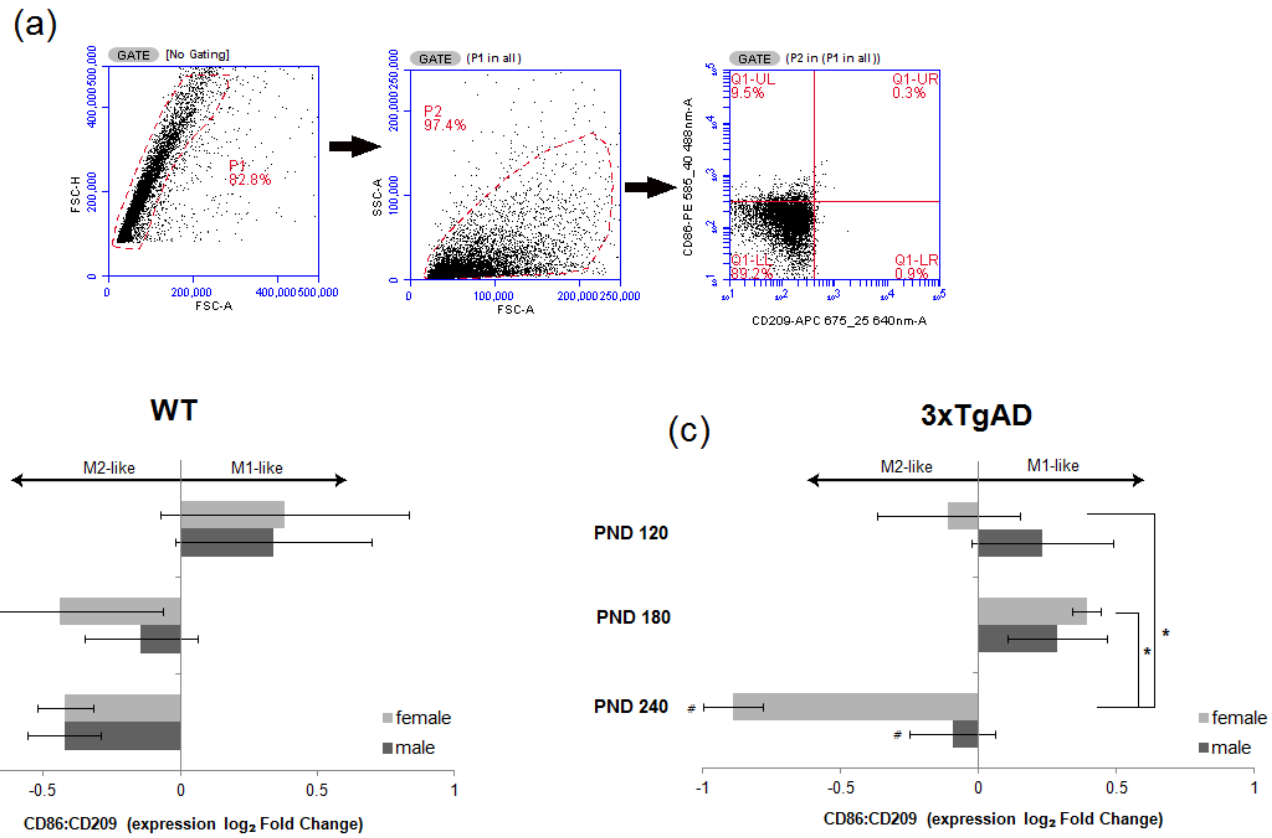
(a)
GATE [No Gating]
P1
82.8%
FSC-H
FSC-A
GATE (P1 in all)
P2
97.4%
SSC-A
FSC-A
GATE (P2 in (P1 in all))
Q1-UL
9.5%
Q1-UR
0.3%
Q1-LL
89.2%
Q1-LR
0.9%
CD86-PE 585_40 488nm-A
CD209-APC 675_25 640nm-A
(b)
WT
M2-like
M1-like
PND 120
PND 180
PND 240
female
male
CD86:CD209 (expression log2 Fold Change)
(c)
3xTgAD
M2-like
M1-like
PND 120
PND 180
PND 240
*
*
#
#
female
male
CD86:CD209 (expression log2 Fold Change)

Fig. 3.2. Ferritin expression is localized to the hilus and CA3 subregions of the hippocampus. (a,b) Representative images of ferritin expression patterns along the mossy fiber pathway, with higher densities in the hilus (a) and terminal CA3 regions (b). (c,d) Representative image of ferritin crystallite aggregate formations (c, arrow), some of which were associated with plaque-like structures (d, inset). (a,c-d) scale bar = 44 µm, (b) scale bar = 70 µm. OML: outer molecular layer.

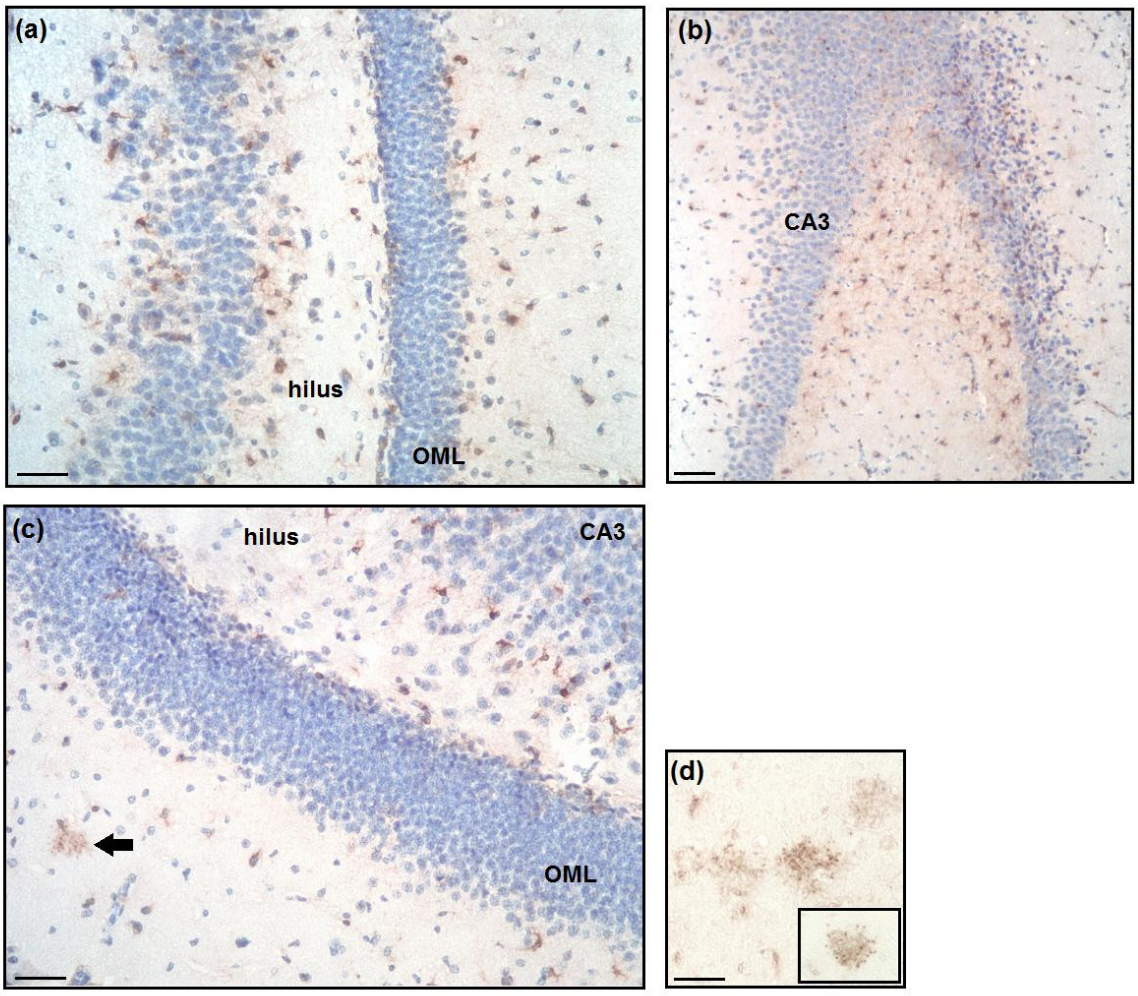
(a)
hilus
OML
(b)
CA3
(c)
hilus
CA3
OML
(d)

Fig. 3.3. Developmental Pb exposure increased hippocampal ferritin expression, moreso in Tg males compared to females. (a-c) Quantification of ferritin immunoreactivity at PND 120 (a), PND 180 (b), and PND 240 (c), expressed as mean % ROI ±SEM. (d) Representative images of Pb-exposed Tg female (left column) and male (right column) hippocampal CA3 regions at PND 120 (top row) and PND 240 (bottom row). n = 3-10 mice/sex/age/treatment/strain. *$p < 0.05$ was considered statistically significant. Scale bar = 60 µm. PND: postnatal day, ROI: region of interest, WT: wildtype, Tg: 3xTgAD transgenic, ctl: control.

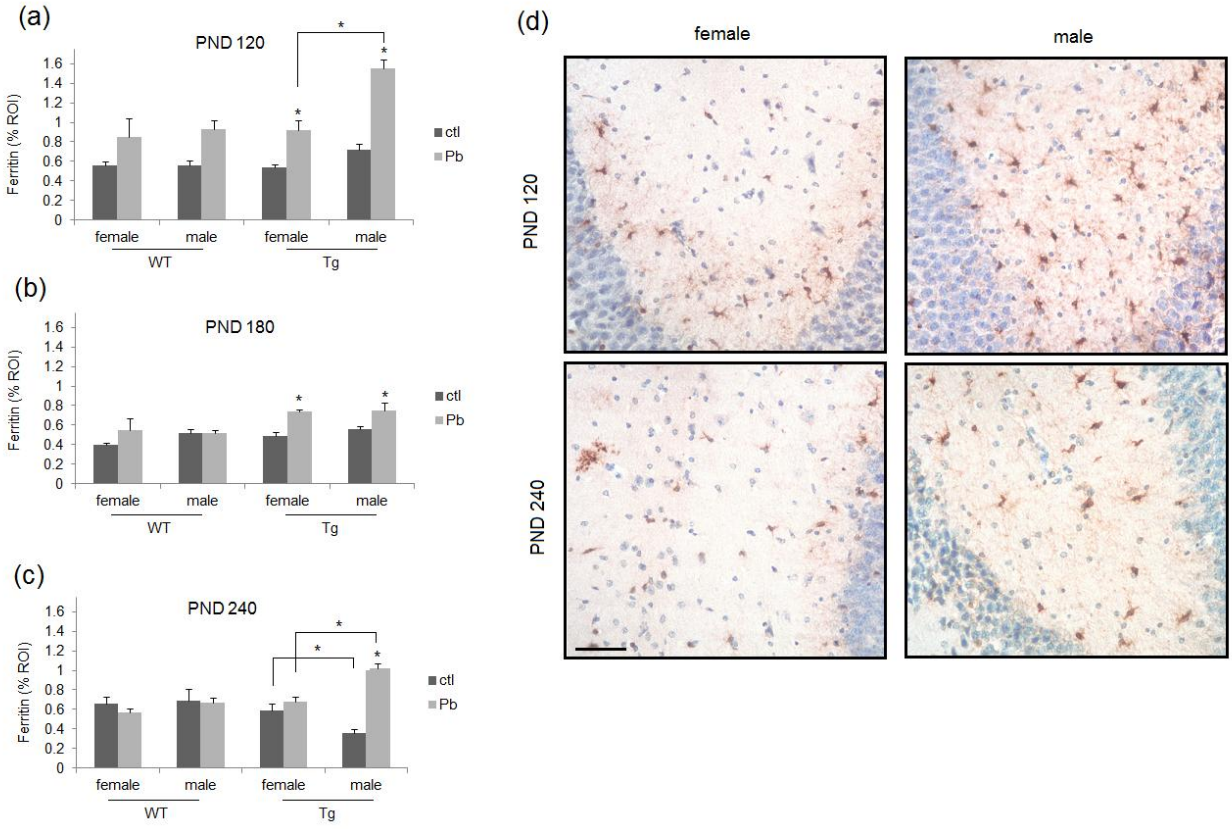
(a)
PND 120
Ferritin (% ROI)
ctl
Pb
female
male
female
male
WT
Tg
(b)
PND 180
(c)
PND 240
(d)
female
male
PND 120
PND 240

Fig. 3.4. Developmental Pb exposure altered expression of synaptic proteins SNAP25 and synaptophysin over time in 3xTgAD mice. (a-d) Quantification and representative western blots for synaptosomal SNAP25 (a-b) and synaptophysin (c-d) expression in 3xTgAD females (a,c) and males (b,d). Data are represented as mean fold change over sex-, age-, and treatment-matched controls ±SEM. n = 3 mice/sex/age/treatment. *$p < 0.05$ was considered statistically significant. PND: postnatal day, ctl: control.

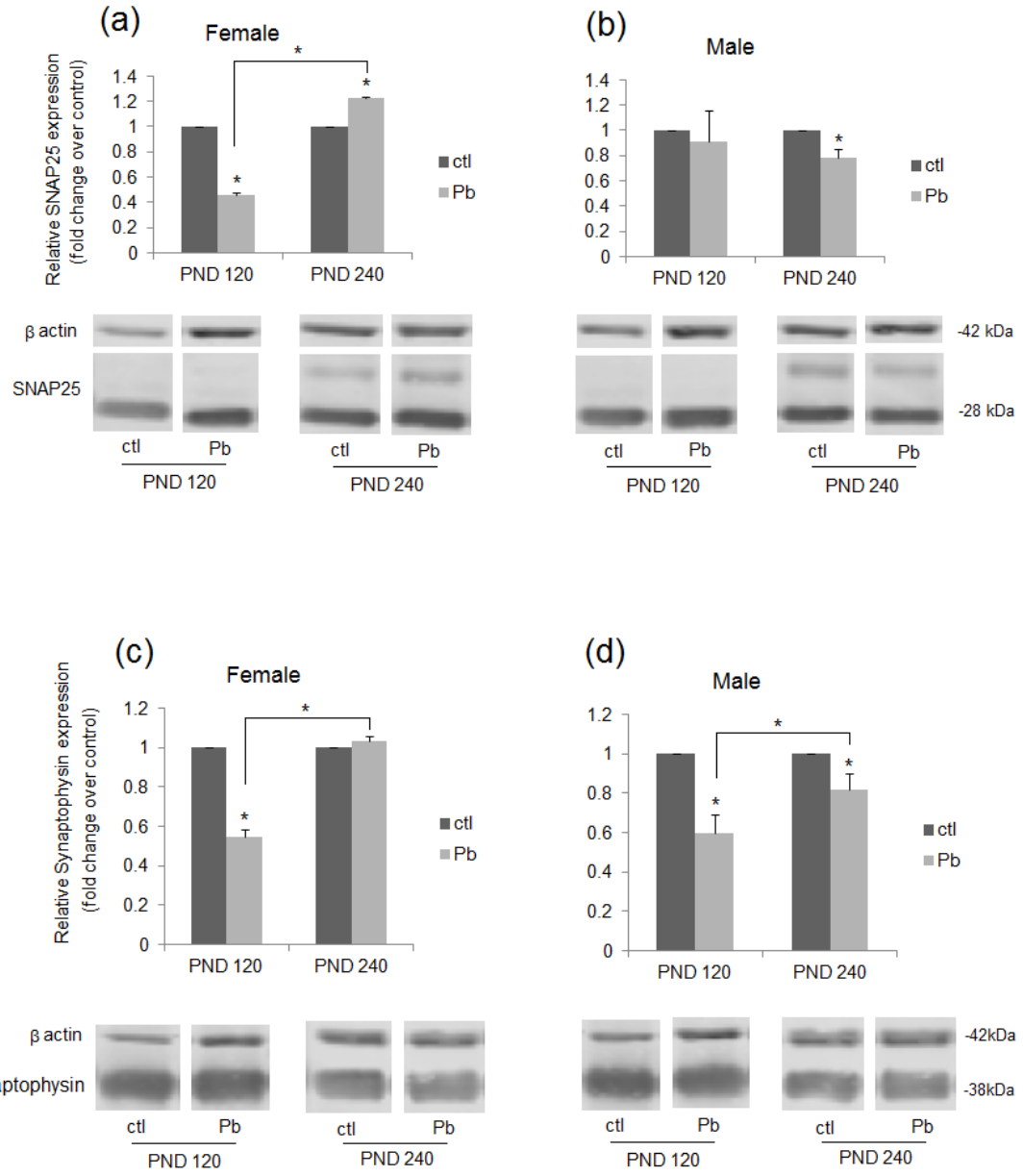
(a)
Female
Relative SNAP25 expression
(fold change over control)
1.4
1.2
1
0.8
0.6
0.4
0.2
0
PND 120
PND 240
ctl
Pb
β actin
SNAP25
ctl
Pb
PND 120
PND 240
(b)
Male
-42 kDa
-28 kDa
(c)
Female
Relative Synaptophysin expression
(fold change over control)
synaptophysin
(d)
Male
-42kDa
-38kDa

Fig. 3.5. TrkB expression in the CA3 subregion of the hippocampus. (a) Representative image of TrkB expression along the hippocampal CA3 region in relation to Iba1 and DAPI staining. (b) Representative staining intensities of TrkB (red), DAPI (blue), and Iba1 (green), as well as merged image of all three colors. (a) scale bar = 95 µm, (b) scale bar = 73 µm.

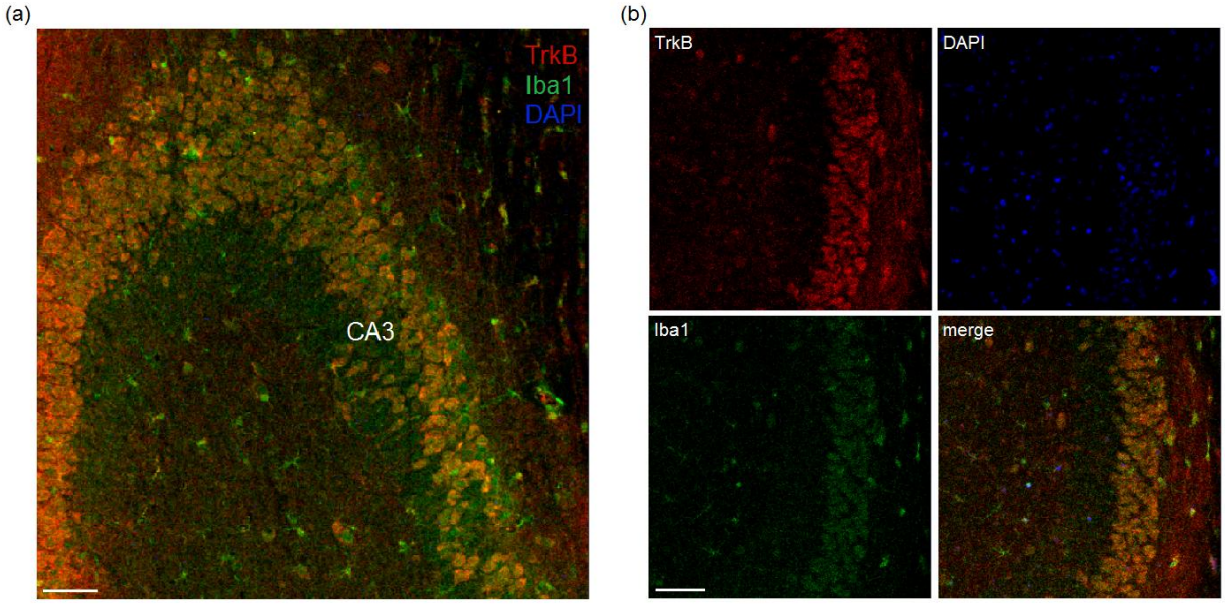
(a)
TrkB
Iba1
DAPI
CA3
(b)
TrkB
DAPI
Iba1
merge

Fig. 3.6. Developmental Pb exposure altered TrkB expression in the CA3 subregion of the hippocampus. (a-b) Quantification of TrkB expression for female and male WT (a) and 3xTgAD (b) mice in the CA3 region. (c) Representative images of TrkB expression in control (far left column) and Pb-exposed (middle and far right columns) mice. Data are represented as mean relative fluorescence intensity ±SEM. n = 3-5 mice/sex/age/treatment. Scale bar = 54 µm. *p < 0.05 was considered statistically significant. PND: postnatal day, ctl: control, ROI: region of interest.

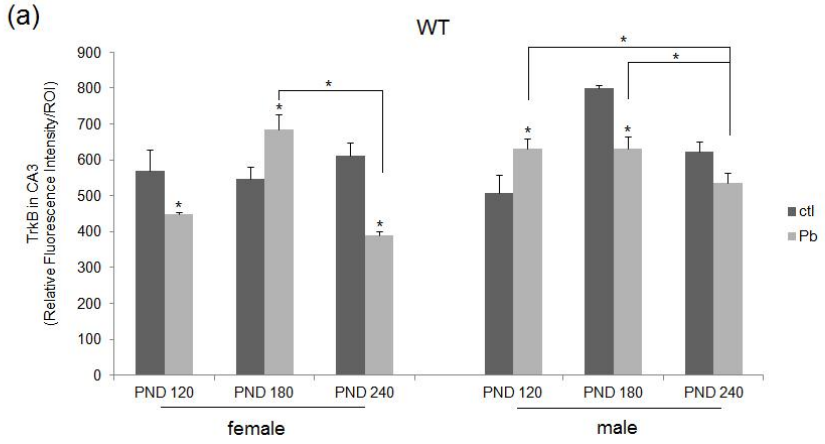
(a)
WT
TrkB in CA3
(Relative Fluorescence Intensity/ROI)
900
800
700
600
500
400
300
200
100
0
ctl
Pb
PND 120
PND 180
PND 240
PND 120
PND 180
PND 240
female
male

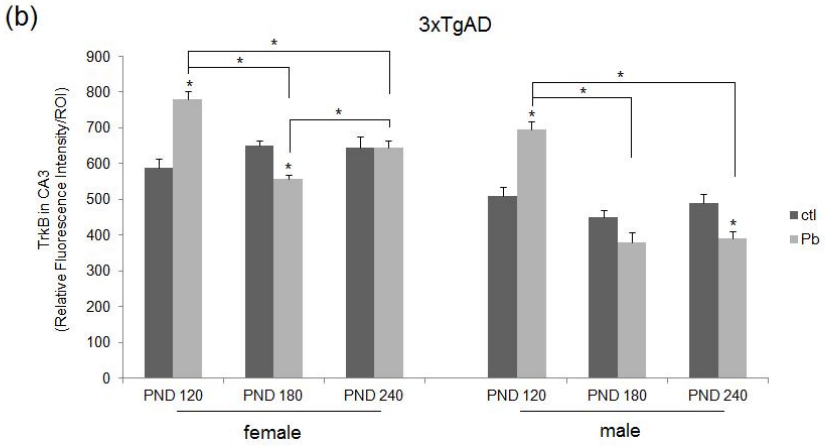
(b)
3xTgAD
TrkB in CA3
(Relative Fluorescence Intensity/ROI)
900
800
700
600
500
400
300
200
100
0
ctl
Pb
PND 120
PND 180
PND 240
PND 120
PND 180
PND 240
female
male

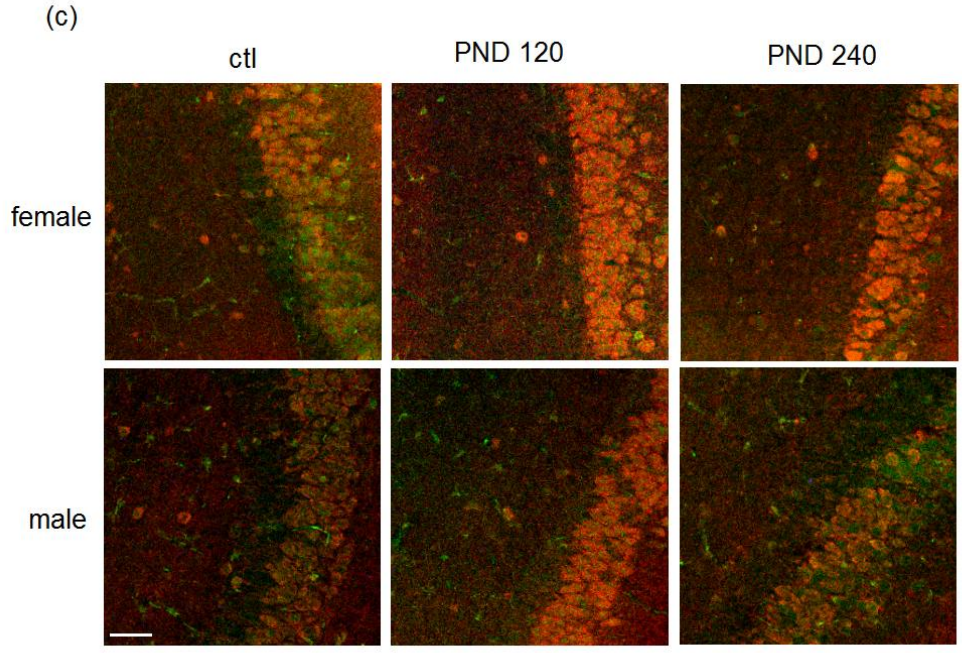
(c)
ctl
PND 120
PND 240
female
male

3.4 Discussion

The potential synaptic dysfunction that underlies some of the earliest known pathological markers for AD has yet to be fully elucidated, much less conclusively interrelated with hypotheses surrounding early origins for adult neurodegeneration. We previously reported that postnatal Pb exposure in a 3xTgAD mouse model of AD is sufficient to increase the susceptibility to amyloid accumulation in conjunction with decreased microglial activation, more so in females compared to males (vonderEmbse et al., 2017). As microglial activation frequently coincides with phagocytic capabilities, such as with amyloid-β (Bolmont et al., 2008), this would suggest decreased microglial neuroprotection. Here, we investigated the implications of female-biased microglial dysfunction on the timing of synapse perturbation, and the importance of homeostatic microglial:neuronal signaling within this gene x environmental model for the developmental origins of AD.

Following pathologic stimuli, microglia drastically change functional phenotype to adopt an activated state congruent with the type, strength, and duration of the stimulus (Luo and Chen, 2012). This polarized activation, although not discriminately bifurcated, can be analyzed by the ratio of the two most general forms of macrophage activation, M1:M2, or expression of CD86:CD209, respectively. This relative ratio of polarization is more likely indicative of microglial responsiveness to alterations to the microenvironment than absolute levels of either CD86 or CD209, particularly when considering the heterogeneity of the cell population and specific demands of the CNS (Crain et al., 2013). Similarly, numerous studies have identified upregulation of both M1 and M2 associated genes in CNS disease and neurodegeneration (Nakagawa and Chiba, 2014; Prokop et al., 2013; Tang and Le, 2015), highlighting the

complexity of microglial response in AD. Although highly variable at PND 120, a female sex bias in microglial polarization is detectable in transgenic mice (Fig 3.1b). By PND 240, flow cytometric analysis revealed activation profiles of all groups become more homogenously polarized toward M2, most significantly in Tg Pb-exposed females (Fig 3.1). Microglia may initiate synaptic stripping to mitigate the risk of glutamate-induced excitotoxicity following a decrease in synaptic activity, such as with impaired maintenance of afferents, after which microglia then provide trophic support for synaptic reorganization (Yamada et al., 2011). Thus, the cognate phenotypic change following immediate neuronal injury would be a temporal switch from M1 to M2, as is seen in Pb-exposed WT mice from PND 120 to 180 (Fig. 3.1c) and Pb-exposed male Tg mice from PND 180 to 240 (Fig. 3.1b). The later shift in the 3xTgAD model compared to WT is likely a result of the accumulation of amyloid beta within this AD model, promoting M1-related proteolysis and phagocytosis.

The prolonged M2 phenotype has been correlated with both immune “priming” (Perry and Teeling, 2013) and a type of “innate immune memory” (Perry et al., 2010) that persists following systemic infection or inflammation and ultimately contributes to chronic neurodegeneration. Chronic, strong M2-polarized microglial activation profiles, seen in Pb-exposed Tg females at PND 240 (Fig 3.1b), are particularly detrimental in neurodegenerative diseases for two reasons, the first being a lack of appropriate, strictly regulated M1/M2 activation balance concordant with region-specific signals derived from the immediate microenvironment. The second reason later-life, strong M2 polarization would be considered a damaging phenotype in our model is due to the resultant decreased pool of ramified microglia. In a recent study, the presence of mature, ramified microglia was shown to be neuroprotective in NMDA-induced hippocampal excitotoxicity, whereas microglial activation coincided with regional neuronal vulnerability; region-specific vulnerability occurred to a greater extent than is

accounted for by endogenous glutamate receptor variability (Vinet et al., 2012). Therefore, postnatal Pb exposure, when combined with a genetic propensity to AD, promotes the female-biased formation of atypical and potentially non-neuroprotective microglial phenotype that is detectable by PND 240.

We further analyzed localized microglia function within the hippocampus via immunohistochemical characterization of ferritin expression. Ferritin is an iron metabolism molecule, comprised of a multi-subunit protein shell with a ferroxidase center (Simmons et al., 2007). The ferritin in neurons, rich in H-chain subunits, is involved in the detoxification of ferrous ion (Fe2+), whereas ferritin in microglia, rich in L-chain subunits, possess glutamate residues to facilitate sequestration and long-term storage of excess extracellular iron (Lopes et al., 2008). Notably, ferritin and amyloid precursor protein (APP) mRNAs are induced by similar translational mechanisms, and both metalloproteins are upregulated as neuroprotective compensation against oxidative stress and acute IL-1 (Rogers et al., 2008). Although the presence of acute ferritin expression is considered a neuroprotective function of microglia, ferritin is also known to promote the rapid transition of microglial activation states from M2 to M1 (Kroner et al., 2014). Our own data support this early correlation between ferritin and M1 activation at PND 120 in WT mice and Tg males, but not M2-skewed Tg females (Fig 3.1 & 3.3), which persisted in all groups at PND 180.

By PND 240, however, the correlation between ferritin and microglia polarization was less linear. One potential explanation could be that pathological amyloid accumulation, not seen in WT animals, alters the efficacy of finely balanced intrinsic neuroprotective mechanisms that is then exacerbated by dysfunctional microglia. Increased ferritin expression at PND 240 in Pb-exposed Tg males (Fig 3.3c) infers male microglia were still responding to excess, neurotoxic

iron occurring at this time, whereas decreased ferritin in Tg females, correlating with the presence of crystallite fragments (Fig 3.3d) and significantly M2-biased microglial polarization (Fig 3.1b), supports a possible mechanism in which the majority of remaining microglia have a dysfunctional, non-neuroprotective M2-skew with limited proliferative potential. Indeed, preferential, microglia-directed damage or even necrosis can occur in ferritin-positive, M1-activated microglia due to the interaction of M1-specific superoxides and release iron via the Fenton reaction (Kroner et al., 2014). Although Pb-exposed Tg males exhibited high ferritin immunoreactivity at PND 120, the recurrent increase by PND 240 in response to amyloid-associated neurotoxicity infers that microglia were able to proliferate, despite potential self-directed toxicity, and respond in a neuroprotective manner. Females, however, were unable to mount this response at PND 240, inferring "martyred" subpopulations of ferritin-containing microglia were no longer functional or present, regardless of relatively comparable pathological stimuli to males for this genetic mouse model of AD. Additionally, ferritin can become dysfunctional over time, eventually degrading into crystallite hemosiderin and releasing iron into the immediate vicinity (Quintana and Gutiérrez, 2010), even without the prompting from M1-associated superoxides. Given these results, we conclude microglia in Pb-exposed Tg females exhibited markers of atypical function earlier and more severely than males, suggesting a sex bias in decreased neuroprotective capabilities.

We next directed our research focus to the hippocampus, a brain region preferentially targeted in AD, and evaluated changes to the mossy fiber pathway (MFP). Along the MFP, granule cells (GCs) from the dentate gyrus project to pyramidal CA3 neurons using non-associative LTP, an NMDA-independent form of synaptic plasticity that relies on repeated stimulation and calcium influx to increase the probability of presynaptic glutamate release. In the 3xTgAD mouse model, decreased neurogenesis is detectable in females as early as 4 months

of age and 6 months of age in males (Rodríguez et al., 2008). Notably, chronic reductions in neurogenesis have been shown to compromise the function and morphology of the CA3 region (Schloesser et al., 2013). As microglia are critical to neurogenesis, alterations to the CA3 region gives specific information regarding adaptation and compensation following microglial deficits in MFP homeostasis.

Ferritin-positive microglia localized with striking specificity in the CA3 and hilar subregions of the hippocampus (Fig 3.1), suggesting both microglial involvement and increased iron release along the MFP, possibly consequent to myelin release from axotomized afferents or necrotic immature GCs. Microglial differentiation and behavior is highly dependent on the brain region, and this is particularly evident within the neurogenic niche. Only a small number of immature neurons in the DG become fully incorporated into the granule cell layer within the four week critical window following neuron birth, with microglial-dependent apoptosis occurring within the first 1-4 days (Sierra et al., 2010). Neurogenic homeostasis is maintained via this early, highly efficient phagocytosis by ramified microglia, as well as other microglial-derived mediators like TGF-β and BDNF. Microglia within the neurogenic niche can also act as mulitpotent stem cells and transdifferentiate into neurons, astrocytes, and oligodendrocytes for regeneration in the normal and injured brain (Yokoyama et al., 2004, 2006). Reductions in either functional phagocytosis or proliferation would drastically affect neurogenic homeostasis and consequent MFP morphology, even more so following neuronal toxicity. Therefore, microglia dysfunction within the neurogenic niche could manifest as 1) decreased proliferative and subsequent regenerative potential, 2) persistent activation and concurrent imbalanced pro-/anti-inflammatory activated phenotypes, and 3) impaired ability to phagocytize apoptotic immature GC neurons before they become necrotic and release inflammatory mediators like iron. Our microglial ferritin and M1/M2 polarization data support this hypothesis of MFP microglial dysfunction, regarding

both neurogenesis and phagocytosis – conditions not unlike the nearly identical postnatal development in which tightly regulated microglial-mediated synaptogenesis and synaptic pruning instruct neuronal circuitry formation and region-specific microglial differentiation and maturation.

Evidence of the neuronal consequences from dysfunctional microglial neurogenic support was explored by analysis of TrkB expression. The tyrosine kinase receptor B (TrkB) is the cognate receptor to brain-derived neurotrophic factor (BDNF), secreted by microglia to promote neuronal homeostasis and synaptogenesis. BDNF-TrkB signaling is crucial to synaptic plasticity, neuronal survival, and differentiation throughout the CNS (Yoshii and Constantine-Paton, 2010). A recent study demonstrated the important role of BDNF-TrkB signaling in non-associative LTP, in which mossy fiber LTP was significantly impaired by both acute and chronic block of BDNF/TrkB signaling (Schidlt et al., 2013). This was substantiated by another study that reported altered mossy fiber terminals in TrkB-deficient mice, including reductions in synaptic vesicles, number of synaptic contacts, and density of axon distribution (Otal et al., 2005). Although altered TrkB expression in the CA3 region gives specific information about changes to excitatory synapses, there are implications for GABAergic interneuron signaling. Untimely sprouting of mossy fibers has been shown to produce increased numbers of synaptic contacts with GABAergic interneurons (Frotscher et al., 2006). The severity of functional outcome is intimately related to signaling through the TrkB receptor, affecting the finely-tuned balance of inhibitory/excitatory inputs through altered network connectivity (Bernard et al., 2007). Another study of network hyperexcitability from altered GC connectivity also implicated a role for TrkB, in which TrkB deletion resulted in increased feed forward inhibition to CA3 pyramidal cells (Danzer et al., 2008). BDNF/TrkB signaling occurs in a very precise, localized manner; in the event of deficits in microglial-derived BDNF, non-microglial BDNF is incapable of

assisting the signaling impairment (Parkhurst et al., 2013). Thus, microglia are critical to TrkB-mediated alterations in GC neurogenesis, MFP connectivity, and balance of inhibitory/excitatory tone to the CA3. We posit altered TrkB expression within the MFP could act as trophic compensation associated with chronic reductions in neurogenesis to maintain balanced synapse dynamics and proper GC maturation. As a response to early postnatal Pb-associated microglial neglect, atypical synaptic connections and early formation of a strong inhibitory GABAergic tone to the CA3 region might then be overcompensated for by gradual development of network hyperexcitability. By evaluating each time point individually within context of the immediate environment, and integrating other neuronal and microglial markers, we interpreted altered expression of TrkB receptor in the CA3 terminus of mossy fiber afferents as indirect evidence of microglial neglect or dysfunction via compensatory neuronal signaling. Western blots for synaptosomal synaptic proteins were also performed to measure sustained, late changes to TrkB-mediated hippocampal LTP (Leal et al., 2014) to corroborate TrkB expression data, and give a more detailed view of synaptic changes involving microglia.

The Pb-associated increase in TrkB expression at PND 120, coupled with the presence of ferritin-positive microglia, is suggestive of neuronal damage along the MFP. In Pb-exposed Tg males, the greater incidence of ferritin-positive microglia and M1-polarization, as well as decreased synaptophysin at PND 120, is suggestive of early microglial-mediated synaptic stripping and greater neuroprotection, respectively, in males. Pb-exposed transgenic females, however, exhibited symptoms of exacerbated and inefficient microglial neuroprotection at PND 120. Not only were there significant decreases in both synaptophysin and SNAP25 in Tg females months after cessation from Pb exposure (Fig. 3.4), but the increase in activity-dependent insertion of TrkB receptors into the membranes of CA3 pyramidal neurons is evidence of neuronal compensation for altered connectivity of mossy fiber terminals that likely

arose from inadequate microglial homeostatic support to the neurogenic niche. Thus, data from PND 120 corroborates the interpretation that AD-like synapse impairments within the MFP occur earlier and more severely in Pb-exposed female mice consequent to regional microglia dysfunction that likely improperly addressed, or even promoted, the formation of imbalanced neuronal circuitry.

Evidence for sex-biased microglial dysfunction accumulated with age. By PND 180, TrkB expression was decreased compared to controls in both male and female Pb-exposed transgenic mice (Fig. 3.6b), whereas ferritin expression remained elevated. Ferritin has been shown to inhibit glutamate uptake (Alekseenko et al., 2008), so decreased TrkB at this time is likely compensatory to mitigate excitotoxicity to CA3 pyramidal thorny protrusions. Furthermore, signaling through the TrkB receptor regulates levels of presynaptic proteins to alter the synaptic terminal phenotype (Leal et al., 2014; Otal et al., 2005). By PND 240, there were significant decreases in both synaptophysin and SNAP25 in Pb-exposed Tg males, likely the result of prolonged suppression of TrkB – that would suggest neuroprotection against the formation of unstable, hyperexcitable mossy fiber circuits. Synaptophysin is upregulated during synaptogenesis as one of the earliest synaptic proteins to accumulate within new synapses to promote stabilization, particularly within the hippocampus (Tarsa and Goda, 2002). As the most abundant protein in the membrane of synaptic vesicles, decreased synaptophysin is correlated with decreased synaptogenesis and fewer synaptic terminals. Additionally, extensive loss of synaptophysin in early and mild AD precedes cognitive decline (Masliah et al., 2001), implicating an early mechanistic role in synapse dysfunction. Synaptosomal-associated protein of 25kDa, or SNAP25, is a t-SNARE protein that assembles with synaptobrevin and syntaxin-1 to promote specificity of vesicular membrane fusion. Its expression is upregulated during development, correlating with synaptogenesis and synaptic maturation, through its dual function

in promoting fusion events and participating in endosomal recycling (Bark et al., 1995). As functional impairment can lead to neurodegeneration (Sharma et al., 2012), alterations in its expression are also suggestive of atypical synapse dynamics related to AD. Therefore, decreased expression of both synaptic proteins in Pb-exposed Tg males at PND 240 (Fig. 3.4b,d) alludes to later-life neurogenic- and synapse-related AD pathologies as stable neuronal compensation.

Conversely, in Pb-exposed Tg females at PND 120, decreased synaptosomal levels of both synaptic proteins in addition to increased CA3 TrkB expression reflect an environment in which significant damage to neuronal synapses promotes trophic signaling within the neurogenic niche. However, the initial decrease in TrkB expression at PND 180, and later comparable levels to controls at PND 240, is suggestive of the continued development of unstable and unbalanced MFP circuitry, unmitigated by neuroprotective microglia as seen in males, and evident of microglial maladaptation rather than compensation. This is further corroborated, specifically, by increased levels of SNAP25 at PND 240. Following lesions of the entorhinal cortex, both ferritin and SNAP25 were shown to be significantly upregulated in the DG molecular layer (Day et al., 1992), implying that, within our own model, if globally increased SNAP25 expression was lesion- or atrophy-associated then the lack of hippocampal ferritin expression is evident of a non-neuroprotective microglial phenotype. Alternatively, non-lesion-associated increases in SNAP25 expression may also substantiate a dysfunctional microglia-based mechanism. At PND 240 there were detectable SNAP25 cleavage products in both male and female transgenic mice (Fig. 3.4a,b). Although this could be a potential artifact of the aging mouse model, various studies have demonstrated that cleavage and subsequent inactivation of a very small subset of functional SNAP25 is enough to induce paralysis by botulinum toxin A (Blasi et al., 1993). Cleavage in the healthy brain, however, is calcium-dependent, inhibiting the

release of neurotransmitters like glutamate and BDNF (Grumelli et al., 2008), so excessive SNAP25 cleavage at this time could be another maladaptive neuronal response in lieu of healthy microglia:neuron crosstalk.

Taken together, the integration of our results supports our hypothesis that the interaction of a genetic susceptibility to AD combined with low-level, postnatal Pb exposure alters healthy microglia:neuronal crosstalk maturation in a female-biased manner that then persists into adulthood and increases susceptibility to neurodegeneration. The exact mechanism by which microglia gradually become dysfunctional over time has yet to be elucidated. Although there is evidence to suggest that a catalytic component may arise from atypical neuronal signaling from unbalanced circuits, the malleability and general resiliency of the healthy brain, and its neuroprotective immune cells, is enough to refute such a linear mechanism. However, the phenotypic plasticity and selective vulnerability of development, and the resultant persistence of effects, may provide novel insight into these slow developing maladaptive responses. Microglia have been implicated in studies of developmental immune activation and later-life cognitive dysfunction (Schwarz and Bilbo, 2012), but there is little to no characterization of the threshold for the development of maladaptation at the molecular level over time. An interesting correlative link may exist in phenotypic adaptation via regulatory elements, as with epigenetics or microRNAs. Further investigation is warranted to determine if, and how, this regulation of phenotypic plasticity goes awry during development, and whether it persists long enough to eventually become maladaptive.

Our study demonstrates a distinct correlation between the combination of a genetic predisposition and early-life toxicant exposure and the exacerbation of later-life neurodegeneration, with strong evidence for a potential etiologic role for early microglia

dysfunction in AD. Furthermore, we have proposed several markers of early maladaptive responses within the neuroimmune parenchyma that parallel and corroborate similar mechanistic hypotheses regarding microglia activation and neurotoxicity in late-stage AD. It is compelling to consider hallmark molecular pathologies associated with AD as indicative of failed compensatory responses and maladaptation, rather than aging-related senescence or metabolic exhaustion. In this way subtle trends may be more telling of mechanistic undercurrents, as opposed to overt effects that likely represent consequence and summation of numerous variables over time. Redirecting the focus of this gene x environment disease paradigm to integrate early dysfunction in microglia:neuron crosstalk opens up a plethora of research avenues to investigate early symptoms and biomarkers of maladaptation and more clearly refine adaptive thresholds for disease-specific parenchyma.

Chapter 4:

Postnatal toxicant exposure in 3xTgAD mice promotes sex-dependent NeurimmiR profiles detrimental to healthy microglia:neuron crosstalk

4.1 Introduction

Developmental plasticity and phenotypic persistence are central to the developmental origins of adult disease (DOAD) hypothesis, and are of particular importance for interpreting the functional implications of parenchymal phenotypes in aging-related diseases like Alzheimer's disease (AD). The consequence of gene x environment (GxE) interactions is much more profound during development due to critical windows in which phenotypic plasticity is instructed by, and extremely sensitive to, exogenous signaling. Moreover, recent studies indicate environmental factors can not only directly contribute to disease, such as with certain cancers, but also indirectly, by promoting detrimental conditions through epigenetic remodeling, prolonged windows of susceptibility, and even altered regulatory elements for primed or dysfunctional phenotypes (Sollome et al., 2016; Dietert, 2011; Miller and O'Callaghan, 2008). However, there has yet to be a fully described mechanistic correlation between toxicant-induced atypical development and increased susceptibility to later-life neurodegeneration, much less a definitive parenchymal target or cognate pathway to neurological disease.

In previous studies using a DOAD model for AD, we have described a female-specific heightened disease susceptibility following postnatal toxicant exposure that promoted the formation of dysfunctional, maladaptive microglia and compensatory synaptic aberrations (vonderEmbse et al., 2017; manuscript under review). As the tissue-resident macrophage of the

central nervous system (CNS), microglia have critical roles involved in not only innate immune surveillance, but also in neuronal development, differentiation, and homeostasis. Healthy microglia:neuron crosstalk vital to adult CNS homeostasis is dynamic throughout life, but instructed early in postnatal development. Thus, imbalances in neuroimmune signaling and function may be developmentally promoted, and, compellingly, may also be detectable as alterations to epigenetic elements.

MicroRNAs are short, non-coding segments of RNA that act as post-transcriptional regulators of gene expression and function. As altered miRNA expression levels are often a direct result of changes to the immediate CNS environment, they are considered a form of epigenetic remodeling of cellular phenotype. Nearly 60% of all protein-encoding genes are thought to be regulated by miRNAs (Friedman et al., 2009), and, with half-lives nearly 10x longer than mRNA (Gantier et al., 2011), numerous studies have already begun exploring the potential of these molecules to act as biomarkers of disease (Reid et al., 2011). Notably, microRNAs are highly involved in CNS development (Bian and Sun, 2011) and may have a central role in the promotion of DOAD. Soreq and Wolf (2011) have recently coined the term “NeurimmiRs” to describe miRNAs that influence both neuronal and immune phenotypes, with evidence for interrelated influence on the function of each cell type. Interestingly, nearly 2/3rds of the 250 miRNAs surveryed in neonatal mouse brains by Morgan and Bale (2012) were shown to be differentially expressed in males and females, implicating miRNAs as major epigenetic regulators of sex differences in the developing brain (Guo et al., 2017; McCarthy and Nugent, 2015), and also highlighting a potential role in the development of sex-related dysfunctional phenotypes. How these sex differences in neurimmiR expression during development is promoted and homeostatically-balanced, and the relative contribution of various signaling

pathways to global phenotypic regulation during poor developmental conditions, has yet to be explored.

The objective of the present study was to delineate early, altered expression of neurimmiRs related to the promotion of dysfunctional microglia:neuron signaling and microglia maladaptation following early toxicant exposure. The adaptive response of immune cells to fine-tune signaling in homeostatic pathways is not only critical in adulthood, but defined during development. Thus, we hypothesized that the combination of a genetic proclivity to AD and postnatal exposure to lead acetate (Pb) would result in persistent, differential changes in interrelated neurimmiRs known to regulate microglial quiescence, neuronal maturation and sprouting, and pro-phagocytic developmental phenotype for microglia, thus promoting an environment ripe for the gradual formation of neuroimmune imbalances associated with increased vulnerability to AD later in life. By including postnatal indomethacin (indo) exposure during a female-specific critical window for later-life microglia dysfunction (vonderEmbse et al., 2017), we aimed to discriminate effects consequent specifically to Pb as an early inflammatory event versus a general disruption of sex-specific neuroimmune maturation, as indo is a potent inhibitor of the brain masculinizing molecule PGE_2 (Amone-Cat et al., 2010), and more clearly describe early re-patterning of microglial response phenotypes. Moreover, the influence of gene x environment interactions on changes to- and prolonged expression of microRNAs was investigated by the addition of a WT model comparison, highlighting the exacerbating effect of the DOAD model in the formation of a development phenotype for later-life susceptibility to neurodegeneration.

4.2 Materials and Methods

4.2.1. *Animal handling*

All handling and experimental manipulations were carried out in accordance with procedures approved by the East Carolina University Institutional Animal Care and Use Committee (IACUC). Pregnant wildtype (SFN) and transgenic dams (3xTgAD; B6;129-*Psen1*^{tm1Mpm}Tg(APPSwe,tauP301L)1Lfa/Mmjax) were obtained from the seed colony in the ECU Department of Comparative Medicine and kept on a 12:12 hour light/dark cycle, with access to food and water *ad libitum*. Litters were culled to eight after birth (postnatal day, PND 1), if needed, and monitored for overt signs of toxicity.

4.2.2 *Dosing and tissue preparation*

Dosing solutions of lead acetate (100 ppm) and indomethacin (1 mg/kg/day) (Sigma-Aldrich, Milwaukee, WI, USA) dissolved in sterile water were prepared weekly. From PND 5-9 neonates were dosed once per day with vehicle, indomethacin, lead acetate, or indomethacin followed by lead acetate 30 minutes later using a modified gavage technique (Butchbach et al., 2007). One mouse per sex, litter, and treatment group was randomly assigned and euthanized at PND 10, 15, or 21. As per ethical use protocol, animals were euthanized with inhaled isofluorane followed by immediate decapitation. The brain was then carefully removed and placed in ice cold PBS. For histochemical analysis the left hippocampus was dissected and fixed for 24 hours in 10% neutral buffered formalin followed by 70% ethyl alcohol before paraffin fixation. The right hemisphere sans cerebellum was flash frozen whole and stored at -80^{0}C.

4.2.3 *Immunohistochemistry*

Formalin-fixed, paraffin-embedded (FFPE) hippocampi were sliced on a rotary microtome at 10 µm and mounted on Superfrost Plus slides (Azer Scientific, Germany). Briefly, slides were dewaxed in Histo-Clear II (Electron Microscopy Sciences, Halfield, PA, USA), followed by washes in 100% and 95% ethyl alcohol and phosphate buffered saline (PBS). Antigen unmasking was accomplished using a heat-mediated citrate buffer, followed by incubation in 0.3% hydrogen peroxide for 30 minutes. All subsequent staining was performed using Sequenza-Coverplate racks (Thermo Scientific, Waldorf, Germany). Sections were permeabilized with PBS with Tween-20 (TPBS) and blocked with diluted normal serum (ABC Vectastain; Vector Laboratories, Burlingame, CA, USA). Slides were then incubated with anti-DAP12 primary antibody (4 µg/mL; Biorbyt, Cambridge, UK), for 60 minutes at room temperature or overnight at 4˚C. Sections were visualized using ABC Vectastain and diaminobenzidine (DAB) kits (Vector Laboratories) and counterstained with Harris' Alum Hematoxylin. After sequential washing in ethyl alcohol and Histo-Clear, slides were coverslipped with Permount (Fisher Scientific, Fair Lawn, NJ, USA) and cured overnight prior to visualization.

Slides were visualized using a Leica DM1000 light microscope at 20x magnification with a SPOT^{TM} Idea camera attachment and Advanced Imaging software. Two regions of interest (ROI) per animal were chosen at random along the dentate gyrus, with the viewing frame containing as much tissue as possible. Immunopositive DAP12 reactivity was determined via FIJI (Schindelin et al., 2012) analysis over a predetermined background threshold and use of a Color Deconvolution plugin, and the % area DAP12 positive/ROI was determined along the CA3 and hilus hippocampal subregion. All data are represented as the mean ± SEM.

4.2.4 *Quantitative real-time polymerase chain reaction (qRT-PCR)*

4.2.4.1 RNA Isolation and cDNA synthesis

Total RNA was purified from no more than 20 mg frozen brain tissue taken from the right hemisphere of 3xTgAD or WT mice using the miRCURY™ RNA Isolation Kit – Cell & Plant (Exiqon Inc., Woburn, MA, USA) and associated Lysis Additive (Exiqon) specific for fatty tissue. Following homogenization and cell lysis, RNA was purified against a proprietary resin spin column separation matrix, washed with the associated buffers, and eluted at 50 µL, as per manufacturer's instructions. Purified RNA was measured on a NanoDrop™ One/One^{C} Microvolume UV-Vis Spectrophotometer (ThermoFisher Scientific, Madison, WI, USA) for purity and concentration, which was then adjusted to 5 ng/µL for subsequent reverse transcription.

For each sample, cDNA was synthesized from 10 ng purified RNA, in duplicate, using the Universal cDNA synthesis kit (Exiqon) and the following protocol: 60 min at 42˚C, followed by heat-inactivation of the reverse transcriptase for 5 min at 95˚C. Newly synthesized cDNA was then stored at -20˚C, and thawed and diluted to 80X in RNase-free water prior to RT-PCR.

4.2.4.2 Real-time PCR

MicroRNA relative quantification was performed on an iQ5 Multicolor Real-Time PCR Detection System thermocycler (Bio-Rad Laboratories, Inc., Hercules, CA, USA), using 96-well PCR plates (VWR, Radnor, PA, USA). A master mix was prepared for each pre-designed LNA™ PCR Primer set (Table 4.1, Exiqon), in conjunction with ExiLENT SYBR® Green master mix (Exiqon), for the target primers (miR-124, miR-132, miR-34a), endogenous reference primer

(SNORD110), and UniSp6 RNA Spike-in control primer included in the kit. Each well consisted of 6 µL master primer mix and 4 µL cDNA template per sample, for a final well volume of 10 µL per sample, performed in duplicate. Reaction conditions included polymerase activation/denaturation at 95°C for 10 min, 40 amplification cycles at 95°C for 10 sec and 60°C for 1 min (1.6°C/s ramp rate), and a melt curve analysis consisting of a setpoint at 60°C and endpoint at 95°C, incrementally increasing by 0.5°C with a 10 sec dwell time.

Automatically generated threshold cycle values (C_t) were evaluated using LinRegPCR (Ruijter et al., 2009) quality assessment to account for amplicon and assay efficiency. Fold change in relative miRNA expression compared to sex-, strain-, and age-matched controls was determined by the Pfaffl method, accounting for differential amplicon efficiencies calculated by LinRegPCR.

Table 4.1 Primer sequences of miRCURY LNA® PCR Primer sets (Exiqon)

microRNA	RT primer sequence 5' -> 3'	
hsa-miR-124-3p	UAAGGCACGCGGUGAAUGCC	target
mmu-miR-132-5p	AACCGUGGCUUUCGAUUGUUAC	target
hsa-miR-34a-5p	UGGCAGUGUCUUAGCUGGUUGU	target
SNORD110	[UGACUUAUAUAUCUGUCAAUCCCCUGAGAG AUCACUGACGACUCCAUGUGUCUGAGCAA]	reference
UniSp6	CUAGUCCGAUCUAAGUCUUCGA	control

RT: reverse transcriptase.

4.2.5 *Statistics*

All statistics were carried out using Statistical Analysis System (SAS Institute, Cary, NC, USA) software. Two-way analysis of variance (ANOVA) for treatment and age was performed for each sex and strain for IHC data, and two-way ANOVA for age and sex was performed for each strain and treatment groups for qRT-PCR. Individual pairwise comparisons were made with a t-test or a Tukey's studentized range distribution method. IHC data are represented as mean DAP12 immunopositive staining/ROI ±SEM, and qRT-PCR data are represented as mean fold change over sex-, strain-, and age-matched controls, with respect to endogenous reference gene levels, ±SEM. $p < 0.05$ was used to denote statistical significance.

4.3 Results

4.3.1 *Postnatal toxicant exposure induced sexually dimorphic aberrations in mouse brain miRNA expression profiles*

To assess early regulatory changes to neuroimmune signaling following a postnatal toxicant exposure, as well as any sex bias and persistence of changes, we performed qRT-PCR for three distinct, yet interrelated microRNAs at PND 10 and 15. We observed considerable sexual dimorphism in differential miRNA expression following postnatal exposure to Pb, indo, or indo+Pb compared to controls. Expression of miR-124 was significantly upregulated in WT females compared to WT males at PND 10 regardless of toxicant, but by PND 21 no detectable sex bias remained (Fig. 4.1). Indo exposure produced early and sustained sex bias in Tg

expression of miR-132 (Fig. 4.2b), with preferential upregulation in females. Likewise, indo exposure resulted in significant sex differences in WT expression of miR-34a, both at PND 10 and PND 21 (Fig. 4.3a), with preferential upregulation in males. Sex bias also occurred in Pb and indo+Pb groups, but was compounded by mouse strain, age, and specific microRNAs evaluated.

4.3.2 *Sex-dependent changes in miR-124 expression with differential developmental exposures*

qRT-PCR analysis of miR-124 expression fold change over sex-, age-, strain-, and treatment-matched controls revealed distinct sex-related differences for each strain of mouse. At PND 10, WT females exhibited increased miR-124 expression compared to control in all treatment groups that differed significantly from decreased levels in WT males (Fig. 4.1a,c,e). Both indo and Pb exposure resulted in acute upregulation in miR-124 expression in WT females that differed significantly from levels at PND 21. A similar trend was seen in indo+Pb-treated WT females (Fig. 4.1e), but by PND 21 expression was more similar to control levels, rather than downregulated as with the other two treatment groups. There was no sex-related difference in WT mice by PND 21. These data suggest that, sans genetic component, an environment (re: toxicant) –derived female proclivity is observed in the upregulation of miR-124 expression immediately following exposure cessation, that is then ablated or compensated for by PND 21.

In brains of Tg mice, the only sex-related difference in miR-124 expression was seen at PND 21 in Pb-exposed animals (Fig. 4.1d), with greater upregulation in females when compared to the control-like levels in males given Pb. Indo exposure, however, resulted in increased expression in both Tg males and females, which then remained upregulated until PND 21 (Fig.

4.1b). These results contrasted sharply with those of the WT indo group, specifically the PND 10-associated increased expression in WT females and PND 21-associated low levels in both WT sexes (Fig. 4.1a), suggesting that the added genetic component of the Tg mouse model had a significant effect on toxicant-specific sex bias and signal perpetuity for changes in expression.

Likewise, Tg mice exposed to indo+Pb exhibited miR-124 expression patterns over time that also differed by sex. Tg females exposed to indo+Pb exhibited a pattern of gradual upregulation with age (Fig. 4.1f), similar to Pb-exposed Tg females (Fig. 4.1d), that would suggest Tg female miR-124 levels were more affected by Pb than indo when combined, or that this indo exposure was not able to effectively mitigate Pb effects, specific to our experimental parameters for concentration and exposure duration. Conversely, Tg males exposed to indo+Pb exhibited low levels at PND 10 followed by a significant upregulation at PND 21 (Fig. 4.1f), more akin to indo-only Tg male expression levels at PND 21 (Fig. 4.1b). These results infer that indo elicited a greater effect than Pb on alterations to miR-124 expression in Tg males when exposed in combination, markedly in the gradual, induced upregulation of miR-124 by PND 21 rather than an acute response at PND 10. Taken together, these results demonstrate female-specific miR-124 expression was acutely and significantly upregulated consequent to any toxicant exposure from PND 5-9; however, the combination of GxE via the Tg model resulted in the diminution of acute sex bias in miR-124 expression at PND 10, and gradual upregulation of miR-124 by PND 21, depending on the type of toxicant, as Pb exposure resulted in eventual female-specific sex bias.

4.3.3 *Pronounced, persistent changes in miR-132 expression varied with sex, depending on combinatorial Pb exposure*

To evaluate additional sex-related and treatment-specific changes in a complimentary neurimmiR involed in anti-inflammatory signaling and neuronal excitability, we measured changes in miR-132 expression compared to sex-, age-, strain-, and treatment-matched controls. Isolated environmental effects, reflected in the WT groups, revealed downregulated miR-132 at PND 10 in WT males treated with either indo (Fig. 4.2a) or Pb (Fig. 4.2c), that then became significantly upregulated by PND 21 in both treatment groups, but considerably more so in Pb-exposed males. Contrarily, WT females treated with either indo or Pb both exhibited downregulation of miR-132 expression by PND 21 (Fig. 4.2a,c), but a Pb-specific upregulation at PND 10. These results infer the presence of a male-specific bias in the gradual upregulation of miR-132 regardless of toxicant exposure for WT mice, as opposed to a more controlled downregulation in WT female response over time. Furthermore, Pb exposure elicited an acute upregulation for females at PND 10 and later upregulation for males at PND 21, revealing a significant sex difference in the timing and potential signaling source for miR-132 expression present in indo exposure but exacerbated in Pb exposure. Interestingly, WT mice treated with both indo+Pb revealed upregulation in females at PND 10 that persisted to PND 21, and the gradual upregulation in males by PND 21 (Fig. 4.2c). This would suggest signaling for increased miR-132 expression occurred abruptly following exposure cessation in females, and developed over time in males; moreover, changes in expression pattern for both sexes incurred with greater sensitivity to Pb, though parallel to indo.

Contrary to indo-exposed WT mice, indo-exposed Tg females exhibited upregulation in miR-132 at PND 10 that persisted until PND 21 (Fig. 4.2b), rather than becoming downregulated at the later time point. Likewise, although similar to the WT at PND 10, indo-exposed Tg males remained downregulated at PND 21, inferring the addition of a genetic component gradually

altered indo-related sex bias by PND 21. Pb exposure in Tg mice produced comparable effects to indo in terms of the eventual mitigation of late-formed sex bias at PND 21 (Fig. 4.2d).

The addition of genetic proclivity to AD via the Tg mouse model significantly altered sex- and treatment-related patterns for miR-132 expression seen in WT mice, in almost all groups except those treated with both indo+Pb (Fig. 4.2f). Sex-related changes to miR-132, and persistence of those changes over time, were nearly identical between Tg and WT indo+Pb-exposed mice (Fig. 4.2f and e, respectively), as well as Tg Pb-exposed mice (Fig. 4.2d). These results suggest altered miR-132 expression was influenced to a greater extent by sex and timing of toxicant exposure, and, to a lesser degree, by Pb exposure in conjunction with either indo pretreatment or a genetic predisposition to AD.

4.3.4 *Significant sex-associated changes in miR-34a expression varied with postnatal toxicant exposure*

To investigate altered regulation of development-specific microglia phenotype and maintenance of pro-inflammatory signals, we measured fluctuations in miR-34a expression following postnatal exposure to Pb, indo, or both indo+Pb. WT mice exposed to either indo (Fig. 4.3a) or both indo+Pb (Fig. 4.3e) exhibited similar sex- and age-related changes in miR-34a expression, underscoring the magnitude of responsiveness of miR-34a expression to indo. Within these two treatment groups, expression was downregulated in WT females at PND 10 and maintained until PND 21, as opposed to the upregulation sustained in WT males (Fig. 4.3a,e). Postnatal Pb exposure resulted in similar sex bias at PND 10, but by PND 21 the sex bias was reversed such that miR-34a was upregulated in WT females and downregulated in WT

males (Fig. 4.3c). Thus, exposure to either toxicant induced similar sex biased expression changes one day following exposure cessation, but signaling for changes to miR-34a were sustained until PND 21 with indo exposure and reversed with Pb exposure in WT mice.

Indo exposure in the Tg mice resulted in a similar sex bias to the WT indo group, with downregulation in females and upregulation in males, but the sex difference was not significant in the Tg group (Fig. 4.3b). By PND 21, expression in both male and female Tg indo mice was upregulated, again, without a significant difference in expression between sex. Conversely, Pb exposure in Tg mice resulted in downregulation in miR-34a expression at PND 10 that was sustained until PND 21 (Fig. 4.3d); Tg females, however, exhibited little discernible change compared to controls at PND 10, but upregulated expression in miR-34a by PND 21, with a significant sex bias that paralleled WT Pb mice at the same time point (Fig. 4.3d,c). Likewise, Tg mice exposed to indo+Pb exhibited considerable downregulation in males at PND 10, and slightly upregulated expression in females (Fig. 4.3f), but by PND 21 patterns in sex bias paralleled the WT indo+Pb group. Tg females exposed to indo+Pb displayed downregulation in miR-34a expression at PND 21 (Fig. 4.3f), contrasting the upregulation with either indo or Pb at the same age (Fig. 4.3b,d). These results reveal a distinct association between sex and toxicant exposure in the differential upregulation of miR-34a by PND 21 in the Tg model, with observed correlations linking indo with male specificity and Pb with female specificity.

4.3.5 *DAP12 immunoreactivity within the CA3 corroborated miRNA data, and revealed the early development of a sex-specific dysfunctional microglial phenotype*

The functional implications of altered miRNA expression early in postnatal development was investigated via changes in DAP12, expressed only in healthy perinatal microglia and critical to synaptic pruning (Roumier et al., 2004), in the CA3 hippocampal subregion. Both WT and Tg control mice exhibited similar age-related changes in DAP12 expression depending on sex, that increased over time in females (Fig. 4.4a-b) to support late, intensive synaptic pruning and remained relatively low in males (Fig. 4.4c-d), with the exception of WT males at PND 15 (Fig. 4.4c). In response to indomethacin, microglia upregulate C3 complement (Prechel et al., 2000), encoded for by a gene directly coupled to that which encodes for DAP12, producing a phenotype that ultimately favors phagocytosis (Salter and Beggs, 2014). Immediately following cessation of indo exposure at PND 10, nearly all groups expressed increased DAP12 immunoreactivity, with the exception of WT males (Fig. 4.4c). However, indo-exposed WT males at PND 10 also expressed increased miR-34a, potentially mediating the effect of indo by decreasing TREM2. Similarly, Pb exposure resulted in increased DAP12 expression at PND 10 in all groups to a greater degree than indo (Fig. 4.4), inferring acute Pb-related damage and subsequent increased DAP12-dependent phagocytosis.

WT females developmentally exposed to Pb exhibited increased DAP12 expression in the hippocampus at PND 10 that dramatically decreased and remained low compared to control from PND 15-21 (Fig. 4.4a). Exposure to indo, conversely, produced a similar expression pattern over time, but less pronounced at each age. Although the combination of indo+Pb in WT females produced significantly increased DAP12 at PND 10, the effect was short-lived, as levels became comparable to controls at PND 15 and 21 (Fig. 4.4a). At PND 10, WT males exhibited increased DAP12 with Pb and indo+Pb exposure, but by PND 15 there was a dramatic decrease with indo and indo+Pb exposure, and only a modest decrease with Pb compared to controls (Fig. 4.4c). By PND 21, WT males exposed to indo+Pb exhibited significantly

decreased DAP12 expression, whereas indo- and Pb-exposed groups were comparable or slightly higher than control levels.

Surprisingly, females in both WT and Tg groups exhibited similar expression patterns for DAP12 in terms of age and exposure, with the exception of Pb-exposed Tg females at PND 15 that exhibited levels comparable to control (Fig. 4.4b). Pb exposure in the Tg males, conversely, resulted in significantly increased DAP12 at PND 10 (Fig. 4.4d), as opposed to the modest increase at PND 10 in the WT Pb-exposed males (Fig. 4.4c), that decreased over time to levels slightly higher than those of age-matched controls. Indo-exposed Tg males maintained near-control levels of DAP12 at PND 10 and 21, but at PND 15 there was a significant spike in expression that was mimicked slightly in the indo+Pb group at the same age (Fig. 4.4d). A similar, yet opposing age-related trend occurred with indo or indo+Pb exposure in WT males at PND 15, suggesting there exists a period of indo-specific sensitivity in males at PND 15 that results in opposing DAP12 expression depending on the mouse strain.

Fig. 4.1. Postnatal toxicant exposure altered miR-124 expression in a sex-dependent manner at PND 10 and 21, varying with strain, age, and treatment. Quantification of miR-124 relative expression expressed as fold change ±SEM over sex-, strain-, and age-matched controls in WT (a,c,e) and Tg (b,d,f) mice. n = 3 mice/sex/age/treatment/strain. $p < 0.05$ was considered statistically significant. * = significant between ages, # = significant between sex. PND: postnatal day, Tg: 3xTgAD, indo: indomethacin, ctl: control.

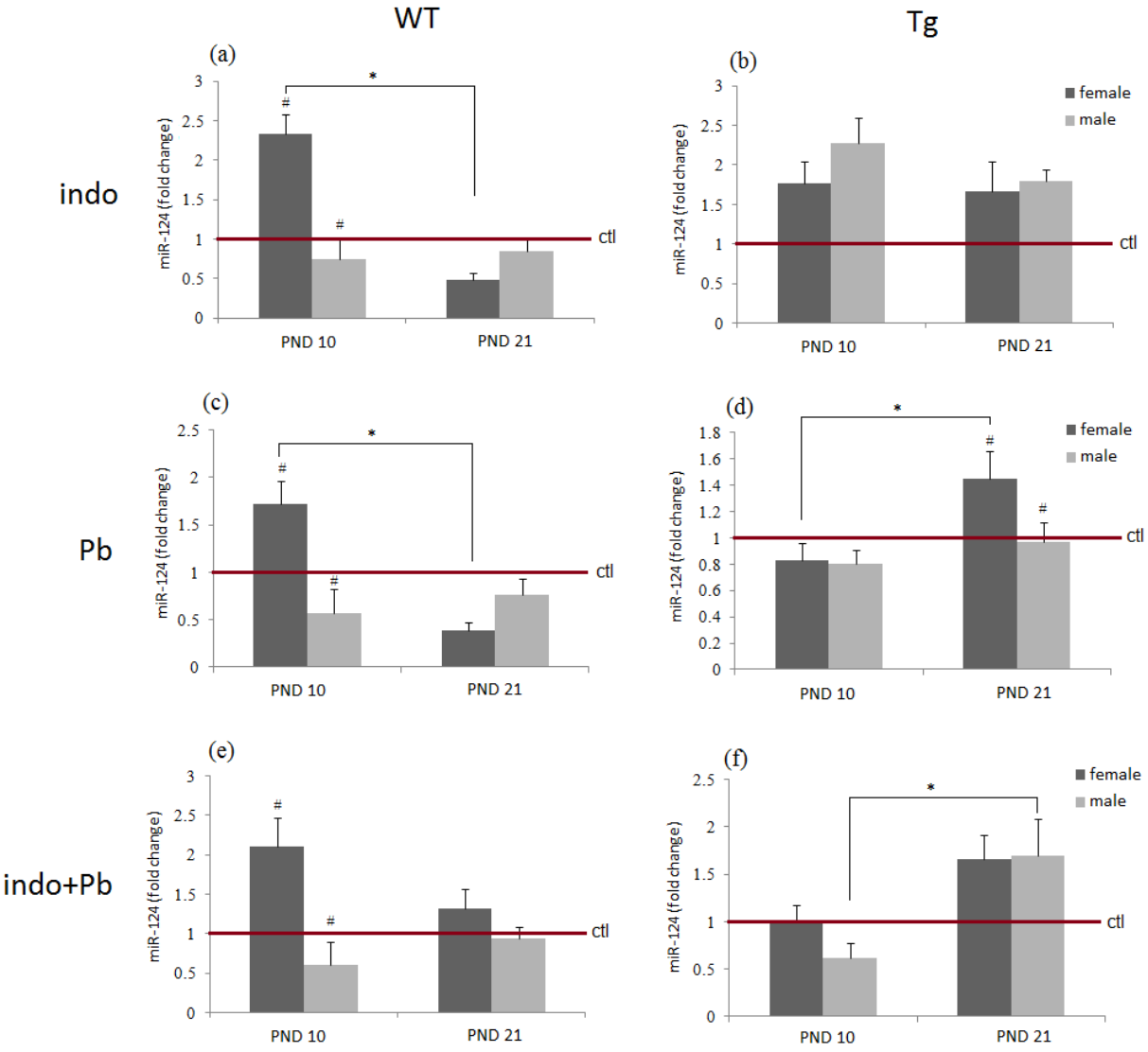
WT
Tg
indo
Pb
indo+Pb
(a)
(b)
(c)
(d)
(e)
(f)
miR-124 (fold change)
PND 10
PND 21
ctl
female
male
*
#

Fig. 4.2. Postnatal toxicant exposure altered miR-132 expression in a sex-dependent manner at PND 10 and 21, varying with strain, age, and treatment. Quantification of miR-132 relative expression expressed as fold change ±SEM over sex-, strain-, and age-matched controls in WT (a,c,e) and Tg (b,d,f) mice. n = 3 mice/sex/age/treatment/strain. $p < 0.05$ was considered statistically significant. * = significant between ages, # = significant between sex. PND: postnatal day, Tg: 3xTgAD, indo: indomethacin, ctl: control.

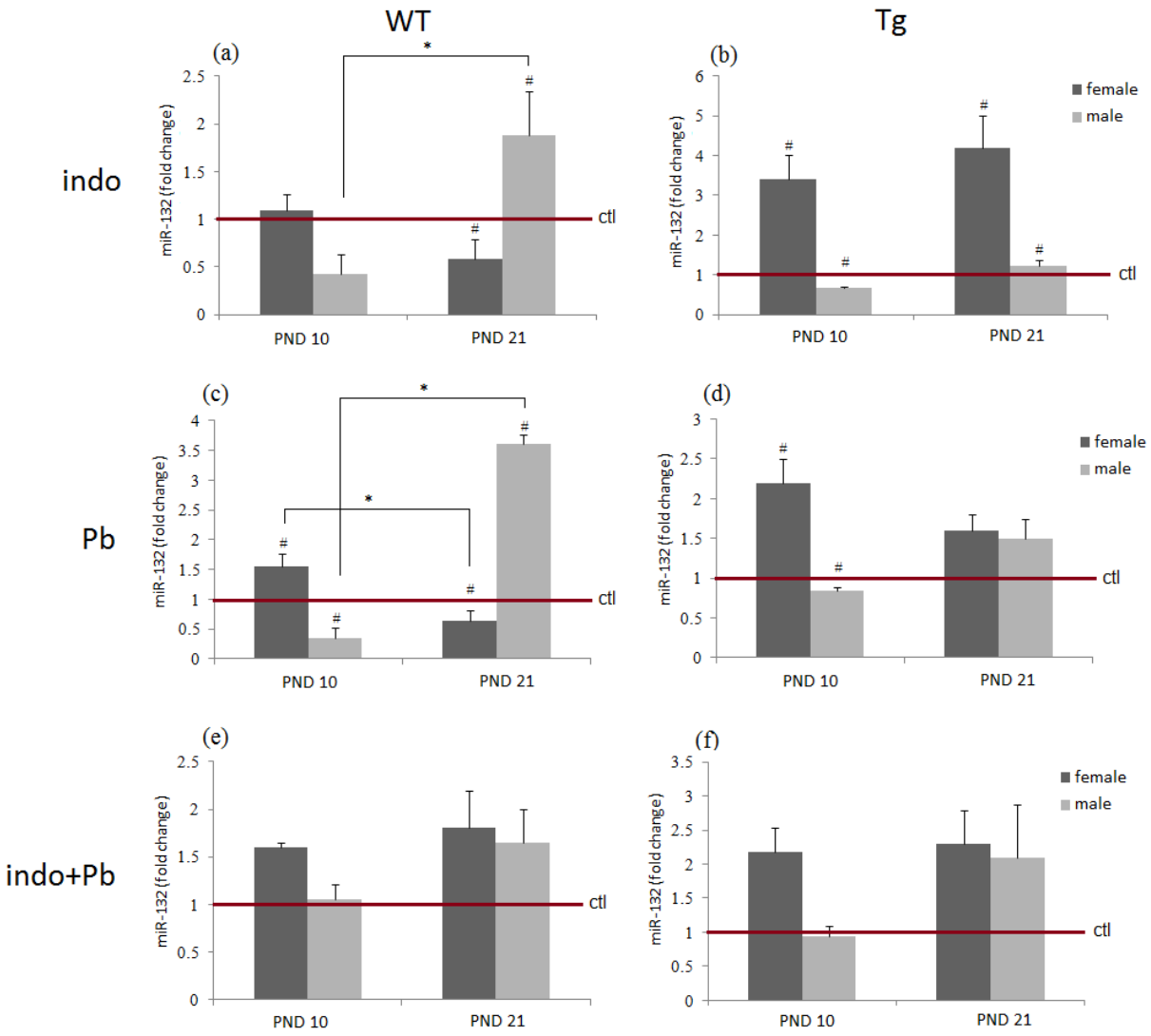
WT
Tg
indo
Pb
indo+Pb
(a)
(b)
(c)
(d)
(e)
(f)
miR-132 (fold change)
PND 10
PND 21
ctl
female
male
*
#

Fig. 4.3. Postnatal toxicant exposure altered miR-34a expression in a sex-dependent manner at PND 10 and 21, varying with strain, age, and treatment. Quantification of miR-34a relative expression expressed as fold change ±SEM over sex-, strain-, and age-matched controls in WT (a,c,e) and Tg (b,d,f) mice. n = 3 mice/sex/age/treatment/strain. $p < 0.05$ was considered statistically significant. * = significant between ages, # = significant between sex. PND: postnatal day, Tg: 3xTgAD, indo: indomethacin, ctl: control.

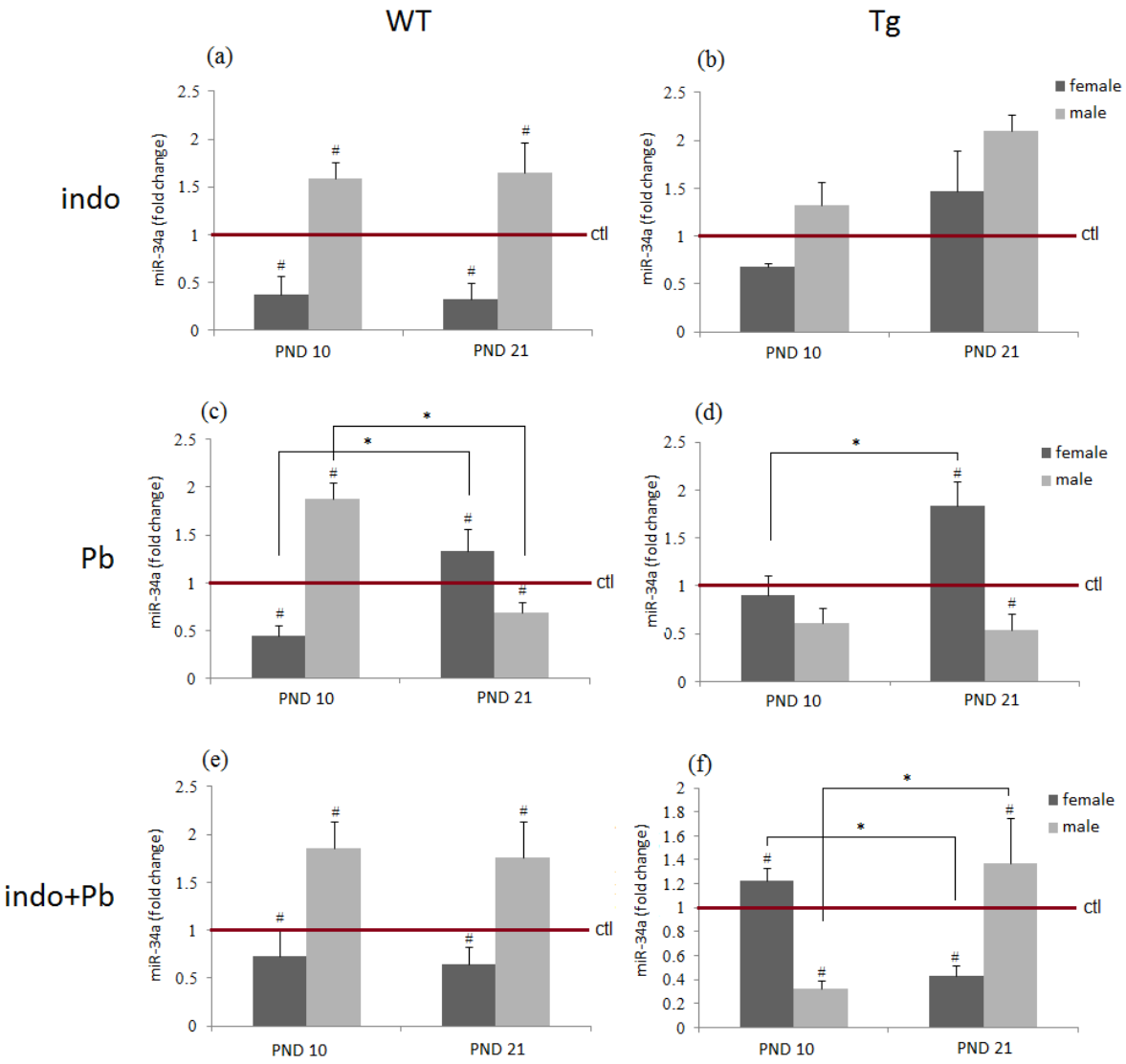
WT
Tg
indo
Pb
indo+Pb
(a)
(b)
(c)
(d)
(e)
(f)
miR-34a (fold change)
ctl
PND 10
PND 21
female
male
*
#

Fig. 4.4. Postnatal toxicant exposure altered DAP12 expression over time, depending on sex and strain. (a-d) Quantification of DAP12-positive immunoreactivity in the CA3 hippocampal subregion of WT (a, female; c, male) and 3xTgAD (b, female; d, male) mice, expressed as mean % ROI ±SEM. n = 3-5 mice/sex/age/treatment/strain. (e) Representative images of 3xTgAD hippocampus at PND 21 treated with control (left column) or Pb (right column). scale bar = 26 μm. *$p < 0.05$ was considered statistically significant. Statistical significance with age represented by lines above graph grouped by treatment. PND: postnatal day, ROI: region of interest, WT: wildtype, indo: indomethacin, ctl: control.

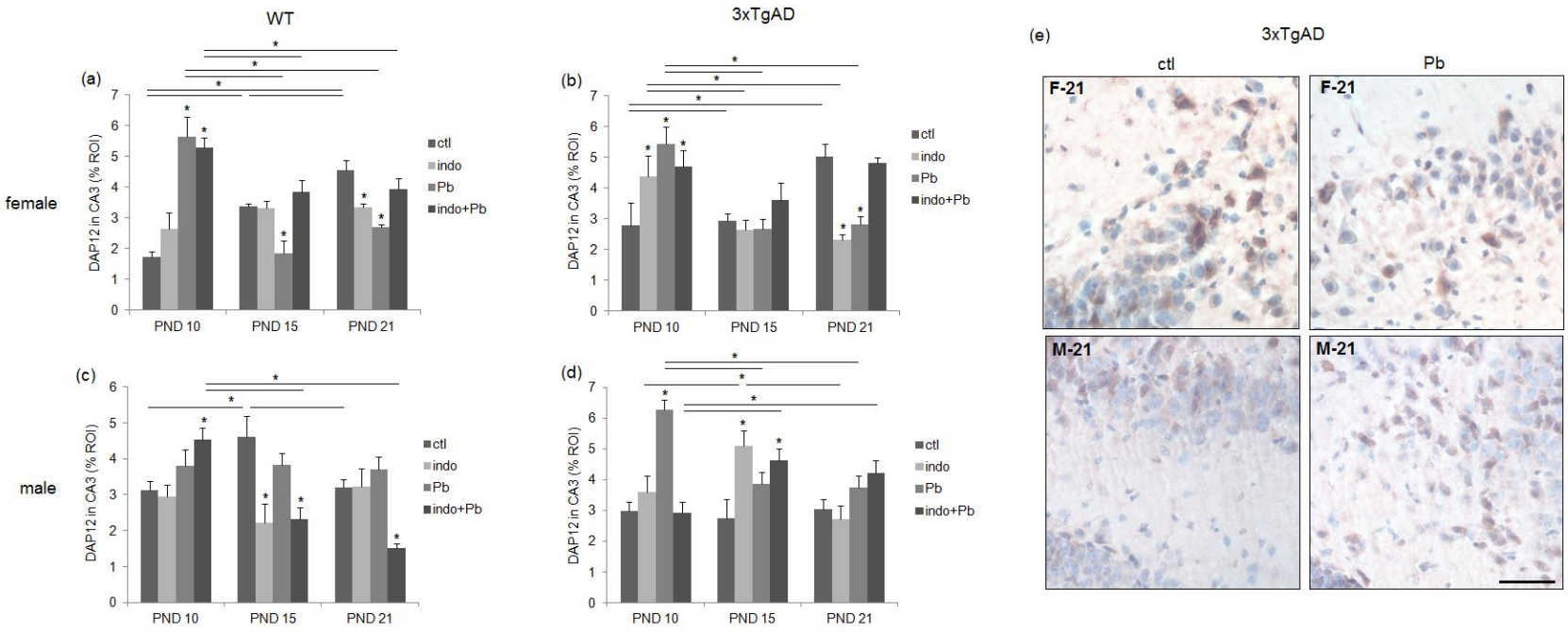
WT
3xTgAD
female
male
(a)
(b)
(c)
(d)
DAP12 in CA3 (% ROI)
PND 10
PND 15
PND 21
ctl
indo
Pb
indo+Pb
(e)
3xTgAD
ctl
Pb
F-21
F-21
M-21
M-21

4.4 Discussion

This is the first study to examine sex-specific changes in developmental neurimmiRs consequent to postnatal toxicant exposure in a DOAD model of AD, supporting our hypothesis that disruption of neuroimmune development initiates sex-biased susceptibility to later-life neurodegeneration through GxE interactions and epigenetic regulation for a susceptible phenotype. This study has three important findings: 1) changes in neurimmiRs due to postnatal toxicant exposure were atypical, further exacerbating poor developmental conditions in the 3xTgAD GxE model compared to WT; 2) distinct sex differences in epigenetic changes were observed, consequent to exposure during harmonic microglia and neuronal maturation; and 3) the results support a GxE, female-specific complimentary neurimmiR expression pattern, relevant to the formation of imbalanced microglia:neuron interactions and subsequent promotion of later-life neurodegeneration, as a “primed” phenotype of latent AD vulnerability.

The GxE interaction of environmental toxicant exposure and genetic proclivity to AD resulted in atypical microRNA expression changes that were distinct from those observed in the WT groups, such that changes were either in opposition to congruent and homeostatic pathways, sustained throughout a sensitive developmental window, or detrimental to normal, sex-specific neuroimmune maturation. The three target neurimmiRs utilized in the present study (miR-124, miR-132, miR-34a) were chosen based on their interrelated regulatory effects on neuronal and microglial phenotypes. Those phenotypes are not only pertinent to healthy development and maturation (Soreq and Wolf, 2011), but are also known to influence neuroimmune functions critical in homeostatic synapse dynamics, as synaptic dysfunction is thought to be one of the earliest pathologies in AD (Du et al., 2010; Masliah et al., 2001).

MicroRNAs are particularly useful in investigating these dysfunctional phenotypes because, as environmentally-sensitive genomic regulators, altered expression of a single miRNA can affect entire, interconnected pathways and signaling cascades rather than single proteins (Sollome et al., 2016). Furthermore, the utility of miRNAs as circulating biomarkers is increasingly recognized in numerous biomedical fields (Reid et al., 2011), with considerable potential for DOAD studies. A recent report by Gillet and colleagues (2016) underscored the correlation between toxicant-altered microRNA expression and neurodevelopmental disorders, as well as the need to interpret these correlations using known developmental neurotoxicants in order to decode biological relevance and pathological roles. The present study aimed to address this need within the context of AD by utilizing Pb, a well-characterized developmental neurotoxicant, as well as a WT model comparison to delineate baseline effects of toxicant-specific changes to microRNAs. Thus, the dramatic difference between WT and Tg changes to sex- and toxicant-specific microRNA expression (Fig. 4.1-4.3) suggest that our GxE DOAD experimental paradigm resulted in a unique microRNA “signature” with implications for a distinct form of exacerbated cellular vulnerability.

This GxE exacerbation is readily observable in expression data for miR-124 (Fig. 4.1), the most abundant miRNA in the brain (Cheng et al., 2009). The half-life of microRNAs was recently investigated, revealing that the majority of microRNAs persist for approximately five days without external stimulus (Gantier et al., 2011). Thus, the persistence of altered expression for the 11 day span between PND 10 and 21 suggests there is continuation of stimulus despite cessation of exposure. In the case of microRNAs not typically expressed during development, such as with miR-124 and miR-34a, sustained expression could also infer a lack of rectifying signals or, perhaps, the formation of rifts between miRNAs involved in compatible signaling pathways. The acute increase in miR-124 in WT females at PND 10 due to either indo or Pb

exposure that was rectified by PND 21 (Fig. 4.1a,c), suggests that the exposure window was specific for female neuroimmune parenchymal targets, and that these targets were capable of preventing the formation of damaging, long-lasting regulatory changes during critical periods of neuroimmune development. However, this was not seen in Tg mice, as exposure either sustained expression until or increased expression at PND 21 (Fig. 4.1b,d,f), with only Pb-exposed Tg males exhibiting a slight resiliency to this effect. These data infer that, although sex and treatment incurred some effect, the promotion of atypical and detrimental epigenetic regulation was substantially exacerbated and influenced by GxE effects. However, the most profound detrimental phenotype occurred in Pb-exposed Tg females, likely a direct result of altering the sex-specific neuroimmune environment and subsequent signaling requirements for healthy development.

Both rodent and human brains undergo sexually dimorphic development, specifically within the postnatal period, during which an early surge of androgens promotes the masculinization of the male brain (Lenz et al., 2013). This sex difference is evident in the number and phenotype of microglia at varying time points in brain development; a spike in the number of amoeboid microglia in males parallels a testosterone surge at PND 4, whereas amoeboid microglia numbers within specific brain regions don't peak in female brains until PND 30 (Schwarz et al., 2012). Previously, the first two postnatal weeks were generally considered a period of male-specific microglial vulnerability to later-life immune-related priming (Schwarz and Bilbo, 2012), but, here, we report a comparable postnatal window of female-specific microglial and neuronal vulnerability to epigenetic regulation for unbalanced later-life crosstalk and response patterning. We explored the relative contribution of the masculinizing signaling microenvironment versus neuroimmune maturation stage by using indo to inhibit PGE_2, which is increased postnatally in males by testosterone and critical to brain masculinization (Lenz et al.,

2013). Indo exposure from PND 5-9 resulted in Tg-specific ablation of significant sex differences at each age for miR-124 (Fig. 4.1b) and miR-34a (Fig 4.2b), but not for miR-132 (Fig. 4.3b); the opposite was observed in the WT model, which retained significant sex differences in microRNA alterations at PND 10 for miR-124 (Fig. 4.1a) and miR-34a (Fig. 4.2a), and the eventual formation of sex-specific miRNA response by PND 21 for miR-132 (Fig. 4.3a). These results suggest, first, that sex-specific brain development and relevant regulatory pathways therein are still partially retained in WT mice exposed to indo, inferring the presence of non-PGE_2-related counterbalanced pathways capable of producing epigenetic changes that are either dysfunctional or no longer tightly regulated for homeostasis in Tg mice. Secondly, these results show a divergence in the sex-related promotion of altered miR-132, compared to miR-124 and miR-34a – specifically, the sustained, dramatic upregulation of miR-132 in Tg females, as opposed to the similarity in pattern over time between WT and Tg males (Fig. 4.2b). It is likely the case that altered miR-132 from indo exposure in Tg females is unrelated to PGE_2, as this pro-inflammatory prostaglandin is decreased postnatally in female microglia. Instead, an exacerbated effect culminating from indo-related anti-inflammatory signals resulted, in addition to or overshadowing those typically derived neuronally, targeting highly sensitive mechanisms that produce epigenetic regulation. Despite an unclear mechanism, the unrestricted or unbalanced nature for epigenetic change with Tg female specificity is notable, especially when considering miR-132, along with any self-restricting signals or complimentary microRNAs, are upregulated during normal postnatal development (Soreq and Wolf, 2011).

The female phenotype of susceptibility promoting dysfunctional neuroimmune crosstalk was specific to postnatal Pb exposure in the Tg mouse model, congruent with our previous studies (vonderEmbse et al., 2017; manuscript under review), with less severe detrimental effects also observed in other experimental groups in a toxicant- and sex-specific manner.

Upregulation of miR-124 during the first few postnatal weeks, when expression is normally suppressed, is detrimental to balanced neuroimmune development in itself, but, in Pb-exposed Tg females, increased miR-124 expression at PND 21 (Fig. 4.1d) has severe implications for the developing female brain. Upregulation of miR-124 has been shown to promote microglial quiescence and restrict proliferation through inhibition of CEBPα, the transcription factor PU.1, and its downstream target CSF1R (Ponomarev et al., 2011). The sex-specific increase in amoeboid microglia around PND 30, preceded by a highly proliferative period to populate various brain regions, was observed in previous studies (Schwarz et al., 2012). This would suggest a premature increase in miR-124 may limit proliferation and subsequent region-specific populations; future studies could utilize miR-424 to analyze cognate epigenetic signaling and feedback loop perturbations, as miR-424 is both upregulated by PU.1 and further upregulates M-CSF receptor expression (Guedes et al., 2013). Likewise, early upregulation of miR-124 may be promoting a microglial phenotype unsupportive to increasing healthy synaptic pruning at this time that is critically dependent on DAP12-positive activated/immature microglia. As anticipated, our data revealed decreased DAP12 expression at PND 21 consequent to Pb exposure in Tg females (Fig. 4.4d), that would suggest decreased phagocytic capabilities of microglia in these mice. In addition, increased miR-34a (Fig. 4.3d) has been shown to decrease TREM2 expression by targeting parts of its mRNA (Bhattacharjee et al., 2016). TREM2, along with its cognate adaptor protein DAP12, is critical to developmental phagocytosis without pro-inflammatory signaling (Takahashi et al., 2005), again corroborating epigenetic regulation in favor of dysfunctional microglia at PND 21.

Expression of miR-34a both strongly promotes, and is itself promoted by, p53 as a cellular stress response leading to apoptosis and senescence (Rokavec et al., 2014). Interestingly, mutations to presenilin2, one of the genes implicated in familial AD, has been

shown to trigger neuronal apoptosis via the miR-34a/p53 axis (Li et al., 2017). Likewise, TP53, the “apoptosis gene” that encodes for p53, is mutated in some cases of AD (Rokavec et al., 2014). Therefore, the increase in miR-34a by PND 21 in Pb-treated females (Fig. 4.3c,d), and indo- or Pb-exposed Tg females (Fig. 4.3b,d) highlights an exacerbated epigenetic stress response in Tg females that is observable to a lesser extent in Pb-exposed WT females and indo-exposed Tg females, and reversed in indo+Pb-exposed Tg females (Fig. 4.3f). This upregulation could be interpreted as evidence of cellular stress and favorable conditions for apoptosis and senescence, without the healthy concomitant neuroprotective presence of phagocytic microglia. As yet another tie-in to neurodegeneration, miR-34a can induce p53 activity through inhibition of *SIRT1* (Rokavec et al., 2014), a deficiency of which in microglia has been demonstrated to have a causative role in aging-related cognitive deficits and neurodegeneration through epigenetic regulation of IL-1β (Cho et al., 2015). In further acknowledgement of mutated TREM2 or DAP12 in Nasu-Hakola disease (Thrash et al., 2009), the multiple AD-like neurodegenerative disorders associated with mutations to or epigenetic regulation of the miR-34a/p53 axis and related targets is uncanny.

The potentiated transition to ramified microglia by either premature or unregulated miR-124 expression may forcibly “mature” female microglia without the necessary, congruent maturation of neurons, disjointing the healthy development of inhibitory signals for activation. This theory is substantiated by reports that impaired activation of *REST*, inhibited by miR-124, delayed the maturation of NMDA receptors by retaining the prevalence of highly excitable GluN2B subunits, which, in ectopic form, have also been associated with amyloid-β production (Rodenas-Ruano et al., 2012; Bordji et al., 2010). Additionally concerning is the initial increase in miR-132 at PND 10 that was sustained until PND 21 (Fig. 4.2d). Although miR-132 is upregulated for the first 2-4 weeks of postnatal development during a period of NMDA-

dependent synaptic pruning, additional upregulation may disrupt the miR-132-promoted positive feedback loop in NMDA depolarization, further exacerbated by what we anticipate to be immature and highly excitable NMDA receptors, and also interfering in GABAergic interneuron maturation (Miller et al., 2012). Furthermore, both miR-124 and miR-132 are known to promote neurite sprouting (Soreq and Wolf, 2011). Thus, our results provide evidence that, at PND 21, Pb-exposed Tg females strongly promoted epigenetic regulation for disjointed microglia:neuron maturation, with implications for the formation of unbalanced, hyperexcitable neuronal circuitry without appropriate microglial support. This detrimental epigenetic phenotype was retained for up to 12 days following cessation of Pb exposure and could set the stage for gradual, atypical adaptation and ultimate maladapation for microglia:neuron crosstalk. In addition, higher levels of miR-132 have been observed during the light portion of the circadian cycle in the suprachiasmatic nucleus, and as well as in the hippocampus of chronically stressed rats (Meerson et al., 2010; Cheng et al., 2007). This would suggest globally elevated miR-132 may be pathologically pertinent to the development of AD-related atypical circadian rhythms or stress-induced brain region specificity.

In the healthy adult brain, transient changes to miRNAs are often the result of the immediate microenvironment, promoting functional changes to parenchymal targets as a cellular adaption to exogenous influences – temporarily shifting the requirements for homeostasis. During development, however, altered miRNAs during critical windows of neuroimmune development have direct consequences on the development of homeostatic baselines, immune maturation and learning, and even patterns of functional response phenotypes. The results of these early, atypical epigenetic changes can have vast implications on later-life adaptability. Consider the parallels in requirements for microglia:neuron crosstalk within the hippocampus during postnatal development and adult neurogenesis – both require strict, region-specific

signals balanced for appropriate promotion of synaptogenesis and synaptic pruning. The associated microglia:neuron crosstalk is extensive and multifaceted, formed during a period of congruent, interrelated development. MicroRNA expression patterns are both evidentiary of past exogenous influences and predictive or future cellular response, such that altered miRNAs promoting the disjointed development of microglia and neurons early in life may likely impact the intertwined functionality of neuroimmune cells throughout life.

As hypothesized, our study demonstrated a clear female bias in the exacerbating effect of GxE interactions in early epigenetic regulation promoting later life maladaptibility and neuroimmune dysfunction, which we have previously correlated with heightened susceptibility to AD (manuscript under review). We have also shown that, although the most detrimental phenotype occurred in Pb-exposed Tg females, there was evidence to suggest that this DOAD model may be useful in investigating toxicant- and timing-specific windows of vulnerabilities for other sex-biased adult diseases. To this end, future studies could utilize alternative transgenic models of disease and specific neurimmiRs critical to microglia:neuron crosstalk, such as those supported by the present study, as well as sex-specific miRNAs upregulated during development. Ultimately, investigation of these early perturbations to epigenetic regulation of cellular phenotype could reveal thresholds of adaptability consequent to atypical developmental conditions, and potential identification of biomarkers for susceptibility.

Chapter 5:

General Discussion and Future Directions

The putative influence of the perinatal environment on adult health and disease is a compelling, if not counterintuitive, hypothesis that has gained the attention of researchers in a wide array of biomedical disciplines. Perhaps most mechanistically elusive is a subset of DOAD research concerning slow-developing diseases in which aging is the primary risk factor, such as Alzheimer's (AD) and Parkinson's disease (PD). Within these late-developing diseases, the majority of cellular phenotypes at time of either diagnosis, emergence of hallmark molecular pathologies, or experimental evaluation are often compensatory in nature or convoluted by the overwhelming presence of complementary signaling cascades and feedback loops. This is particularly evident in recent research investigating the role of microglia in AD pathogenesis. Despite the field's gradual transition towards the Dystrophic Microglia Hypothesis and the accumulating data corroborating the late senescent morphology, few studies have attempted detection of a pre-dystrophic, susceptible phenotype, apart from those focused on cellular exhaustion and hyper-reactive priming. Given the relatively normal functionality of microglia throughout the majority of the organism's life and likelihood of multiple waves of compensation over time, it is no surprise that this stochastic lifelong phenotype has yet to be comprehensively characterized. In addressing this endeavor within the DOAD context of AD, our global research directive incorporated a macroscopic-to-microscopic approach to, first, establish a functional model by which thresholds of adaptation might be quantifiable, and, second, evaluate plausible gene x environment (GxE)-related provocateurs of latent, susceptible phenotypes, such as detrimental epigenetics, that would attempt to reconcile conflicting correlational-vs-causational data.

Within the present thesis, postnatal toxicant exposure in 3xTgAD (Tg) mice was utilized to model GxE interactions exacerbating disease susceptibility consequent to poor developmental conditions, and, in support of our hypothesis, demonstrated a decisive female bias in microglia dysfunction and concurrent pathological vulnerability at multiple pathological stages. Additionally, integration of data reported in this thesis substantiates a critical pathological role in AD for the latent maladaptation of microglia, initiated by an early ripple of functional phenotypic imbalances that are incapable of resolution due to derivation during critical windows of development. This interpretation contrasts sharply with current hypotheses surrounding aging-related microglial senescence and theories of metabolic exhaustion. Microglia inhabit an exceptionally unique role in the CNS, expansive both in breadth and depth, that, given their relative longevity and limited proliferative pool, challenges the stability of an aging hypothesis whose central tenet is a truncated time limit for the sole resident immune cell, critical glial cell, and multipotent stem cell of the CNS. Were that the case, AD cases would be far more commonplace, if not guaranteed by a certain age, and manifest with far more pathological variability.

The lead (Pb)-exposed Tg female-specific vulnerability was present throughout all three correlative studies, and was detectable early in postnatal development as detrimental neurimmiR profiles and DAP12 expression (Chapter 4). In consideration of the unique demands of the neuroimmune system during sexually dimorphic development, these GxE females expressed abnormally high levels of miR-124 and miR-34a globally, and low levels of DAP12 in the CA3, early in a critical period of hippocampal synaptic pruning for females at PND 21. Not only do these atypical miRNA levels represent unbalanced stimulation for epigenetic regulation, itself a red flag for homeostasis and lifelong phenotypic plasticity, but they also suggest that the

respective development of microglia and neurons and subsequent maturation of dynamic crosstalk were becoming disjointed. The quintessential variable for this disordered neuroimmune development was the premature upregulation of miR-124, which simultaneously acts to delay neuronal maturation and promote microglia quiescence (Guedes et al., 2013), among other equally disadvantageous effects for females at this age. Overexpression of miR-124 has been shown to promote neurite sprouting and limit synaptic long term facilitation, with implications for gross imbalances in excitability supported by exceptionally high levels of miR-132 at PND 10 that were sustained or continually promoted until PND 21 (Fig. 4.2d). The reduced expression of DAP12 compared to controls (Fig. 4.4b) and upregulation of miR-34a (Fig. 4.3d) at PND 21 inferred epigenetic, functional downregulation for the “silent” amoeboid microglia phenotype necessary for synaptic pruning. Taken together, these data suggest the presence of unbalanced epigenetic regulation related to poor developmental conditions specific to females that likely elicited the permanent re-patterning of response phenotypes in microglia:neuron signaling.

In Chapter 3, the results demonstrated precisely that. Microglia:neuron signaling in Pb-exposed Tg females transitioned from adaptive to maladaptive within an amyloid-stressed neuronal environment, evident of tersely functional, yet non-homeostatic phenotypic regulation that could be anticipated to result from chronic waves of compensatory signaling. Studies of microglial DAP12 loss-of-function have shown alterations to synaptic plasticity and dramatic reductions in neuronal TrkB expression (Roumier et al., 2004), implicating that early reductions in DAP12 expression during a critical window (Ch. 4) and later imbalanced-turned-detrimental signaling through the TrkB receptor (Ch. 3) could be connected via a common variable: the persistence of a temporally unstable phenotype, such as is developmentally-derived via epigenetics. Similarly, the forced, premature expression of miR-124 (Fig. 4.1), implying

consequent inhibition of PU.1 and reduced CSF1R, may limit the proliferative potential of migrating microglia at PND 21 and subsequent pool of region-specific mature microglia, corroborated by depleted neuroprotective ferritin by PND 240 (Fig. 3.3). Furthermore, premature miR-124 could encourage altered sensitivity to neuronally-derived activating signals, as is noted in the decisively aberrant microglial polarization profiles from PND 120-240 (Ch. 3). Despite slight variability in length of postnatal exposure, the consistent female bias throughout the three studies underscores a definitive critical window of neuroimmune development for female microglial "priming" for later-life susceptibility to accelerated aging and neurodegeneration. The overlapping exposure windows encompassed a postnatal period of considerable sexual dimorphism in microglial maturation, substantiating the interpretation that sex-specific susceptibility later in life was mediated through our purported parenchymal target. Likewise, sex- and toxicant-specific contributions to atypical epigenetic reprogramming, evaluated in Chapter 4, further support our characterization of a critical period of postnatal development for microglia, with substantial influence of sex on variability in phenotypic perturbations.

Through novel demonstration of early epigenetic neuroimmune reprogramming and gradual maladaptation in the amyloid-stressed adult CNS, we have attempted to describe DOAD effects for AD-related dystrophic microglial phenotypes that likely participate in female AD susceptibility observed in Chapter 2. Moreover, we have established GxE synergism as a significant contributing factor in postnatal neuroimmune vulnerability. While this is not the first set of experiments to posit a role for developmental toxicity in AD, it stands apart by utilizing a pathogenically holistic, yet hypothesis-driven approach to elucidate temporally-targeted molecular mechanisms spanning the course of an organism's lifetime. Slow-developing biomarkers of disease have been notoriously difficult to definitively characterize *in vivo*,

highlighting the utility and efficacy of this DOAD model for the investigation of complex disease etiologies via a high degree of variability in scope and scale.

It is important to note that, within the present thesis, there are still considerable gaps in knowledge yet to be addressed in order to parse out more direct, linear mechanisms; in that endeavor, more traditional DIT experimental paradigms may be necessary. However, in consideration of the enormity and complexity of scientific knowledge now being generated, our DOAD experimental paradigm acts to some degree as a variation on "integrative pluralism," first proposed by Mitchell (2009) to describe a new conceptual framework by which scientific practice investigates contextually dynamic, multifaceted systems. Not without its own shortcomings, the utilization of such integrative scientific practices in an attempt to more effectively and holistically interact with vast quantities of interdependent data may become commonplace. The emergence of the DOAD hypothesis is, itself, testimony to such scientific evolution. It could even be argued that this new conceptualization is both necessary and pertinent to qualitatively balance another burgeoning form of scientific evolution – high-throughput, *in vitro* assays, 'omics (e.g. metabolomics, proteomic, exposomics, etc.), and genome-wide arrays, to name a few "quantity"-focused techniques. Nevertheless, the growing trends in data non-reproducibility and ineffectiveness of therapeutics derived from rodent studies demand revision of current practice. This thesis is our early contribution to said reformation.

References

Alekseenko AV, Waseem TV, Fedorovich SV. 2008. Ferritin, a protein containing iron nanoparticles, induces reactive oxygen species formation and inhibits glutamate uptake in rat brain synaptosomes. Brain Res. 1241:193-200.

Ajmone-Cat M, Bernardo A, Greco A, Minghetti L. 2010. Non-steroidal anti-inflammatory drugs and brain inflammation: effects on microglial functions. Pharmaceuticals. 3(6): 1949-1965. doi:10.3390/ph3061949

Armstrong RA. 2009. The molecular biology of senile plaques and neurofibrillary tangles in Alzheimer's disease. Folia Neuropathol. 47(4): 289-299.

Baglioni S, Casamenti F, Bucciantini M, Luheshi LM, Taddei N, Chiti F, Dobson CM, Stefani M. 2006. Prefibrillar amyloid aggregates could be generic toxins in higher organisms. J Neurosci. 26(31): 8160-8167.

Banati RB, Gehrmann J, Schubert P, Kreutzberg GW. 1993. Cytotoxicity of microglia. Glia. 7:111-118.

Bark IC, Hahn KM, Ryabinin, Wilson MC. 1995. Differential expression of SNAP-25 protein isoforms during divergent vesicle fusion events of neural development. Proc. Natl. Acad. Sci. U.S.A. 92(5):1510-1514.

Basha, M.R., Wei, W., Bakheet, S.A., Benitez, N., Siddiqi, H.K., Ge, Y.W., Lahiri, D.K., Zawia, N.H. 2005. The fetal basis of amyloidogenesis: exposure to lead and latent overexpression of amyloid precursor protein and β-amyloid in the aging brain. J Neurosci. 25(4): 823-829.

Becher B, Antel JP. 1996. Comparison of phenotypic and functional properties of immediately ex vivo and cultured human adult microglia. Glia.18:1-10.

Bernard PB, MacDonald DS, Gill DA, Ryan CL, Tasker RA. 2007. Hippocampal mossy fiber sprouting and elevated trkB receptor expression following systemic administration of low dose domoic acid during neonatal development. Hippocampus. 17(11):1121-1133.

Bessis A, Béchade C, Bernard D, Roumier A. 2007. Microglial control of neuronal death and synaptic properties. Glia. 55(3):233-238. doi:10.1002/glia.20459.

Bhattacharjee S, Zhao Y, Dua P, Rogaev EI, Lukiw WJ. 2016. microRNAs-34a-mediated down-regulation of the microglial-enriched triggering receptor and phagocytosis-sensor TREM2 in age-related macular degeneration. PLOS ONE. 11(4): e0153292

Bian S, Sun T. 2011. Functions of noncoding RNAs in neural development and neurological diseases. Mol Neurobiol. 44: 359-373. doi:10.1007/s12035-011-8211-3.

Bilbo SD. 2010. Early-life infection is a vulnerability factor for aging-related glial alterations and cognitive decline. Neurobiol Learn Mem. 94(1):57-64.

Bilbo SD, Schwarz JM. 2009. Early-life programming of later-life brain and behavior: a critical role for the immune system. Front Behav Neurosci. 3(14): 1-14.

Blasi J, Chapman ER, Link E, Binz T, Yamasaki S, de Camilli P, Südhof TC, Niemann H, Jahn R. 1993. Botulinum neurotoxin A selectively cleaves the synaptic protein SNAP-25. Nature. 365:160-163.

Bolmont T, Haiss F, Eicke D, Radde R, Mathis CA, Klunk WE, Kohsaka S, Jucker M, Calhoun ME. 2008. Dynamics of microglial/amyloid interaction indicate a role in plaque maintenance. Neurobiol Dis. 28(16):4283-4292.

Bordji K, Becerril-Ortega J, Nicole O, Buisson A. 2010. Activation of extrasynaptic, but not synaptic, NMDA receptors modified amyloid precursor protein expression pattern and increases amyloid-β production. J Neurosci. 30(47): 15927-15942.

Burns-Naas LA, Hastings KL, Ladics GS, Makris SL, Parker GA, Holsapple MP. 2008. What's so special about the developing immune system? Int J Toxicol. 27:223-254.

Butchbach MER, Edwards JD, Schussler KR, Burghes AHM. 2007. A novel method for oral delivery of drug compounds to the neonatal SMNΔ7 mouse model of spinal muscular atrophy. J Neurosci Meth. 161(2):285-290.

Campanella M, Sciorati C, Tarozzo G, Beltramo M. 2002. Flow cytometric analysis of inflammatory cells in ischemic rat brain. Stroke. 33:586-592.

Carson MJ, Thrash JC, Walter B. 2006. The cellular response in neuroinflammation: the role of leukocytes, microglia and astrocytes in neuronal death and survival. Clin Neurosci Res. 6(5): 237-245.

Chamniansawat S, Chongthammakun S. 2015. Inhibition of hippocampal estrogen synthesis by reactive microglia leads to down-regulation of synaptic protein expression. NeuroToxicology. 46:25-34.

Chan WY, Kohsaka S, Rezaie P. 2007. The origin and cell lineage of microglia – new concepts. Brain Res Rev. 53(2): 344-354.

Cheng LC, Pastrana E, Tavazoie M, Doetsch F. 2009. miR-124 regulates adult neurogenesis in the subventricular zone stem cell niche. Nat Neurosci. 12(4):399-408. doi:10.1038/nn.2294.

Cheng HYM, Papp JW, Varlamova O, Dziema H, Russell B, Curfman JP, Nakazawa T, Shimizu K, Okamura H, Impey S. microRNAs modulation of circadian-clock period and entrainment. Neuron. 54(5): 813-829.

Chin-Chan M, Navarro-Yepes J, Quintanilla-Vega B. 2015. Environmental pollutants as risk factors for neurodegenerative disorders: Alzheimer and Parkinson diseases. Front Cell Neurosci. 9(124): 1-22.

Cho SH, Chen JA, Sayed F, Ward ME, Gao F, Nguyen TA, Krabbe G, Sohn PD, Lo I, Minami S, Devidze N, Zhou Y, Coppola G, Gan L. 2015. SIRT1 deficiency in microglia contributes to cognitive decline in aging and neurodegeneration via epigenetic regulation of IL-1β. J Neurosci. 35(2): 807-818.

Cikla U, Chanana V, Kintner DB, Udho E, Eickhoff J, Sun W, Marquez S, Covert L, Otles A, Shapiro RA, Ferrazzano P, Vemuganti R, Levine JE, Cengiz P. 2016. ERα signaling is required for TrkB-mediated hippocampal neuroprotection in female neonatal mice after hypoxic ischemic encephalopathy. eNeuro. 3(1):1-14. doi:10.1523/eneuro.0025-15.2015.

Combs CK, Karlo JC, Kao SC, Landreth GE. 2001. β-Amyloid stimulation of microglia and monocytes results in TNFα-dependent expression of inducible nitric oxide synthase and neuronal apoptosis. J Neurosci. 21(4):1179-1188.

Coppieters N, Dieriks BV, Lill C, Faull RLM, Curtis MA, Dragunow M. 2014. Global changes in DNA methylation and hydroxymethylation in Alzheimer's disease human brain. Neurobiol Aging. 35(6): 1334-1344.

Crain JM, Nikodemova M, Watters JJ. 2013. Microglia express distinct M1 and M2 phenotypic markers in the postnatal and adult central nervous system in male and female mice. J Neurosci Res. 91:1143-1151.

Cras P, Kawai M, Siedlak S, Mulvihill, Gambetti P, Lowery D, Gonzalez-DeWhitt P, Greenberg B, Perry G. 1990. Neuronal and microglial involvement in β-amyloid protein deposition in Alzheimer's disease. Am J Pathol. 137(2):241-246.

Dalmau I, Vela JM, González B, Finsen B, Castellano B. 2003. Dynamics of microglia in the developing rat brain. J Comp Neurol. 458(2):144-157. doi:10.1002/cne.10572.

Danzer SC, Kotloski RJ, Walter C, Hughes M, McNamara JO. 2008. Altered morphology of hippocampal dentate granule cell presynaptic and postsynaptic terminals following conditional deletion of TrkB. Hippocampus. 18:668-678.

Davis KE, Fox S, Gigg J. 2014. Increased hippocampal excitability in the 3xTgAD mouse model for Alzheimer's disease in vivo. PLOS ONE. 9(3): e91203.

Day JR, Min BH, Laping NJ, Martin G III, Osterburg HH, Finch CE. 1992. New mRNA probes for hippocampal responses to entorhinal cortex lesions in the adult male rat: A preliminary report. Exp. Neurol. 117:97-99.

Demars M, Hu YS, Gadadhar A, Lazarov O. 2010. Impaired neurogenesis is an early event in the etiology of familial Alzheimer's disease in transgenic mice. J Neurosci Res. 88(10): 2103-2117.

DeWitt JC, Peden-Adams MM, Keil DE, Dietert RR. 2012. Current status of developmental immunotoxicity: early-life patterns and testing. Toxicol Path. 40:230-236.

Dietert R. 2011. Role of developmental immunotoxicity and immune dysfunction in chronic disease and cancer. Reprod Toxicol. 31:319-326.

Dietert RR, Zelikoff JT. 2009. Pediatric immune dysfunction and health risks following early-life immune insult. Curr Ped Rev. 5(1):36-51.

Du H, Guo L, Yan S, Sosunov AA, McKhann GM, Yan SSD. 2010. Early deficits in synaptic mitochondria in an Alzheimer's disease mouse model. Proc. Natl. Acad. Sci. U.S.A. 107(43):18670-18675.

El Khoury J, Hickman SE, Thomas CA, Loike JD, Silverstein SC. 1998. Microglia, scavenger receptors, and the pathogenesis of Alzheimer's disease. Neurobiol Aging. 19(1S):S81-S84.

Ford AL, Goodsall AL, Hickey WF, Sedgwick JD. 1995. Normal adult ramified microglia separated from other central nervous system macrophages by flow cytometry sorting. J Immunol. 154:4309-4321.

Forny-Germano L, Lyra e Silva NM, Batista AF, et al. 2014. Alzheimer's disease-like pathology induced by amyloid-β oligomers in non-human primates. J Neurosci. 34(41): 13629-13643.

Fox DA, Grandjean P, de Groot D, Paule MG. 2012. Developmental origins of adult diseases and neurotoxicity: epidemiological and experimental studies. NeuroToxicology. 33(4): 810-816.

Friedman RC, Farh KKH, Burge CB, Bartel DP. 2009. Most mammalian mRNAs are conserved targets of microRNAs. Genome Res. 19:92-105.

Frotscher M, Jonas P, Sloviter RS. 2006. Synapses formed by normal and abnormal hippocampal mossy fibers. Cell Tissue Res. 326:361-367.

Gantier MP, McCoy CE, Rusinova I, Saulep D, Wang D, Xu D, Irving AT, Behlke MA, Hertzog PJ, Mackay F, Williams BRG. 2011. Analysis of microRNAs turnover in mammalian cells following *Dicer1* ablation. Nucleic Acids Res. 1-12. doi:10.1093/nar/gkr148.

Garay PA, McAllister AK. 2010. Novel roles for immune molecules in neural development: implications for neurodevelopmental disorders. Front. Synaptic Neurosci. 2:136. doi:10.3389/fnsyn.2010.00136.

Gehrmann J, Matsumoto Y, Kreutzberg GW. 1995. Microglia: Intrinsic immuneffector cell of the brain. Brain Res Rev. 20(3):269-287.

Gillet V, Hunting DJ, Takser L. 2016. Turing revisited: decoding the microRNAs messages in brain extracellular vesicles for early detection of neurodevelopmental disorders. Curr Envir Health Rpt. 3:188-201. doi:10.1007/s40572-016-0093-0.

Gluckman PD, Hanson MA, Buklijas T. 2010. A conceptual framework for the developmental origins of health and disease. J Dev Orig Health Dis. 1(1): 6-18.

Goldberg AD, Allis CD, Bernstein E. 2007. Epigenetics: a landscape takes shape. Cell. 128(4): 635-638.

Grathwohl SA, Kälin RE, Bolmont T, Prokop S, Winkelmann G, Kaeser SA, Odenthal J, Radde R, Eldh T, Gandy S, Aguzzi A, Staufenbiel M, Mathews PM, Wolburg H, Heppner FL, Jucker M. 2009. Formation and maintenance of Alzheimer's disease β-amyloid plaques in the absence of microglia. Nat Neurosci. (12)11:1361-1363.

Grumelli C, Berghuis P, Pozzi D, Caleo M, Antonucci F, Bonanno G, Carmignoto G, Dobszay MB, Harkany T, Matteoli M. 2008. Calpain activity contributes to the control of SNAP-25 levels in neurons. Mol. Cell Neurosci. 39(3):314-323.

Guedes J, Cardoso ALC, Pedroso de Lima MC. 2013. Involvement of microRNAs in microglia-mediated immune response. Clin Dev Immunol. 2013: 186872. doi:10.1155/2013/186872.

Guo L, Zhang Q, Ma X, Wang J, Liang T. 2017. miRNA and mRNA expression analysis reveals potential sex-biased miRNA expression. Sci Rep. 7:39812.

Hanisch UK. 2013. Functional diversity of microglia – how heterogeneous are they to begin with? Front Cell Neurosci. 7(65): 47-64.

Harry JG, Kraft AD. 2012. Microglia in the developing brain: A potential target with lifetime effects. NeuroToxicology. 33:191-206.

Hickman SE, Allison EK, Khoury JE. 2008. Microglial dysfunction and defective β-amyloid clearance pathways in aging Alzheimer's disease mice. J Neurosci. 28(33):8354-8360.

Hooper C, Pinteaux-Jones F, Fry VAH, Sevastou IG, Baker D, Heales SJ, Pocock JM. 2009. Differential effects of albumin on microglia and macrophages; implications for neurodegeneration following blood-brain barrier damage. J Neurochem. 109:694-705.

Hoozemans JJM, Veerhuis R, Van Haastert ES, Rozemuller JM, Baas F, Eikelenboom P, Scheper W. 2005. The unfolded protein response is activated in Alzheimer's disease. Acta Neuropath. 110(2): 165-172.

Kaneko Y, Kitamoto T, Tateishi J, Yamaguchi K. 1989. Ferritin immunohistochemistry as a marker for microglia. Acta Neuropathol. 79:129-136.

Kierdorf K, Erny D, Goldmann T, et al., 2013. Microglia emerge from erythromyeloid precursors via Pu.1- and Irf8-dependent pathways. Nat Neurosci. 16: 273-280.

Kiialainen A, Hovanes K, Paloneva J, Kopra O, Peltonen L. 2005. Dap12 and Trem2, molecules involved in innate immunity and neurodegeneration, are co-expressed in the CNS. Neurobiol Dis. 18: 314-322.

Kim K, Son SM, Mook-Jung I. 2013. Contributions of microglia to structural synaptic plasticity. J Exp Neurosci. 7: 85-91.

Klintsova AY, Helfer JL, Calizo LH, Dong WK, Goodlett CR, Greenough WT. 2007. Persistent impairement of hippocampal neurogenesis in young adult rats following early postnatal alcohol exposure. Alcohol Clin Exp Res. 31(12): 2073-2082.

Koo JW, Park CH, Choi SH, Kim NJ, Kim HS, Choe JC, Suh YH. 2003. The postnatal environment can counteract prenatal effects on cognitive ability, cell proliferation, and synaptic protein expression. FASEB J. 17: 1556-1558.

Kroner A, Greenhalgh AD, Zarruk JG, Passos dos Santos R, Gaestel M, David S. 2014. TNF and increased intracellular iron alter macrophage polarization to a detrimental M1 phenotype in the injured spinal cord. Neuron. 83(5):1098-1116.

Krstic D, Madhusudan A, Doehner J, Vogel P, Notter T, Imhof C, Manalastas A, Hilfiker M, Pfister S, Schwerdel C, Riether C, Meyer U, Knuesel I. 2012. Systemic immune challenges trigger and drive Alzheimer-like neuropathology in mice. J Neuroinflamm. 9:151.

Lambert JC, Pasquier F, Cottel D, Frigard B, Amouyel P, Chartier-Harlin MC. 1998. A new polymorphism in the *Apoe* promoter associated with risk of developing Alzheimer's disease. Hum Mol Genet. 7(3):533-540.

Leal G, Comprido D, Duarte CB. 2014. BDNF-induced local protein synthesis and synaptic plasticity. Neuropharmacology. 76:639-656.

Lee HG, Casadesus G, Zhu X, Takeda A, Perry G, Smith MA. 2004. Challenging the amyloid cascade hypothesis: senile plaques and amyloid-β as protective adaptations to Alzheimer's disease. Ann N Y Acad Sci. 1019. doi:10.1196/annals.1297.001.

Lee DC, Ruiz CR, Lebson L, Selenica MJB, Rizer J, Hunt JB Jr, Rojiani R, Reid P, Kammath S, Nash K, Dickey CA, Gordon M, Morgan D. 2013. Aging enhances classical activation but mitigates alternative activation in the central nervous system. Neurobiol. Aging. 34(6):1610-1620.

Leifer CA, Dietert RR. 2001. Early life environment and developmental immunotoxicity in inflammatory dysfunction and disease. Toxicol Environ Chem. 93(7):1463-1485.

Lenz KM, Nugent BM, Haliyur R, McCarthy MM. 2013. Microglia are essential to masculinization of brain and behavior. J Neurosci. 33(7):2761-2772.

Li LH, Tu QY, Deng XH, Xia J, Hou DR, Guo K, Zi XH. 2017. Mutant presenilin2 promotes apoptosis through the p53/miR-34a axis in neuronal cells. Brain Res. 1662: 57-64.

Li S, Hong S, Shepardson NE, Walsh DM, Shankar GM, Selkoe D. 2009. Soluble oligomers of amyloid β protein facilitate hippocampal long-term depression by disrupting neuronal glutamate uptake. Neuron. 62(6): 788-801.

Liu JT, Dong MH, Zhang JQ, Bai Y,Kuang F, Chen LW. 2015. Microglia and astroglia: the role of neuroinflammation in lead toxicity and neuronal injury in the brain. Neuroimmunol Neuroinflammation. 2(3): 131-137.

Liu MC, Liu XQ, Wang W, Shen XF, Che HL, Guo YY, Zhao MG, Chen JY, Luo WJ. 2012. Involvement of microglia activation in the lead induced long-term potentiation impairment. PLoS ONE. 7(8):e43924. doi:10.1371/journal.pone.0043924.

Lopes KO, Sparks DL, Streit WJ. 2008. Microglia dystrophy in the aged and Alzheimer's disease brain is associated with ferritin immunoreactivity. Glia. 56:1048-1060.

Luo XG, Chen SD. 2012. The changing phenotype of microglia from homeostasis to disease. Transl. Neurodegener. 1:9.

Marlatt MW, Bauer J, Aronica E, van Haastert ES, Hoozemans JJM, Joels M, Lucassen PJ. 2014. Proliferation in the Alzheimer hippocampus is due to microglia, not astroglia, and occurs at sites of amyloid deposition. Neural Plast. 693851.

Masliah E, Mallory M, Alford M, DeTeresa R, Hansen LA, McKeel DW Jr, Morris JC. 2001. Altered expression of synaptic proteins occurs early during progression of Alzheimer's disease. Neurology. 56(1):127-129.

Matcovitch-Natan O, Winter DR, Giladi A, et al. 2016. Microglia development follows a stepwise program to regulate brain homeostasis. Science. 353: aad8670. doi:10.1126/science.aad8670.

Mathew V, Ayyar SV. 2012. Developmental origins of adult diseases. Indian J. Endocrinol. Metab. 16(4):532-541. doi:10.4103/2230-8210.98005.

McCarthy MM, Nugent BM. 2015. At the frontier of epigenetics of brain sex differences. Front Behav Neurosci. 9(221): 1-8.

Meerson A, Cacheaux L, Goosens KA, Sapolsky RM, Soreq H, Kaufer D. 2010. Changes in brain microRNAs contribute to cholinergic stress reaction. J Mol Neurosci. 40:47-55.

Miller DB, O'Callaghan JP. 2008. Do early-life insults contribute to the late-life development of Parkinson and Alzheimer diseases? Metab Clin Exp. 57(2): S44-S49. doi:10.1016/j.metabol.2008.07.011.

Miller BH, Zeier Z, Xi L, Lanz TA, Deng S, Strathmann J, Willoughby D, Kenny PJ, Elsworth JD, Lawrence MS, Roth RH, Edbauer D, Kleiman RJ, Wahlestedt C. 2012. microRNAs-132 dysregulation in schizophrenia has implications for both neurodevelopment and adult brain function. PNAS. 109(8): 3125-3130.

Mitchell SD. 2009. Unsimple Truths: Science, Complexity, and Policy. The University of Chicago Press.

Morgan CP, Bale TL. 2012. Sex differences in microRNAs regulation of gene expression: no smoke, just miRs. Biol Sex Differ. 7:1034-1039. doi:10.1186/2042-6410-3-22.

Moser VC, Walls I, Zoetis T. 2005. Direct dosing of preweaning rodents in toxicity testing and research: deliberations of an ILSI RSI expert working group. Int J Toxicol. 24:87-94.

Naidoo N. 2009. ER and aging – protein folding and the ER stress response. Ageing Res Rev. 8(3): 150-159.

Nakagawa Y, Chiba K. 2014. Role of microglial M1/M2 polarization in relapse and remission of psychiatric disorders and diseases. Pharmaceuticals (Basel). 7:1028-1048. doi:10.3390/ph7121028.

Näslund J, Haroutunian V, Mohs R, Davis KL, Greengard P, Buxbaum JD. 2000. Correlation between elevated levels of amyloid β–peptide in the brain and cognitive decline. JAMA. 283(12): 1571-1577.

Nayak D, Roth TL, McGavern DB. 2014. Microglia development and function. Annu Rev Immunol. 32: 367-402.

Nikodemova M, Watters JJ. 2012. Efficient isolation of live microglia with preserved phenotypes from adult mouse brain. J Neuroinflamm. 9(147):1-10.

Oddo S, Caccamo A, Kitazawa M, Tseng BP, LaFerla FM. 2003. Amyloid deposition precedes tangle formation in a triple transgenic model of Alzheimer's disease. Neurobiol Aging. 24:1063-1070.

Olah M, Biber K, Vinet J, Boddeke HWGM. 2011. Microglia phenotype diversity. CNS Neurol Disord. 10(1):1-11.

Otal R, Martínez A, Soriano E. 2005. Lack of TrkB and TrkC signaling alters the synaptogenesis and maturation of mossy fiber terminals in the hippocampus. Cell Tissue Res. 319:349-358.

Overk CR, Perez SE, Ma C, Taves MD, Soma KK, Mufson EJ. 2013. Sex steroid levels and AD-like pathology in 3xTgAD mice. J Neuroendocrinol. 25(2): 131-144.

Paolicelli RC, Bolasco G, Pagani F, et al. 2011. Synaptic pruning by microglia is necessary for normal brain development. Science. 333(6048): 1456-1458.

Parakalan R, Jiang B, Nimmi B, et al. 2012. Transcriptome analysis of amoeboid and ramified microglia isolated from the corpus callosum of rat brain. BMC Neurosci. 13:64.

Parkhurst CN, Yang G, Ninan I, Savas JN, Yates JR III, Lafaille JJ, Hempstead BL, Littman DR, Gan WB. 2013. Microglia promote learning-dependent synapse formation through brain-derived neurotrophic factor. Cell. 155:1596-1609.

Pericak-Vance MA, Haines JL. 1995. Genetic susceptibility to Alzheimer disease. Trends Genet. 11(12): 504-508.

Perry VH, Teeling J. 2013. Microglia and macrophages of the central nervous system: the contribution of microglia priming and systemic inflammation to chronic neurodegeneration. Semin Immunopathol. 35:601-612.

Perry VH, Nicoll JAR, Holmes C. 2010. Microglia in neurodegenerative disease. Nat. Rev. Neurol. 6:193-201.

Ponomarev ED, Veremeyko T, Barteneva N, Krichevsky AM, Weiner H. 2011. microRNAs-124 promotes microglia quiescence and suppresses EAE by deactivating macrophages via the C/EBP-α-PU.1 pathway. Nat Med. 17: 64-70. doi:10.1038/nm.2266.

Prechel MM, Ding C, Washington RL, Kolodziej MS, Young MR. 2000. In vivo indomethacin treatment causes microglial activation in adult mice. Neurochem Res. 25(3):357-362.

Prokop S, Miller KR, Heppner FL. 2013. Microglia actions in Alzheimer's disease. Acta Neuropathol. 126:461-477.

Quintana C, Gutiérrez L. 2010. Could a dysfunction of ferritin be a determinant factor in the aetiology of some neurodegenerative diseases? Biochim. Biophys. Acta. 1800:770-782.

Reid G, Kirschner MB, van Zandwijk N. 2011. Circulating microRNAs: Association with disease and potential use as biomarkers. Crit Rev Oncol Hematol. 80(2): 193-208.

Rodenas-Ruano A, Chávez AE, Cossio MJ, Castillo PE, Zukin RS. 2012. REST-dependent epigenetic remodeling promotes the developmental switch in synaptic NMDA receptors. Nat Neurosci. 15(10): 1382-1390. doi:10.1038/nn.3214.

Rodríguez JJ, Jones VC, Tabuchi M, Allan SM, Knight EM, LeFerla FM, Oddo S, Verkhratsky A. 2008. Impaired adult neurogenesis in the dentate gyrus of a triple transgenic mouse model of Alzheimer's disease. PLoS ONE. 3(8):e2935. doi:10.1371/journal.pone.0002935.

Rogers JT, Bush AI, Cho HH, Smith DH, Thomas AM, Friedlich AL, Lahiri DK, Leedman PJ, Huang X, Cahill CM. 2008. Iron and the translation of the amyloid precursor protein (APP) and ferritin mRNAs: riboregulation against neural oxidative damage in Alzheimer's disease. Biochem. Soc. Trans. 36:1282-1287. doi:10.1042/BST0361282.

Rokavec M, Li H, Jiang L, Hermeking H. 2014. The p53/miR-34 axis in development and disease. J Mol Cell Biol. 6:214-230. doi:10.1093/jmcb/mju003.

Roumier A, Béchade C, Poncer JC, Smalla KH, Tomasello E, Vivier E, Gundelfinger ED, Triller A, Bessis A. 2004. Impaired synaptic function in the microglial KARAP/DAP12-deficient mouse. J Neurosci. 24(50):11421-11428. doi:10.1523/jneurosci.2251-04.2004.

Ruijter JM, Ramakers C, Hoogaars WM, Karlen Y, Bakker I, van den Hoff MJ, Moorman AF. 2009. Amplification efficiency: Linking baseline and bias in the analysis of quantitative PCR data. Nucleic Acids Res. 37(6):e45. doi:10.1093/nar/gkp045.

Salter MW, Beggs S. 2014. Sublime microglia: expanding roles for the guardians of the CNS. Cell. 158(1):15-24. doi:10.1016/j.cell.2014.06.008.

Santambrogio L, Belyanskaya SL, Fischer FR, Cipriani B, Brosnan CF, Ricciardi-Castagnoli P, Stern LJ, Strominger JL, Riese R. 2001. Developmental plasticity of CNS microglia. PNAS. 98(11)6295-6300.

Schidlt S, Endres T, Lessmann V, Edelmann E. 2013. Acute and chronic interference with BDNF/TrkB-signaling impair LTP selectively at mossy fiber synapses in the CA3 region of the mouse hippocampus. Neuropharmacology. 71:247-254.

Schindelin J, Arganda-Carreras I, Frise E. 2012. Fiji: an open-source platform for biological-image analysis. Nat. methods. 9(7): 676-682.

Schloesser RJ, Jimenez DV, Hardy NF, Paredes D, Catlow BJ, Manji HK, McKay RD, Martinowich K. 2014. Atrophy of pyramidal neurons and increased stress-induced glutamate levels in CA3 following chronic suppression of adult neurogenesis. Brain Struct. Funct. 219:1139-1148.

Schmidt R, Kienbacher E, Benke T, et al. 2008. Sex differences in Alzheimer's disease. Neuropsychiatr. 22(1): 1-15.

Schwarz JM, Bilbo SD. 2012. Sex, glia, and development: Interactions in health and disease. Horm Behav. doi:10.1016/j.yhbeh.2012.02.018.

Schwarz JM, Sholar PW, Bilbo SD. 2012. Sex differences in microglial colonization of the developing rat brain. J Neurochem. 120:948-963.

Sedgwick, J.D., Schwender, S., Imrich, H., Dörries, R., Butcher, G.W., Meulen, V.T. 1991. Isolation and direct characterization of resident microglial cells from the normal and inflamed central nervous system. Proc Natl Acad Sci. 88:7438-7442.

Sharma M, Burré J, Bronk P, Zhang Y, Xu W, Südhof TC. 2012. CSPα knockout causes neurodegeneration by impairing SNAP-25 function. EMBO J. 31:829-841.

Shi L, Zhang Z, Su B. 2016. Sex biased gene expression profiling of human brains at major developmental stages. Sci. Rep. 6:21181. doi:10.1038/srep21181.

Sierra A, Encinas JM, Deudero JJP, Chancey JH, Enikolopov G, Overstreet-Wadiche LS, Tsirka SE, Maletic-Savatic M. 2010. Microglia shape adult hippocampal neurogenesis through apoptosis-coupled phagocytosis. Cell Stem Cell. 7:483-495.

Simmons DA, Casale M, Alcon B, Pham N, Narayan N, Lynch G. 2007. Ferritin accumulation in dystrophic microglia is an early event in the development of Huntington's disease. Glia. 55:1074-1084.

Smith AM, Dragunow M. 2014. The human side of microglia. Trends Neurosci. 37(3): 125-135.

Sobin C, Montoya MGF, Parisi N, Schaub T, Cervantes M, Armijos RX. 2013. Microglial disruption in young mice with early chronic lead exposure. Toxicol Let. 220: 44-52.

Solito E, Sastre M. 2012. Microglia function in Alzheimer's disease. Front Pharmacol. 3(14)1-10. doi:10.3389/fphar.2012.00014.

Sollome J, Martin E, Sethupathy P, Fry RC. 2016. Environmental contaminants and microRNAs regulation: transcription factors as regulators of toxicant-altered microRNAs expression. Toxicol Appl Pharmacol. 312:61-66. doi:10.1016/j.taap.2016.06.009.

Soreq H, Wolf Y. 2011. NeurimmiRs: microRNAs in the neuroimmune interface. Trends Mol Med. 17(10):548-555.

Spangenberg EE, Lee RJ, Najafi AR, Rice RA, Elmore MRP, Blurton-Jones M, West BL, Green KN. 2016. Eliminating microglia in Alzheimer's mice prevents neuronal loss without modulating amyloid-β pathology. Brain. 139:1265-1281. doi:10.1093/brain/aww016.

Stalder M, Phinney A, Probst A, Sommer B, Staufenbiel M, Jucker M. 1999. Association of microglia with amyloid plaques in brains of APP23 transgenic mice. Am J Pathol. 154(6):1673-1684.

Sterniczuk R, Antle MC, LaFerla FM, Dyck RH. 2010. Characterization of the 3xTg-AD mouse model of Alzheimer's disease: Part 2. Behavioral and cognitive changes. Brain Res. 1348: 149-155.

Stevens SL, Bao J, Hollis J, Lessov NS, Clark WM, Stenzel-Poore, M.P. 2001. The use of flow cytometry to evaluate temporal changes in inflammatory cells following focal cerebral ischemia in mice. Brain Res. 932:110-119.

Streit WJ, Xue QS, Tischer J, Bechmann I. 2014. Microglia pathology. Acta Neuropathol. 2(142):1-17.

Streit WJ. 2010. Microglial activation and neuroinflammation in Alzheimer's disease: a critical examination of recent history. Front Aging Neurosci. 2:22.

Streit WJ, Braak H, Xue QS, Bechmann I. 2009. Dystrophic (senescent) rather than activated microglial cells are associated with tau pathology and likely precede neurodegeneration in Alzheimer's disease. Acta Neuropathol. 118: 475-485.

Streit WJ. 2006. Microglial senescence: does the brain's immune system have an expiration date? Trends Neurosci. 29(9): 506-510.

Takahashi K, Rochford CDP, Neumann H. 2005. Clearance of apoptotic neurons without inflammation by microglial triggering receptor expressed on myeloid cells-2. J Exp Med. 201(4): 647-657.

Tang Y, Le W. 2015. Differential roles of M1 and M2 microglia in neurodegenerative diseases. Mol. Neurobiol. 53:1181. doi:10.1007/s12035-014-9070-5.

Tarsa L, Goda Y. 2002. Synaptophysin regulates activity-dependent synapse formation in cultured hippocampal neurons. Proc. Natl. Acad. Sci. U.S.A. 99(2): 1012-1016. doi:10.1073/pnas.022575999.

Thrash JC, Torbett BE, Carson MJ. 2009. Developmental regulation of TREM2 and DAP12 expression in the murine CNS: implications for Nasu-Hakola disease. Neurochem Res. 34:38. doi:10.1007/s11064-008-9657-1.

Toscano CD, Guilarte TR. 2005. Lead neurotoxicity: From exposure to molecular effects. Brain Res Rev. 49:529-554.

Vinet J, van Weering HRJ, Heinrich A, Kälin RE, Wegner A, Brouwer N, Heppner FL, van Rooijen N, WGM Boddeke H, Biber K. 2012. Neuroprotective function for ramified microglia in hippocampal excitotoxicity. J Neuroinflammation. 9:27. doi:10.1186/1742-2094-9-27.

vonderEmbse AN, Hu Q, DeWitt JC. 2017. Developmental toxicant exposure in a mouse model of Alzheimer's disease induces differential sex-associated microglial activation and increased susceptibility to amyloid accumulation. J. Dev. Orig. Health Dis. 1-9. doi:10.1017/S2040174417000277.

Wake H, Moorhouse AJ, Jinno S, Kohsaka S, Nabekura J. 2009. Resting microglia directly monitor the functional state of synapses *in vivo* and determine the fate of ischemic terminals. J Neurosci. 29(13): 3974-3980.

Wakselman S, Béchade C, Roumier A, Bernard D, Triller A, Bessis A. 2008. Developmental neuronal death in hippocampus requires the microglial CD11b integrin and DAP12 immunoreceptor. J Neurosci. 28(32): 8138-8143.

Walker FR, Beynon SB, Jones KA, Zhao Z, Kongsui R, Cairns M, Nilsson M. 2014. Dynamic structural remodeling of microglia in health and disease: a review of the models, the signals and the mechanisms. Brain Behav Immun. 37: 1-14.

Walker DG, Lue LF. 2015. Immune phenotype of microglia in human neurodegenerative disease: challenges to detecting microglia polarization in human brains. Alzheimer's Res Ther. 7:56. doi:10.1186/s13195-015-0139-9.

West-Eberhard MJ. 1989. Phenotypic plasticity and the origins of diversity. Annu Rev Ecol Syst. 20: 249-278.

Williamson LL, Sholar PW, Mistry RS, Smith SH, Bilbo SD. 2011. Microglia and memory: modulation by early-life infection. J Neurosci. 31(43): 15511-15521.

Wu J, Basha MR, Brock B, Cox DP, Cardozo-Pelaez F, McPherson CA, Harry J, Rice DC, Maloney B, Chen D, Lahiri DK, Zawia NH. 2008. Alzheimer's Disease (AD)-like pathology in aged monkeys after infantile exposure to environmental metal lead (Pb): evidence for a developmental origin and environmental link for AD. J Neurosci. 28(1): 3-9.

Yamada J, Nakanishi H, Jinno S. 2011. Differential involvement of perineuronal astrocytes and microglia in synaptic stripping after hypoglossal axotomy. Neuroscience. 182:1-10. doi:10.1016/j.neuroscience.2011.03.030.

Yokoyama A, Sakamoto A, Kameda K, Imai Y, Tanaka J. 2006. NG2 proteoglycan-expressing microglia as multipotent neural progenitors in normal and pathologic brains. Glia. 53(7):754-768. doi:10.1002/glia.20332.

Yokoyama A, Yang L, Itoh S, Mori K, Tanaka J. 2004. Microglia, a potential source of neurons, astrocytes, and oligodendrocytes. Glia. 45(1):96-104. doi:10.1002/glia.10306.

Yoshii A, Constantine-Paton M. 2010. Postsynaptic BDNF-TrkB signaling in synapse maturation, plasticity, and disease. Devel Neurobiology. 70(5):304-322.

Ziebell JM, Adelson PD, Lifshitz J. 2015. Microglia: dismantling and rebuilding circuits after acute neurological injury. Metab Brain Dis. 30(2): 393-400.

Zoetis T, Walls I. 2005. Principles and Practices for direct dosing of pre-weaning mammals in toxicity testing and research. A report of the ILSI Risk Science Institute Expert Working Group on Direct Dosing of Pre-weaning Mammals in Toxicity Testing, ILSI Press, Washington DC.

Appendix A

East Carolina University

Animal Care and Use Commitee
212 Ed Warren Life Sciences Building
East Carolina University
Greenville, NC 27834

252-744-2436 office
252-744-2355 fax

May 6, 2013

Jamie DeWitt, Ph.D.
Department of Pharmacology
Brody 6S-10
ECU Brody School of Medicine

Dear Dr. DeWitt:

Your Animal Use Protocol entitled, "Exacerbation of Alzheimer's Pathology by Early-Life Exposure to Lead" (AUP #W236) was reviewed by this institution's Animal Care and Use Committee on 5/6/13. The following action was taken by the Committee:

"Approved as submitted"

Please contact Dale Aycock at 744-2997 prior to hazard use

A copy is enclosed for your laboratory files. Please be reminded that all animal procedures must be conducted as described in the approved Animal Use Protocol. Modifications of these procedures cannot be performed without prior approval of the ACUC. The Animal Welfare Act and Public Health Service Guidelines require the ACUC to suspend activities not in accordance with approved procedures and report such activities to the responsible University Official (Vice Chancellor for Health Sciences or Vice Chancellor for Academic Affairs) and appropriate federal Agencies.

Sincerely yours,

Susan McRae, Ph.D.
Chair, Animal Care and Use Committee

SM/jd

enclosure

East Carolina University

Animal Care and
Use Commitee
212 Ed Warren Life
Sciences Building
East Carolina University
Greenville, NC 27834

252-744-2436 office
252-744-2355 fax

December 16, 2015

Jamie DeWitt, Ph.D.
Department of Pharmacology
Brody 6S-30
ECU Brody School of Medicine

Dear Dr. DeWitt:

Your Animal Use Protocol entitled, "Developmental Dysregulation of Microglia and Increased Susceptibility to Alzheimer's Disease Neuropathologies" (AUP #W248) was reviewed by this institution's Animal Care and Use Committee on December 16, 2015. The following action was taken by the Committee:

"Approved as submitted"

Please contact Dale Aycock at 744-2997 prior to hazard use

*Administrative changes were made by adding PI emergency contact information and marking out the comment about IBC approval since it is not required.

A copy is enclosed for your laboratory files. Please be reminded that all animal procedures must be conducted as described in the approved Animal Use Protocol. Modifications of these procedures cannot be performed without prior approval of the ACUC. The Animal Welfare Act and Public Health Service Guidelines require the ACUC to suspend activities not in accordance with approved procedures and report such activities to the responsible University Official (Vice Chancellor for Health Sciences or Vice Chancellor for Academic Affairs) and appropriate federal Agencies. **Please ensure that all personnel associated with this protocol have access to this approved copy of the AUP and are familiar with its contents.**

Sincerely yours,

Susan McRae, Ph.D.
Chair, Animal Care and Use Committee

SM/jd

enclosure